FOCUS-Africa

Research and Innovation Action (RIA)

This project has received funding from the European Union's Horizon 2020 research and innovation programme under grant agreement No 869575

Start date : 2020-09-01 Duration : 48 Months

Report on the selection and analysis of high resolution climate projections of the region

Authors : Nicolas Fournier (MO), Scott Burgan (MO), Christopher Jack (UCT), Lisa van Aardenne (UCT), Izidine Pinto(UCT), Lila Collet (EDF), Hiba Omrani (EDF), Francois Englebrecht (WITS), Jonathan Padavatan (WITS), Hamid Bastani (WMO), Sebastian Grey (WMO)

FOCUS-Africa - Contract Number: 869575

Project officer: Anna-Natasa ASIK

Document title	Report on the selection and analysis of high resolution climate projections of the region
Author(s)	Nicolas Fournier, Scott Burgan (MO), Christopher Jack (UCT), Lisa van Aardenne(UCT), Izidine Pinto (UCT), Lila Collet (EDF), Hiba Omrani (EDF), Francois Englebrecht (WITS), Jonathan Padavatan (WITS), Hamid Bastani (WMO), Sebastian Grey (WMO)
Number of pages	68
Document type	Deliverable
Work Package	WP3
Document number	D3.1
Issued by	MO
Date of completion	2021-10-06 09:40:46
Dissemination level	Public

Summary

The SADC countries are particularly vulnerable to climate variability, change and extremes. Water resources, agriculture, hydropower generation, ecosystems and basic infrastructures are especially under stress because of increased frequency and intensity of floods, droughts, and landslides. The development of improved climate information and forecasts of decision-relevant parameters is essential to address these challenges FOCUS-Africa s climate services will be developed by ensuring the full value chain is implemented, starting from close involvement of end-users to assess their climate-related challenges and risks (WP2), understanding regional climate processes (WP3), developing methods and tools (WP4), creating prototypes of end-user tailored climate services (WP5), assessing their economic value, and exploiting results (WP6) and capacity building (WP7). This will be demonstrated by piloting eight case studies in six countries involving a wide range of fellow-users. The case studies will illustrate how the use of WP3 climate science, forecasts and projections can maximize socio-economic benefits in the Southern Africa region and potentially in the whole of Africa. Indeed, WP3 builds up the climate foundation of the project and focuses specifically on advancing the underpinning science required to provide robust climate services and development of climate-integrated applications for the energy, water, infrastructure, and food security sectors. To achieve this, WP3 explores the performances of the latest climate projections (Task 3.1, M12) and predictability at seasonal forecast time scales s (Task 3.2, M18) as well as analyse the extremes in the region (Task 3.3, M24). The Task 3.1 report is the first of the series and analyses the most recent climate models information, namely, CMIP6, CMIP5, CORDEX as well as higher resolution simulations from CP4A and CCAM over the SADC region. Task 3.1 investigates, firstly, the performance of these models against present-day air temperature and rainfall observations. Secondly, it examines their future climate projections over the SADC region. It is demonstrated that the selected models perform reasonably well at simulating the present-day conditions for near-surface air temperature and rainfall over the SADC region. The simulations from CP4A (4.5 km) and CCAM (8 km) exhibit some improvements compared to the lower resolution models especially for the DJF rainfall. There was thus no reason to exclude any of these models in our evaluation of the future SADC climate projections. For the end of century climate projections, there is a common agreement from all the models on an air temperature increase across the SADC region. However, the high-resolution models exhibit larger values with increase average around 5oC. For the precipitation, there is a general reduction projected across the region except for (1) DJF months in the Upper ESAF and SEAF regions, (2) MAM months in SEAF. However, there are significant discrepancies between the models in (1) Lower ESAF in DJF and MAM, (2) Upper ESAF in MAM and (3) SEAF in SON. However, it should be kept in mind that there are large differences between the models and thus some uncertainties. Therefore, for the case studies and their risk-based decision making, further assessment of the reliability of these models must be performed to characterize better the formulation of these models and the reliability of the mechanisms involved in their future climate responses.

Approval

Date	By
2021-10-06 09:41:12	Mr. Nicolas FOURNIER (MO)
2021-10-06 10:59:58	Mrs. Roberta BOSCOLO (WMO)

FOCUS-AFRICA

Full-value chain Optimised Climate User-centric Services for Southern Africa

Climate Projections Analysis Over the SADC Region

Deliverable D3.1

Lead Beneficiary: Land Bank (South Africa), Local Farmer's Association (Malawi), Smallholder Farmers (Mozambique), Tanzania Agricultural Research Institute, COWI (Tanzania), TANESCO (Tanzania), Total (Tanzania), EDF (Malawi), Water and Agriculture Local communities (Mauritius).

September 2021

Scott Burgan[1], Christopher Jack[2], Lisa van Aardenne[2], Izidine Pinto[2], Lila Collet[3], Hiba Omrani[3], Francois Englebrecht[4], Jonathan Padavatan[4], Hamid Bastani[5], Sebastian Grey[5], Nicolas Fournier[1]

[1] *Met Office (MO), Exeter, UK*
[2] *Climate System Analysis Group, University of Cape Town (UCT), Cape Town, South Africa*
[3] *Electricité De France (EDF), Paris, France*
[4] *Global Change Institute – University of the Witwatersrand (WITS), Johannesburg, South Africa*
[5] *World meteorological organization (WMO), Geneva, Switzerland*

www.focus-africaproject.eu

This project has received funding from the European Commission's Horizon 2020 Research and Innovation Programme. The content in this presentation reflects only the author(s)'s views. The European Commission is not responsible for any use that may be made of the information it contains.

Document Information

Grant Agreement:	869575
Project Title:	Full-value chain Optimised Climate User-centric Services for Southern Africa
Project Acronym:	Focus-Africa
Project Start Date:	1 September 2020
Related work package:	WP 3
Related task(s):	Task 3.1
Lead Organisation:	Met Office
Submission date:	21 September 2021
Dissemination Level:	1

History

Date	Submitted by	Reviewed by	Version (Notes)
21/09/2021	N. Fournier	WMO	V1

About FOCUS-Africa

FOCUS-Africa – Full-value chain Optimised Climate User-centric Services for Southern Africa – is developing sustainable tailored climate services in the Southern African Development Community (SADC) region for four sectors: agriculture and food security, water, energy and infrastructure.

It will pilot eight case studies in six countries involving a wide range of end-uses to illustrate how the application of new climate forecasts, projections, resources from Copernicus, GFCS and other relevant products can maximise socio-economic benefits in the Southern Africa region and potentially in the whole of Africa.

Led by WMO, it gathers 14 partners across Africa and Europe jointly committed to addressing the recurring sustainability and exploitation challenge of climate services in Africa over a period of 48 months.

For more information visit: www.focus-africaproject.eu

Coordinator Contact
Roberta Boscolo | Climate & Energy Scientific Officer
Applied Climate Services Division
Services Department
World Meteorological Organization (WMO)
CP 2300, 1211 Geneva SWITZERLAND
email: rboscolo@wmo.int

Table of Content

List of Acronyms

CCAM - Conformal-Cubic Atmospheric Model

CMIP5 - Coupled Model Inter-comparison Project Phase 5

CMIP6 - Coupled Model Inter-comparison Project Phase 6

CORDEX - Coordinated Regional climate Downscaling Experiment

CP4A - Climate Predictions for Africa

CPM – Convection-permitting Model

CRU – Climatic Research Unit

DJF – December January February

ECMWF – European Centre for Medium-Range Weather Forecasts

ENDGAME – Even Newer Dynamics for General Atmosphere Modelling

ERA-Interim – ECMWF Re-Analysis Interim

ESAF - East Southern-Africa

GCM – Global Climate Model

GHG – Green House Gas

HadGEM2-ES – Hadley Centre Global Environment Model

JJA – June July August

MAM – March April May

RCM – Regional Climate Model

RCP - Representative Concentration Pathway

SEAF – South Eastern-Africa

SON – September October November

SADC – Southern African Development Community

SSP - Socio-economic Pathways

WASF – West Southern-Africa

WP – Work Package

Executive Summary

The SADC countries are particularly vulnerable to climate variability, change and extremes. Water resources, agriculture, hydropower generation, ecosystems and basic infrastructures are especially under stress because of increased frequency and intensity of floods, droughts, and landslides. The development of improved climate information and forecasts of decision-relevant parameters is essential to address these challenges

FOCUS-Africa's climate services will be developed by ensuring the full value chain is implemented, starting from close involvement of end-users to assess their climate-related challenges and risks (WP2), understanding regional climate processes (WP3), developing methods and tools (WP4), creating prototypes of end-user tailored climate services (WP5), assessing their economic value, and exploiting results (WP6) and capacity building (WP7).

This will be demonstrated by piloting eight case studies in six countries involving a wide range of fellow-users. The case studies will illustrate how the use of WP3 climate science, forecasts and projections can maximize socio-economic benefits in the Southern Africa region and potentially in the whole of Africa.

Indeed, WP3 builds up the climate foundation of the project and focuses specifically on advancing the underpinning science required to provide robust climate services and development of climate-integrated applications for the energy, water, infrastructure, and food security sectors. To achieve this, WP3 explores the performances of the latest climate projections (Task 3.1, M12) and predictability at seasonal forecast time scales s (Task 3.2, M18) as well as analyse the extremes in the region (Task 3.3, M24).

The Task 3.1 report is the first of the series and analyses the most recent climate models information, namely, CMIP6, CMIP5, CORDEX as well as higher resolution simulations from CP4A and CCAM over the SADC region. Task 3.1 investigates, firstly, the performance of these models against present-day air temperature and rainfall observations. Secondly, it examines their future climate projections over the SADC region.

It is demonstrated that the selected models perform reasonably well at simulating the present-day conditions for near-surface air temperature and rainfall over the SADC region. The simulations from CP4A (4.5 km) and CCAM (8 km) exhibit some improvements compared to the lower resolution models especially for the DJF rainfall. There was thus no reason to exclude any of these models in our evaluation of the future SADC climate projections.

For the end of century climate projections, there is a common agreement from all the models on an air temperature increase across the SADC region. However, the high-resolution models exhibit larger values with increase average around 5°C. For the precipitation, there is a general reduction projected across the region except for (1) DJF months in the Upper ESAF and SEAF regions, (2) MAM months in SEAF. However, there are significant discrepancies between the models in (1) Lower ESAF in DJF and MAM, (2) Upper ESAF in MAM and (3) SEAF in SON. However, it should be kept in mind that there are large differences between the models and thus some uncertainties. Therefore, for the case studies and their risk-based decision making, further assessment of the reliability of these models must be performed to characterise better the formulation of these models and the reliability of the mechanisms involved in their future climate responses.

Keywords

Climate Projections, Regional Climate Model, South Africa, Climate change and variability

1 Introduction

Southern Africa epitomizes the link between climate and the water–energy–food nexus, as multiple challenges collide across a very diverse socioeconomic spectrum of countries (Mabhaudhi et al., 2021; Siderius et al., 2021). According to the World Bank Classification (see Table 1 below) of the countries that comprise SADC (Southern African Development Community); six are defined as low income including Malawi, Mozambique, and Tanzania which are the focus of 5 of our project's case studies.

Table 1 – Income group of the countries that comprise SADC

INCOME GROUP		SADC COUNTRY
LOW		Lesotho **Malawi** **Mozambique** **Tanzania** Zambia Zimbabwe
MIDDLE	LOWER	Angola Botswana Namibia Swaziland
	UPPER	**Mauritius** **South Africa**

Food security is the main sector of interest in our project and agriculture's contribution to regional Gross Domestic Product (GDP) is 17% for the whole SADC region, and up to 28% for the low-income countries. At the same time, ca. 75% of the land in SADC is either arid or semi-arid, and agriculture is estimated to consume 70% of the renewable water resources of the region (Nhemachena et al., 2020). Major water scarcity issues are expected in the SADC because of ongoing exploitation and degradation, coupled with increased demand and climate change (IPCC, 2021). With 27 million food insecure people, the 2015/16 El Niño-induced drought provides an example of how increased water demand for agriculture can aggravate water, energy, and food insecurity (Nhemachena et al., 2020; Kolusu et al., 2019).

Climate change is expected to impact infrastructures, renewable energy, and agricultural production in SADC in multiple ways. Indeed, approximately 30% of the region is critically exposed to a variety of climate hazards such as drought, flood, climate variability and high temperatures (Ramirez-Villegas et al., 2021). The SADC countries are particularly vulnerable to climate variability, change and extremes: particularly water resources, agriculture, hydropower generation, ecosystems and basic infrastructures are especially under stress because of increased frequency and intensity of floods, droughts, and landslides. The 2015/16 drought, one of the most severe on record, contributed to over 40 million people to be food insecure, and dam water levels to be reduced, leading to intermittent

power outages in most countries in the region (Conway et al., 2017). Climate change is also projected to reduce the amount of suitable land for cropping and crop, pasture, livestock productivity (Pequeno et al., 2021, Ekine-Dzivenu et al., 2020) as well as to double the risk of drought such as the 2015/16 event occurring (Kolusu et al., 2019). Decreased suitable land for cropping and reduced crop and livestock productivity would exacerbate water scarcity and insecurity, and decrease national self-sufficiency ratios, and impact food availability locally, with devastating effects on food insecurity in the region. Water, energy, and food are thus inextricably linked across multiple scales in SADC and are heavily interdependent.

Therefore, to address these existing and emerging infrastructure-water-energy-food issues requires a better understanding and characterization of the main climate hazards of the SADC region. This is the objective of Task 3.1 described in this report. We are building up the climate foundation of this project by analysing the most recent climate model data available over the SADC region. This will then enable selecting in the next tasks (i.e., Task 4.2) the most suitable climate projections to be used in the case studies for specific countries and climate parameters.

In this report, Section 2 describes the different climate models and Section 3 the observations used to assess their present-day performance in Section 5. Section 4 provides an overview of the methodology employed to conduct this performance assessment and Section 6 focuses on the analysis of the future climate projections over our regions of interest.

FOCUS-AFRICA

2 Models

2.1 Models' selection

In this task, we considered a range of the latest available GCMs (Global Circulation Model), RCMs (Regional Climate Model) and one CPM (Convection-permitting Model) over the region allowing us to evaluate performances and projections across a wide range of resolutions (280 km to ~4.5 km). The selected GCMs comprise 37 CMIP5 and 30 CMIP6 models (Climate Model Intercomparison Project Phase 5 in 2014 and Phase 6 in 2019; Appendix 8.1). The RCMs include a range of 25-50km CORDEX simulations and 6 CCAM 8km downscaled simulations. Finally, the CPM is CP4A (Climate Predictions for Africa, Senior et al., 2021) with 4.5km spatial resolution. These models are described in more details in the following sections.

2.1.1 CMIP5 & 6

GCMs are widely used in the assessment of current and future climates on global and regional scales. Due to current knowledge on processes affecting the climate system on centennial timescales, models are constructed from basic components (e.g., atmosphere, ocean, cryosphere, land surface). Since not all these processes can be fully described from basic principles and fully resolved at GCM spatial scales, several assumptions are needed in building GCMs, resulting in a varied range of climate simulations. Therefore, in this task 37 models from the CMIP5 ensemble are considered, as well as their ensemble mean, to compare their output to that of higher resolution models that are available. The full overview of the CMIP5 ensemble can be found in Taylor, Stouffer and Meehl (2012). Furthermore, the more recent 30 CMIP6 models are also included with an increased spatial resolution, allowing for a better representation of smaller scale physical processes (Eyring et al., 2016; O'Neill et al., 2016; Stouffer et

al., 2017), as well as additional forcing's which include the Shared Socio-Economic Pathway (SSP) scenario matrix (Eyring et al., 2016; Riahi et al., 2017; Stouffer et al., 2017).

2.1.2 CORDEX

Due to an increasing demand for regional climate change information at a high spatial resolution, several international projects began to generate high-resolution ensembles, including the Coordinated Regional climate Downscaling Experiment (CORDEX) initiative. Originally, this initiative produced RCMs with a 50 km resolution (Nikulin et al., 2012), but recent developments by the WCRP CORDEX Common Regional Experiment (CORE) framework, produced a new ensemble with a spatial resolution of 25 km across a number of regions (Remedio et al., 2019). In this task, we will be evaluating both the 50 and 25 km models (23 and 10), but also a sub-set of three 25km CORDEX CORE ensemble. The subset of models selected are driven by HadGEM2-ES, allowing us to make a direct comparison of the RCMs performance compared to its GCM driver and includes REMO2015, RegCM4-7 and CCLM5-0-15. REMO2015 was originally developed within the Max Planck Institute for Meteorology, REMO is now maintained and developed by GERICS. It combines a numerical weather prediction model (EUROPA-MODELL) with a GCM (ECHAM4), creating this a model suitable for climate modelling and weather forecast (more info - https://www.remo-rcm.de/059966/index.php.en). RegCM4-7 was developed at the National Centre for Atmospheric Research (NCAR) and is now maintained the International Centre for Theoretical Physics (ICTP). This is the latest version of this model which was updated in 2010 to include a new pre- and post-processor, as well as updated physics parameterisations (more info-https://www.ictp.it/research/esp/models/regcm4.aspx). Finally, the CCLM5-0-15 is a Nonhydrostatic regional climate model developed and maintained by the Climate Limited-area Modelling (CLM) community and is a climate version of the COSMO LM model (Steppeler et al., 2003)(more info - COSMO core documentation (cosmo-model.org)).

2.1.3 CP4A

CP4A is the highest resolution model in the evaluation and is driven by the Met Office Unified Model Stratton *et al.* (2018). This driving model is most comparable to HadGEM2-ES from the CMIP5 ensemble. Some of the key differences between the Met Office Unified Model and HadGEM2-ES are the updated physics and dynamical schemes. This Unified model is also an atmospheric only model, which uses sea surface temperature. However, they are still structurally related which allows us comparing its performance to that of the HadGEM2-ES, as well as the selected CORDEX-CORE models. CP4A differs from the other models in this evaluation due to its ability to represent convection explicitly. This is termed "convection-permitting" which is achievable due to its high resolution of ~4.5 km. The other models in this evaluation (CMIP5-6, CORDEX, CCAM) use parameterizations to represent the effects of convection which is a known potential source of model error. Additionally, convection-permitting models have been found to improve the representation of extreme precipitation (on an hourly time scale), the diurnal cycle of precipitation, as well as the depiction of precipitation structures (Prein et al., 2015; Senior et al., 2021). These are important factors to consider in the development of the climate services of the case studies.

2.1.4 CCAM

Another RCM used in this task is the Conformal-Cubic Atmospheric Model (CCAM), a variable-resolution global climate model developed by the Commonwealth Scientific and Industrial Research Organisation (CSIRO) (McGregor, 2005). CCAM is coupled to a dynamic land-surface model CABLE (CSIRO Atmosphere Biosphere Land Exchange model). The model was applied at the Global Change Institute in South Africa, as part of the FOCUS-Africa project, to downscale ERA-Interim reanalysis data to an 8 km spatial resolution over southern Africa, for the period 1979-2017.

The experimental design followed that of Horowitz et al. (2017), by first nudging CCAM in the ERA Interim data to obtain 50 km quasi-uniform resolution simulations - forced at its lower boundary with the bias-corrected sea-surface temperatures (SSTs) and sea-ice concentrations (SICs) from a CMIP5 GCM simulation. No atmospheric forcing from the GCM was applied. This approach avoids biases from the GCM, for example the common Pacific cold tongue bias or the overestimation of SSTs along the west coast of southern Africa, impacting on the regional simulations. The 8 km resolution runs over southern Africa were spectrally nudged within the output of the 50 km resolution global simulations following the approach of Engelbrecht et al. (2019). This approach to downscaling implies that the uncertainty range across the different downscaling's can be attributed largely to the differential SST and SIC forcing from the host GCMs (internal variability likely plays a minor role). However, whether teleconnections from say changes in ENSO attributes, or changes in regional SSTs drive the projected changes in regional climate, is not trivial to determine and beyond the scope of the analysis presented here. For a more detailed description of the features and advantages of this downscaling methodology, see Engelbrecht et al. (2015).

A second set of CCAM simulations analysed here has been obtained by downscaling the projections of future climate change of 6 CMIP5 GCMs under a low mitigation scenario, Representative Concentration Pathway 8.5 (RCP8.5), for the period 1961-2100. The GCM simulations were first downscaled to 50 km resolution globally (Archer et al., 2018) and subsequently to 8 km resolution over southern Africa. The 6 GCMs downscaled are the Australian Community Climate and Earth System Simulator (ACCESS1-0); the Geophysical Fluid Dynamics Laboratory Coupled Model (GFDL-CM3); the National Centre for Meteorological Research Coupled Global Climate Model, version 5 (CNRM-CM5); the Max Planck Institute Coupled Earth System Model (MPI-ESM-LR); the Norwegian Earth System Model (NorESM1-M) and the Community Climate System Model (CCSM4). This set of simulations were performed as part of the Future Climate for Africa project Fractal (FRACTAL: FUTURE RESILIENCE FOR AFRICAN CITIES AND LANDS - fcfa (futureclimateafrica.org) by the Council for Scientific and Industrial Research in South Africa. The simulations were bias corrected following the methodology of Engelbrecht et al. (2015).

3 Observations

In this task, the climate models' performances were evaluated based on their present-day representation of the two main variables of interest for the case studies:

- Near-surface temperature
- Precipitation

Precipitation was evaluated against a range of datasets. This is in part due the sparsity of *in situ* observations making validation of satellite data difficult, as well as impacting the accuracy of gauge and satellite datasets. There is also another dataset available called ERA-Interim but this is neither observed nor assimilated data but is a result of a model forecast and reanalysis system (Berrisford et al., 2009). With a variety of methods available, there is bound to be variability between datasets, as shown in Figure 1. Therefore, four data sets were considered in this task as illustrated in Table 2. Near-surface temperature observations do not show such variability, and therefore one dataset was used for the validation: CRU v4 .02 (Harris, Jones, Osborn, & Lister, 2014).

Table 2 - Precipitation variables used in this study

Dataset	Method	Resolution (degrees)	Reference
CRU v4 .02	Gauge	0.5°	Harris et al., 2014
GPCC	Gauge	0.5°	Schneider et al., 2011
GPCP	Gauge & satellite	1°	Huffman et al., 2009
CHIRPS	Gauge & satellite	0.25°	Funk et al., 2015
DCCMS	Gauge	0.5°	http://www.metmalawi.gov.mw/dccms_station.php

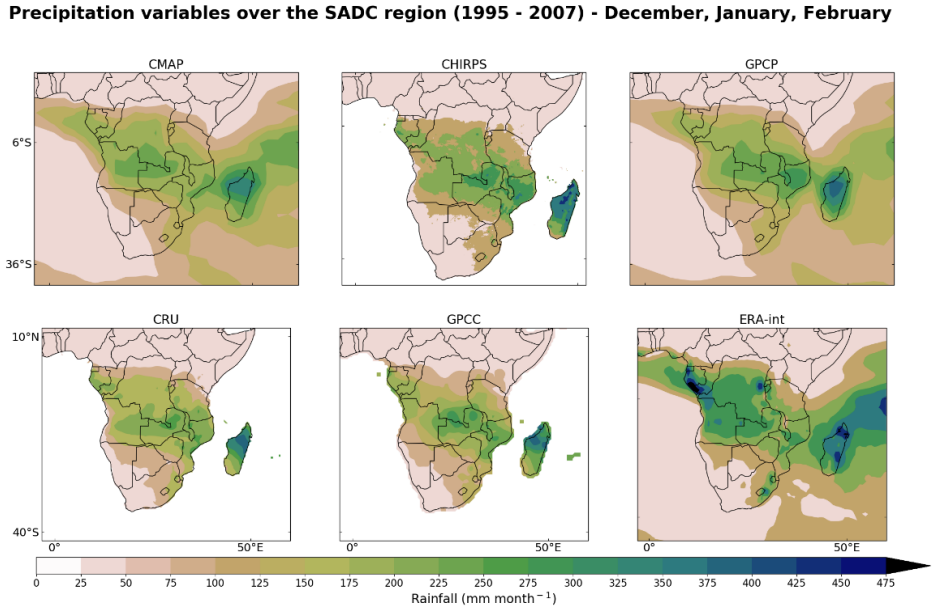

Figure 1 - Examples of the mean precipitation data sources available over SADC. Both CMAP and ERA-Interim were not used in this project.

4 Analysis methodology

4.1 Regions

Africa has a complex and varied climate with numerous climatic zones, which makes defining reference regions a challenge. For this task, SADC was divided into four zones by adapting the climate reference regions defined by IPCC (Iturbide et al., 2020) as shown in **Error! Reference source not found.**. The South Eastern-Africa (SEAF; Zone 1) region was kept unmodified but the amendments concern:

- Reduction of the West Southern-Africa (WSAF; Zone 4) region to focus primarily on South Africa.
- Division of the East Southern-Africa (ESAF) with one zone for eastern South Africa (Zone 2) and another for central East Africa (Zone 3).

These modifications were made to better represent the countries of interest within the FOCUS-Africa project.

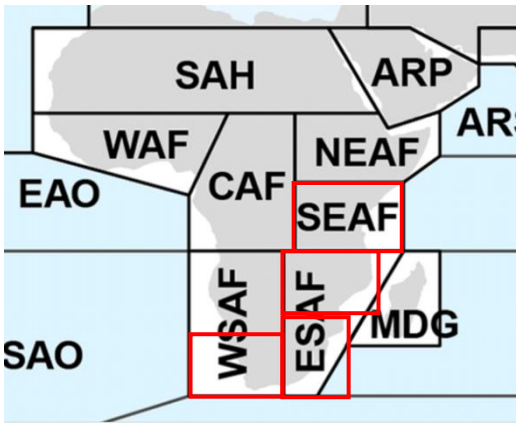

Figure 2 - Adaptation of the updated IPCC climate reference regions for both land (grey shading) and ocean (blue shading) (Iturbide et al., 2020). The modified regions used in this task are highlighted in red.

4.2 Simulations' time periods

As CP4A simulations only cover 10-year time slices (1997-2006, 2095-2105), all other models were also reduced to similar 10-year time slices (1995–2005, 2090-2100). This allows us comparing consistently the models' bias across the four zones. The slightly differing time periods above are due to data availability, with CORDEX and CMIP5 data sets both ending in 2005. Therefore, averages over these 10 years were used to provide a 'start of century' and 'end of century' representation of the climate. The five-year discrepancy between CP4A and the other models is not expected to cause any issues in the historical period due to the contribution of natural variability being comparable to climate change. The same cannot be said for the future time-slice and, hence, this is considered in the analysis of the results. These results will indeed show where the projected changes are not statistically significant given natural variability and the 10-year sample size, and a threshold of $p < 0.5$ for a two-sided t-test.

4.3 Emission scenarios considered

In this task, the predominant emission scenario used is RCP8.5. This assumes that greenhouse gases emissions will continue to rise and, thus, it gives us a worst-case scenario depiction of the future climate. This emission pathway was used for all the models except CMIP6. CMIP6 uses the latest emission scenarios which represent different future shared socio-economic pathways (SSP). These vary depending on socio-economic projection and political environments, in addition to the greenhouse gas concentrations and mitigation pathways. This task focused on two of the latest scenarios SSP5-8.5 and SSP2-4.5. The SSP5-8.5 scenario is based on a future with low socioeconomic challenges to adaptation and high socio-economic challenges to mitigation (O'Neill et al., 2016), alongside the high greenhouse gas emissions of RCP8.5. SSP2-4.5 represents a future with little shift

from historical patterns and development, growth continues albeit unevenly, and uses the RCP4.5 concentration pathway. It is also worth noting that there are discrepancies between the forcing's used in CMIP and those used in CP4A. The key difference here is in the absence of anomalous aerosols in CP4A's forcing, leading to an increased warming in CP4A compared to its driving model.

5 Evaluation of Historical Climate Simulations

In this section, a basic analysis of the models listed in section 2 is undertaken by investigating their ability to quantitively and spatially represent temperature and precipitation over the historical time. Firstly, we analyse annual rainfall and temperature for SADC using CMIP5, a CORDEX subset and CP4A including their spatial representations (Sections 5.1 and 5.2). Secondly, we examine the CMIP6 ensemble (Section 5.3) and CCAM downscaled simulations over SADC (Section 5.4). Section 5.5 summarises the results of this evaluation.

5.1 Annual cycles

5.1.1 Zone 1 – SEAF (South Eastern-Africa)

For precipitation in SEAF, most of the models show conformity with observations through DJF and JJA, however, it is in the transitional months of MAM and SON, that discrepancies arise (Figure 3). HadGEM2-ES is a good example of this, underestimating rainfall by 75 – 80 mm in March and April and overestimating in SON. The subset of CORDEX models driven by HadGEM2-ES follow the pattern of their driving model, with similar precipitation values throughout the year. However, these show marked improvements in SON, with values closer to observations than HadGEM2-ES. CP4A consistently overestimates rainfall throughout the year when compared to observations, particularly in April where it exceeds observations by roughly 75 mm. However, it does manage to correctly identify April as the wettest month and does follow monthly trends better than the CORDEX sub-set.

Temperature is better represented in the models, with most being within ± 1.5 ^{o}C of observations (Figure 3). The large spread in CMIP5 data is caused predominantly by one model, incm4, which has a very cold bias. HadGEM2-ES has a lower annual fluctuation in temperature, underestimating temperatures in summer, and overestimating in winter, but It does manage to replicate temperature well through the start of the year (February – April). CP4A is very similar to HadGEM2-ES throughout the year, with a slightly warmer bias leading to slight improvements in December/January. Both REMO2015 and RegCM4-7 have higher temperatures than their driving model, improving their performance through SON, but enhancing the overestimation made by their driving model between March to August. CCLM5-0-15 is the opposite, with a general reduction in temperature compared to HadGEM2-ES, improving its performance through the colder month (March – August), but enhancing the cold bias during the warmer seasons.

5.1.2 Zone 2 – Upper ESAF (Eastern Southern-Africa)

Precipitation in this region peaks in DJF (Figure 4), with observations of 200 – 250 mm a month, and minimal rain through the dry cooler months (May – September). This is emulated well by HadGEM2-ES through the start of the year, with results very close to observations. HadGEM2-ES does overestimate precipitation slightly through October, November, and December, but not drastically. CP4A continues to overestimate rainfall, particularly in the wetter months, but does well through the drier seasons. This is also the case for RegCM4-7, which has higher precipitation than HadGEM2-ES and observations through most of the year. REMO has reduced precipitation when compared to

HadGEM2-ES during the wettest season (DJF), which makes it conform better with observations. This changes through the drier months with more rain than its driving model, leading to an overestimation like RegCM4-7. CCLM5-0-15 has lower precipitation than HadGEM2-ES year-round and is the driest model tested during March (~ 100 mm below observations and HadGEM2-ES). This drier bias is detrimental through the start of the year where the driving model performed well compared to observations, however, it does improve on HadGEM2-ES's wetter bias through the second half of the year, with CCLM5-0-15 falling between observed ranges through JJASON.

The model's representation of temperature (Figure 4) follows a similar pattern to that seen in zone 1 (Figure 3), with HadGEM2-ES underestimating warm seasons, however, it does replicate temperature well in the summer months. CCLM5-0-15 is warmer than HadGEM2-ES through the start of the year, unlike in Zone 1, however, it is colder than HadGEM2-ES from May – December, and as a result becomes colder than observed temperatures. Both REMO2015 and RegCM4-7 have a warmer bias than their driving model through the year, with temperatures slightly higher than HadGEM2-ES. CP4A has the lowest annual range of the higher resolution models but follows HadGEM2-ES's general pattern well. The colder bias is in SOND in CP4A, moving it further away from observations when compared to HadGEM2-ES.

5.1.3 Zone 3 - Lower ESAF

Observed precipitation in this region shows low variability between the data sets through the wetter months (October – March) (Figure 5), with a larger range through the drier portion of the year. HadGEM2-ES follows observed precipitation values well in this region, except for October, November, and December, where it does overestimate. RegCM4-7, REMO2015 are wetter than HadGEM2-ES throughout the year, leading to the overestimating rainfall year-round. As seen before, CP4A is wetter than HadGEM2-ES during the wet seasons, but like HadGEM2-ES, falls within observations during the dry months. CCLM5-0-15 continues to show a drier bias than its driving model, and as a result falls within observed ranges for much of the year (April – December).

Temperatures are well represented by most models in this zone (Figure 5). HadGEM2-ES follows observations well, particularly through March-October. The warmer months (Nov – Feb) are underestimated slightly, but still fall within ~1.5°C. Both REMO2015 and CCLM5-0-15 have a slightly colder bias compared to their driving model and this moves their representation of temperature further away from observations when compared to HadGEM2-ES. RegCM4-7 has a warmer bias than HadGEM2-ES from May onwards, but still complies well with observations and improves accuracy in October, November, and December. Finally, CP4A has again a smaller temperature range year-round, overestimating temperature in the cold months and underestimating in warmer months.

5.1.4 Zone 4 – Western South Africa (WSAF)

This is the driest of the four regions, with observed precipitation remaining below 50 mm year-round and is represented well by most of the RCMs in the study (Figure 6). HadGEM2-ES follows observations well here, falling within the observed range for much of the year. REMO2015 and RegCM4-7 overestimate rainfall in this region during the wetter months (December – May). REMO2015 does then conform well to its driving model and as a result, follows observations well for the remainder of the year. RegCM4-7 on the other hand, has a wet bias for most of the year, overestimating rainfall most months. CCLM5-0-15, like its driving model, follows observations year-round. CP4A continues to have a wetter bias through the start and end of the year but represents rainfall well in the drier months. Temperature in this zone is again, well represented by HadGEM2-ES, with it having a slightly colder bias than observations (Figure 6). CCLM5-0-15 continues to be colder than HadGEM2-ES, underestimating temperature year-round, particularly in the colder months. CP4A follows the same trends as in previous zones, with a smaller annual range, underestimating warm months and overestimating cold months. RegCM4-7 has a much warmer bias than its driving model, being ~2°C

warmer year-round, leading to overestimation of temperature in this zone. REMO2015 also has a slight warm bias compared to its driving model, however, this corrects the colder bias of HadGEM2-ES and leads to REMO2015 following observations closely.

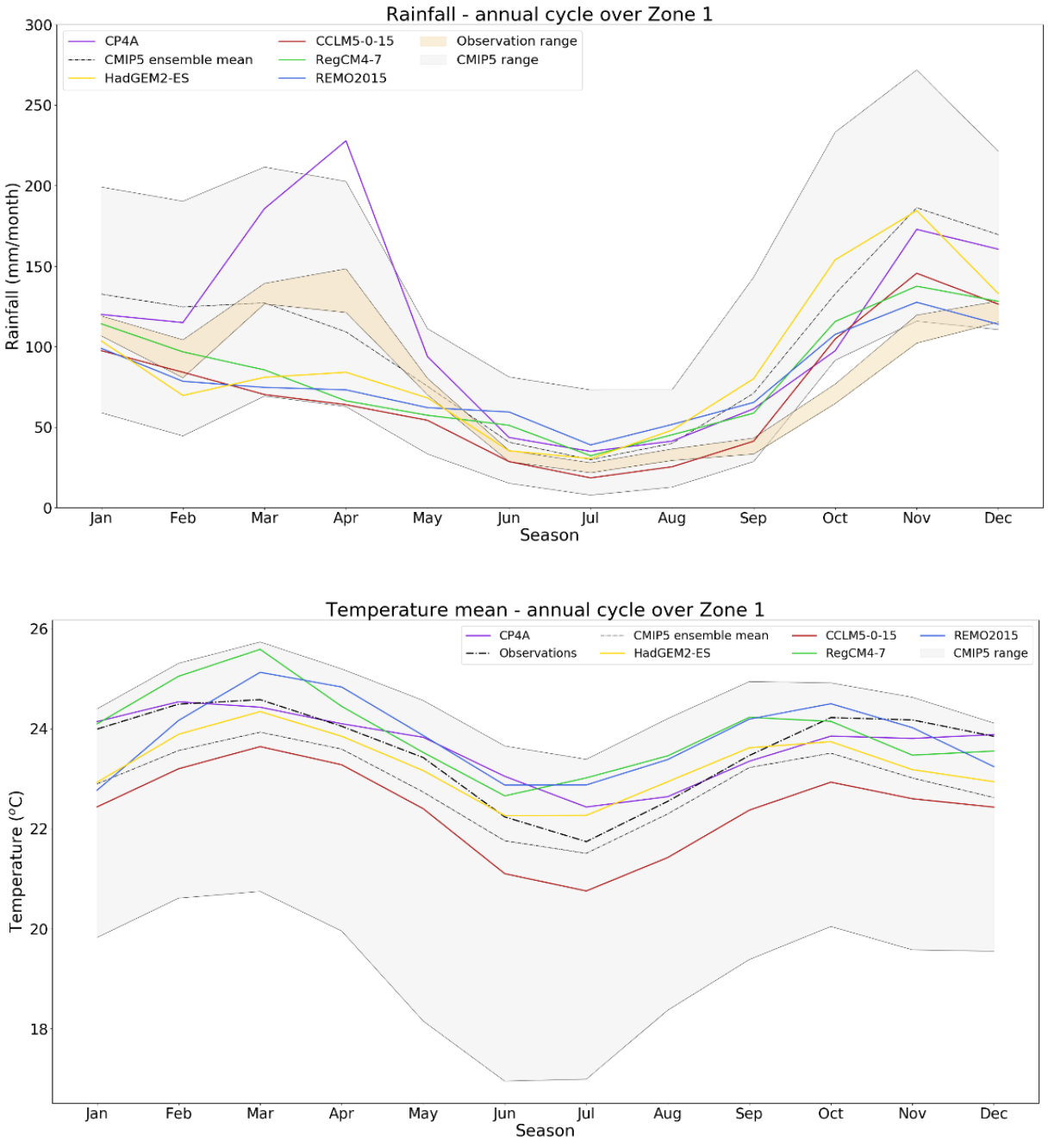

Figure 3 - Annual cycle for rainfall (top) and mean temperature (bottom) across all modes in zone 1

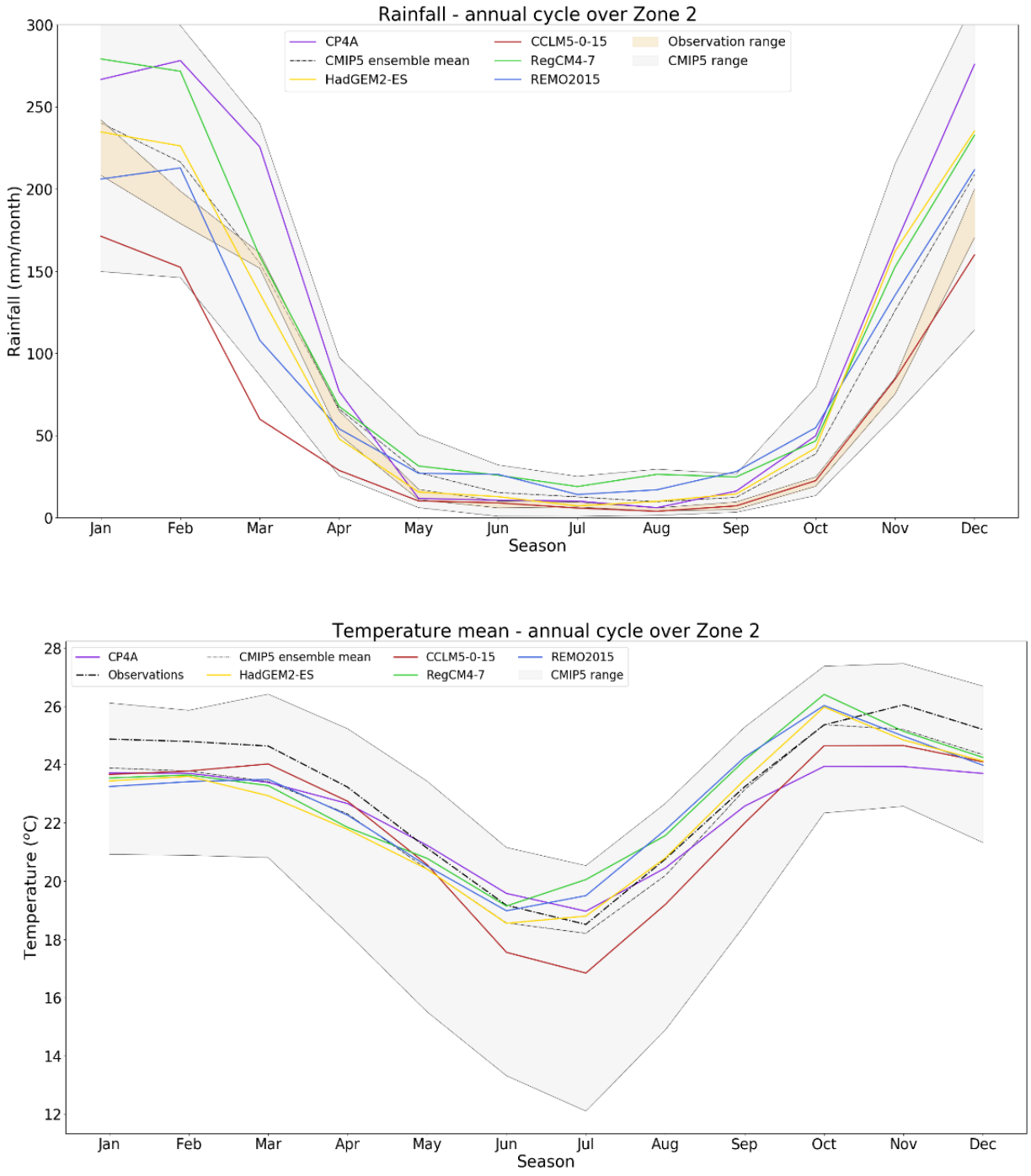

Figure 4 - Annual cycle for rainfall (top) and mean temperature (bottom) across all modes in zone 2

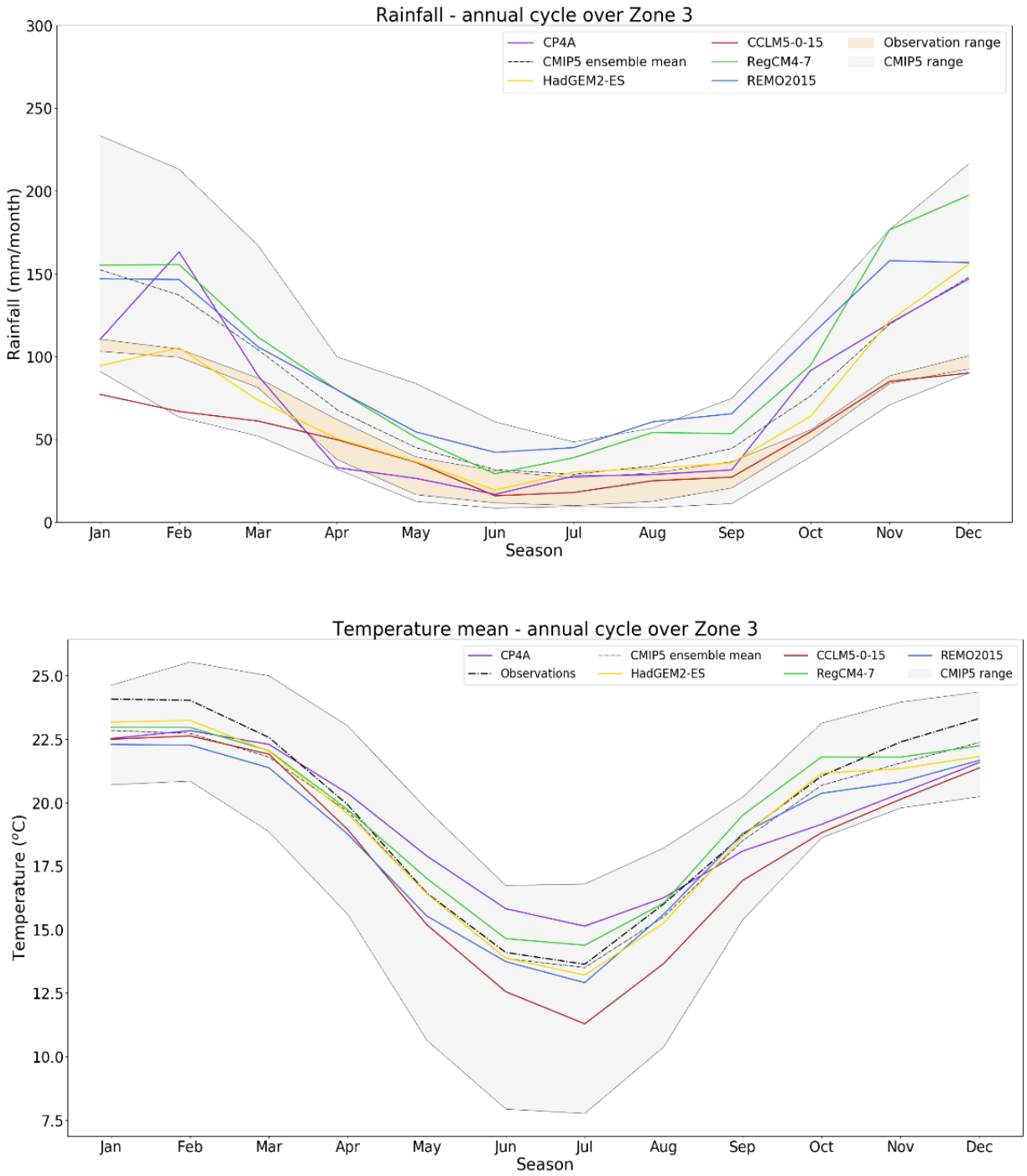

Figure 5 - Annual cycle for rainfall (top) and mean temperature (bottom) across all modes in zone 3

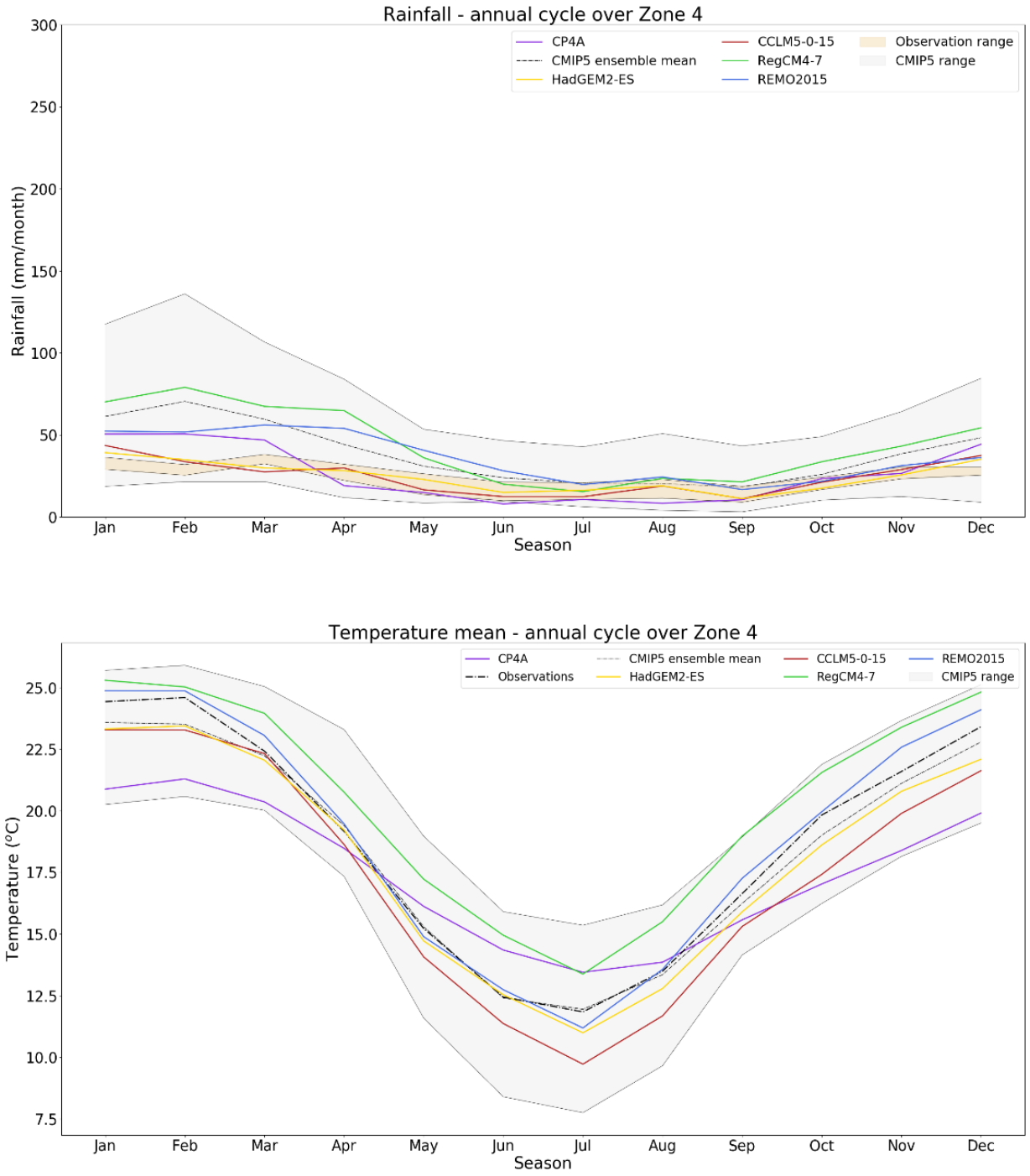

Figure 6 - Annual cycle for rainfall (top) and mean temperature (bottom) across all modes in zone 4

5.2 Spatial representation

In this section, we analyse how well the models capture observed precipitation and temperature spatial patterns over the 10-year present-day period into four seasons due to half of the regions lying in the mid-latitudes. Madagascar is not discussed in the analysis as it lies outside our focus regions and case studies.

5.2.1 DJF

In DJF, observations show a clear band of precipitation which runs through the centre of SADC (Figure 7). The highest average precipitation is in the east, along the coast and at higher elevations, and the slowly decreases towards the northwest. Some of the highest observed temperatures are also found along the east coast, as well as in Namibia and Botswana. Central Africa and higher elevations, such as in Lesotho, are the coolest regions during this period. The regional models all show the same observed rainband across SADC, although with varying levels of success (Figure 7). As seen in Figure 5, CCLM5-0-15 produces noticeably less rainfall in zone 3, particularly along the east coast of Mozambique (Figure 7), this is seen in the driving model as well, but has been amplified due to this model's drier bias. However, in the zones with lower rainfall (WSA and ESA) this model performs very well, conforming to HadGEM2-ES. RegCM4-7 and CP4A both represent the spatial structure of this rainband well much like HadGEM2-ES, however, they do have higher than observed rainfall at high elevations, which is not as prominent in HadGEM2-ES (Figure 11). Spatially, all the regional models show similar results to observations when looking at temperature. The Namibian and Angolan coast are the only exceptions, with all CORDEX models having higher temperatures that observations, which is also seen in their driving model.

5.2.2 MAM

Precipitation observations here show a clear dipole pattern, with southern countries having less precipitation (up to around 75 mm/month) when compared to the north (150 – 250 mm/month) (Figure 8). The same divide can be seen in observed temperatures, with the north of the SADC region being far warmer than the south, with temperatures around Lesotho averaging ~11-12^{o}C. The wetter bias in CP4A is evident in this season with higher precipitation in Tanzania and the coast of northern Mozambique when compared to HadGEM2-ES, which has a dry bias compared to observations in zones 1 and 2. Temperature in CP4A is spatially very similar to HadGEM2-ES, with both having a colder bias for this season. CCLM5-0-15 has a clear dry bias for this season, which is also seen in HadGEM2-ES and affects most of SADC (Figure 12). Like HadGEM2-ES, all three CORDEX models show drier conditions than observations in northeast SADC, however, both REMO2015 and RegCM4-7 have wetter conditions in the south and northwest of SADC, which is not seen in HadGEM2-ES. The three CORDEX models all have a similar spatial pattern for temperature. CCLM5-0-15 is again predominantly colder across all of regions like HadGEM2-ES. REMO2015, also has a colder bias in most zones like its driving model, however, it does have a warm bias over Tanzania, unlike HadGEM2-ES. RegCM4-7 also has a warmer bias over Tanzania, but also differs slightly from the other CORDEX models and HadGEM2-ES, with temperatures in WSA exceeding observations by 2^{o}C.

5.2.3 JJA

Observations during this season show a predominantly dry SADC (Figure 9). The north/northwest does still experience precipitation (150 - >200 mm/month), as does the east and south coast, although to a lesser extent (15 - ~75 mm/month). The spatial pattern of precipitation in this season is well represented across all models, particularly CP4A. Both REMO2015 and RegCM4-7 do have higher precipitation averages along the coastal regions, which is not seen in their driving model (Figure 13). All models also show lower levels of precipitation in and around the Western Cape which is also present in HadGEM2-ES although quite minor. Temperatures are well represented by all models compared to observations and HadGEM2-ES. CCLM5-0-15 still has a cold bias, as CP4A, across large areas of SADC, especially in the study regions. Unlike HadGEM2-ES, RegCM4-7 has a warm bias across

most of the SADC, with temperatures over 8°C warmer than observations in places. However, across the regions this study will focus on, temperatures are closer to observations (within ± 2/3°C). REMO2015 also has a warmer bias during this season compared to both HadGEM2-ES and observations.

5.2.4 SON

Observations show continued precipitation in the north / northwest, and an increase across central SADC, as well as in coastal areas (Figure 10). There is still little to no precipitation in the south east of the continent, however, precipitation in western South Africa does begin to increase particularly over higher elevations. Temperatures are lowest in South Africa (~13-19°C) and peak in the north east (~ 28°C). The key spatial characteristics of temperature observations are picked up by all the models here, much like HadGEM2-ES. Both CP4A and CCLM5-0-15 have a cold bias across most of SADC, whereas RegCM4-7 and REMO2015 are more balanced. However, there is more of a warm bias in the latter over the study region when compared to their driving model, HadGEM2-ES, observations (Figure 14). The model's representation of precipitation is also spatially like observations and HadGEM2-ES. However, most have a wet bias for this season, much like their driving model, with CCLM5-0-15 being the only exception. Both RegCM4-7 and REMO2015 have much higher rainfall over eastern South Africa compared to observations (> +100 mm/month), which is also seen in HadGEM2-ES (Figure 14). The drier bias seen in CCLM5-0-15 improves its representation of precipitation with rainfall like that of observations. Finally, although CP4A has a wet bias, it is not as prominent over the study area, reducing the wet bias of HadGEM2-ES in some region (Tanzania) but increasing it in others (Mozambique).

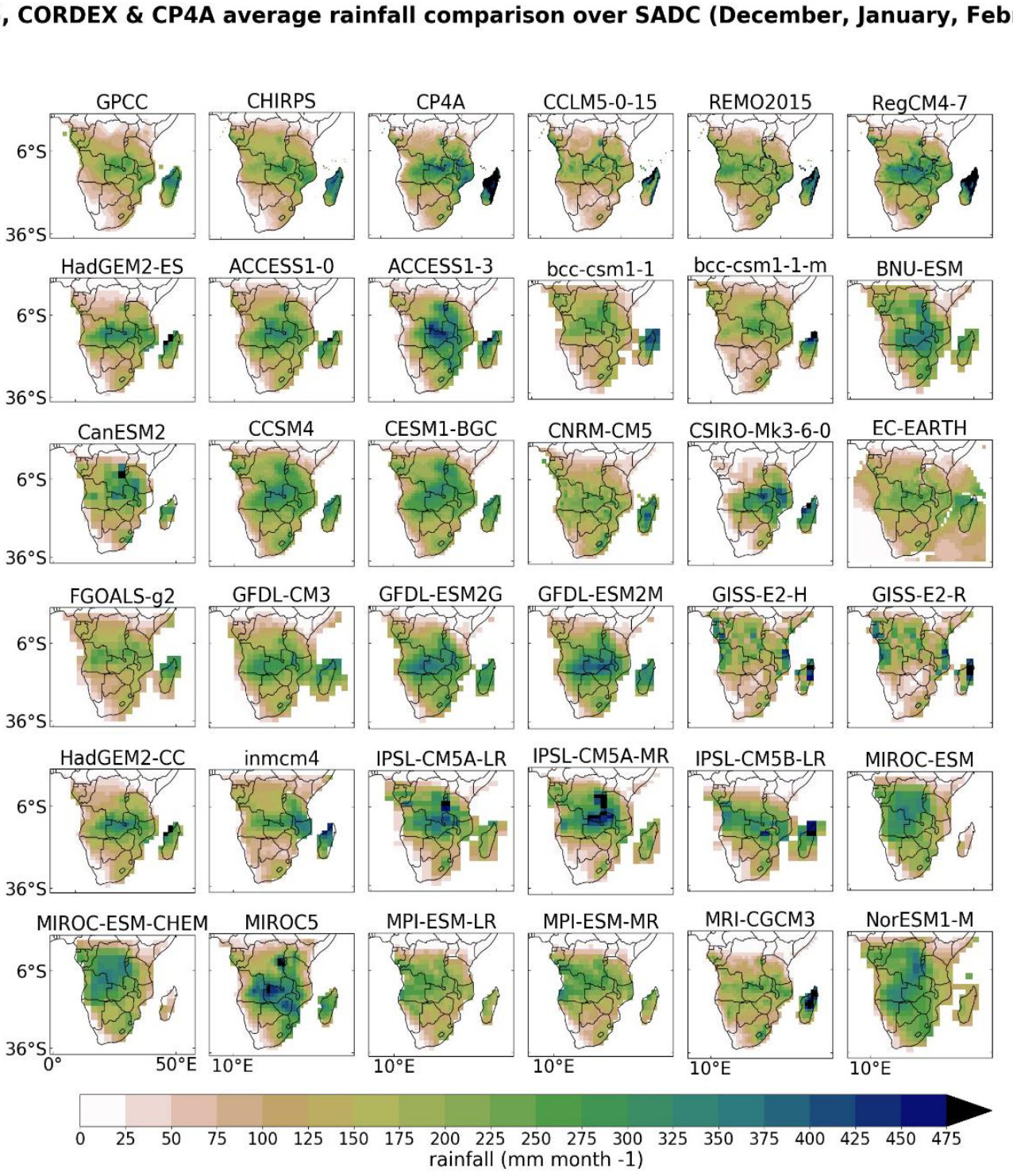

Figure 7 - Spatial representation of average rainfall for December, January, and February

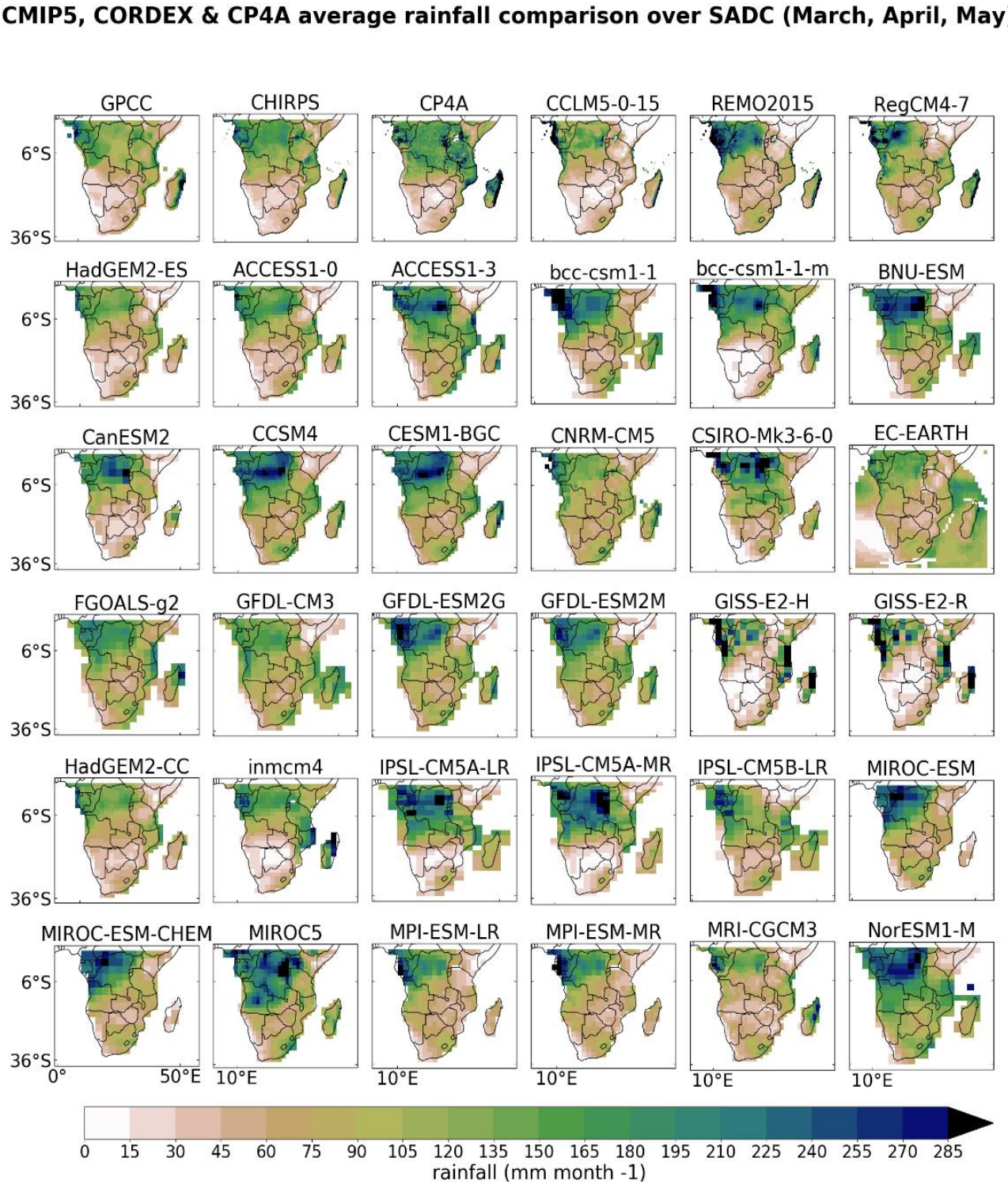

Figure 8 - Spatial representation of average rainfall for March, April, and May

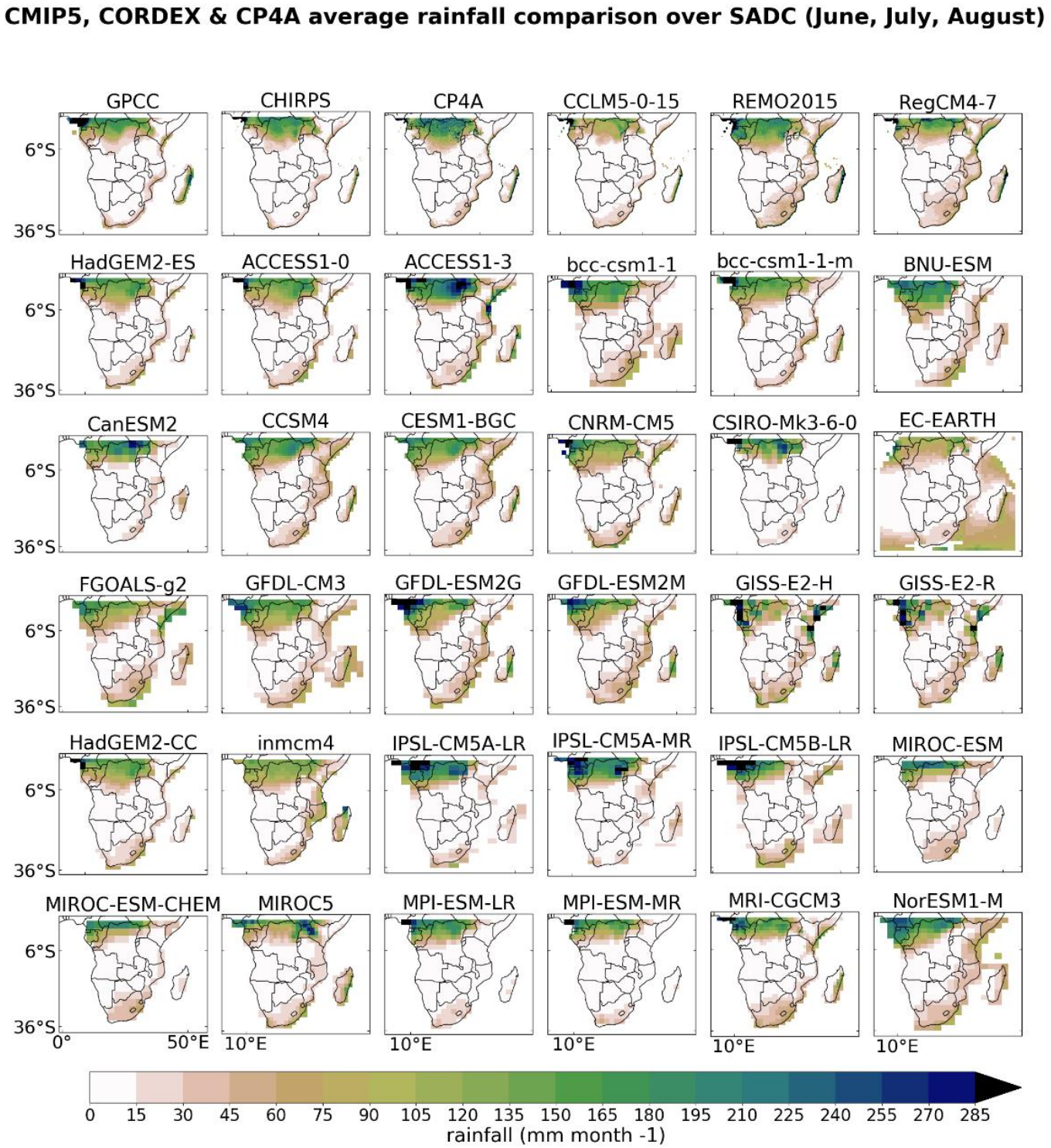

Figure 9 - Spatial representation of average rainfall for June, July, and August

CMIP5, CORDEX & CP4A average rainfall comparison over SADC (September, October, November)

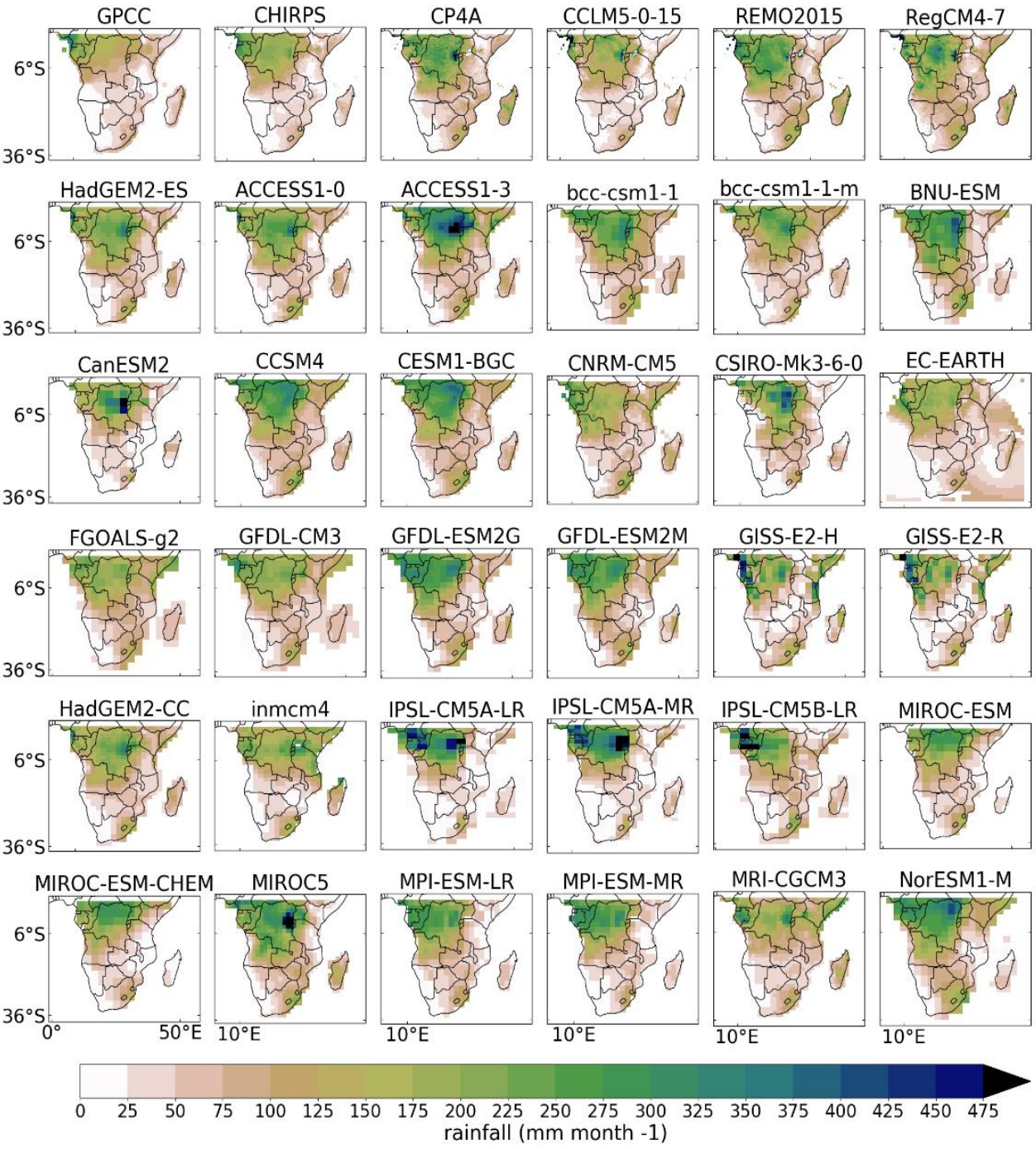

Figure 10 - Spatial representation of average rainfall for September, October, and November

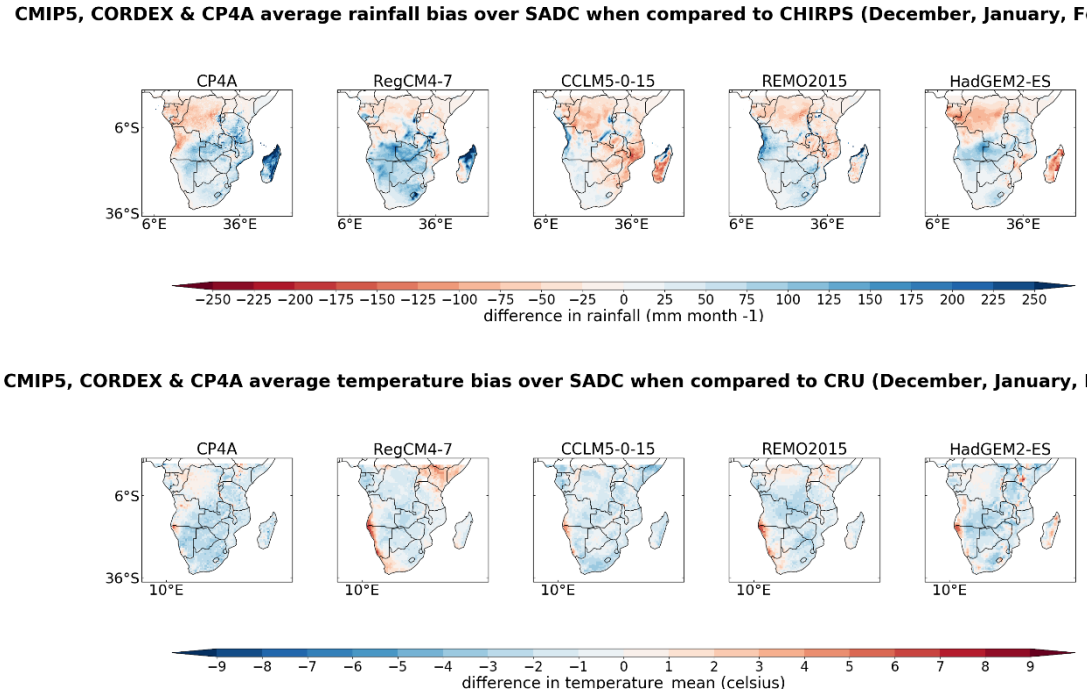

Figure 11 - Rainfall (top) and temperature (bottom) bias in December, January, and February when compared to CHIRPS

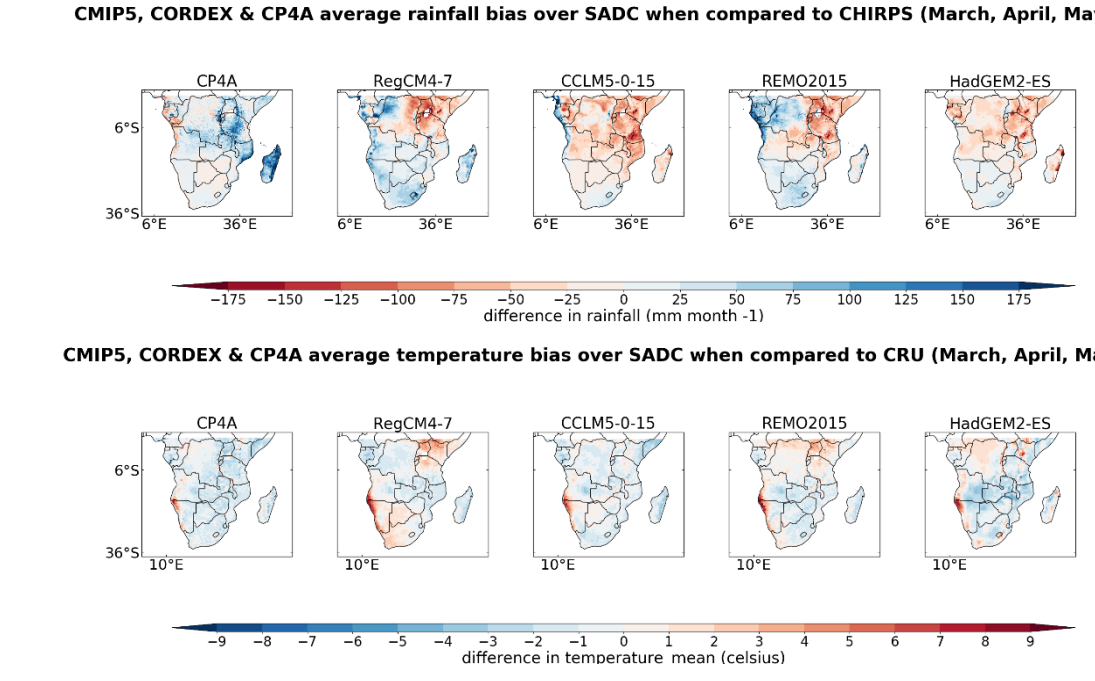

Figure 12 - Rainfall (top) and temperature (bottom) bias in March, April and May when compared to CHIRPS

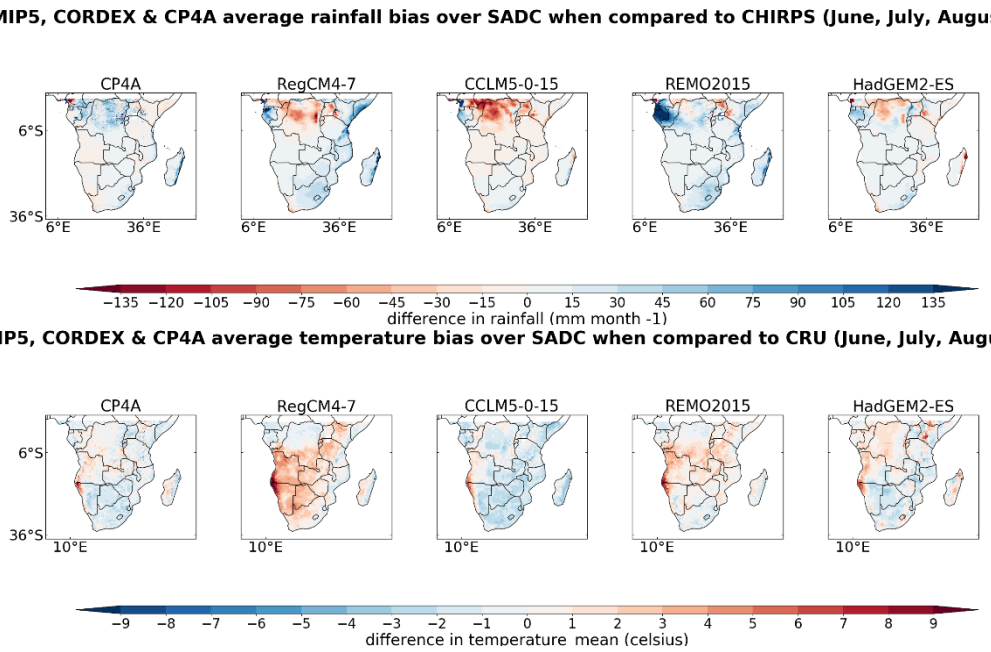

Figure 13 - Rainfall (top) and temperature (bottom) bias in June, July, and August when compared to CHIRPS

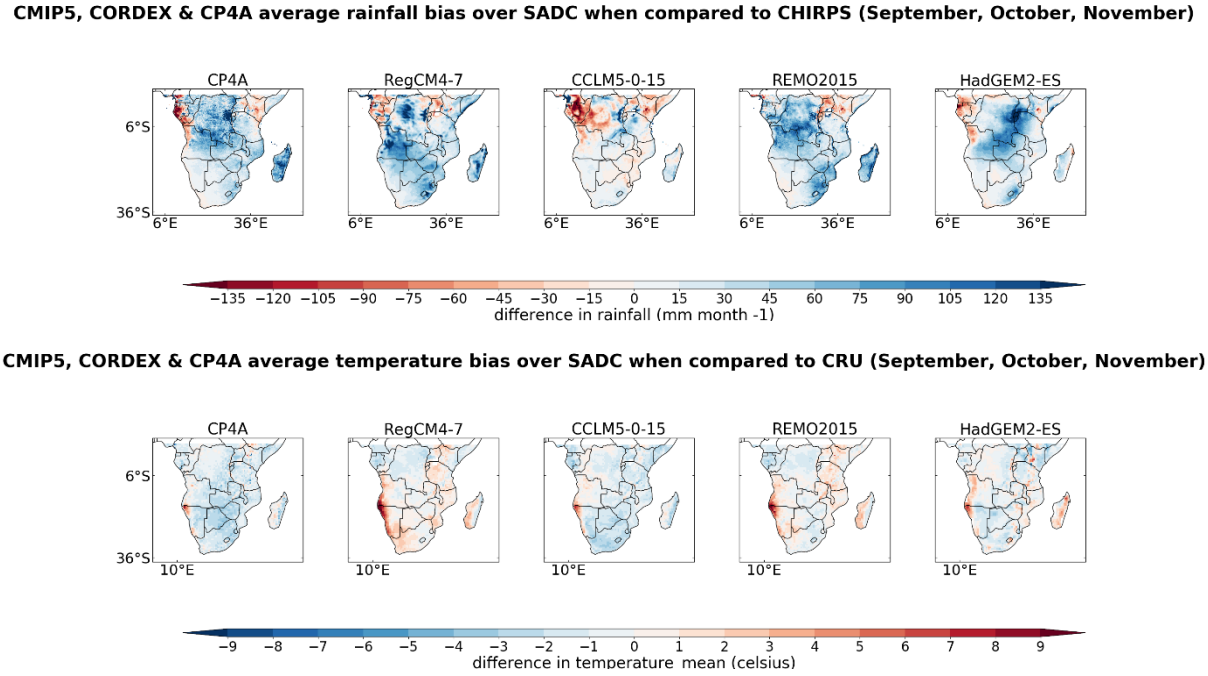

Figure 14 - Rainfall (top) and temperature (bottom) bias in September, October, and November when compared to CHIRPS

5.3 CMIP6 Spatial plots

Figure 15 (DJF) and Figure 16 (JJA) below illustrate the bias (model – observed) of the CMIP6 ensemble models relative to the CHIRPS proxy rainfall values across the region for the reference period of 1995-2005. Longer reference periods over 30 years were also tested and do not significantly affect the observed patterns.

For the DJF season, the wet season across the region, the models have quite wide-ranging biases but tend towards a wet bias across most of the region, especially across the western sections. Models of the same family show similar bias patterns (e.g., EC-EARTH family and MPI family). Both FGOALS and IITM-ESM show strong dry biases across most of the region. NorESM-LM and KACE-1-0-G have the smallest absolute biases across the area though would need to be explored further to establish their realism with respect to other measures.

For the relatively dry JJA season, biases are of course smaller. However almost all models have a wet bias over South Africa during this dry season. NorESM-LM and KACE-1-0-G continue to perform well though much less clearly given the low rainfall.

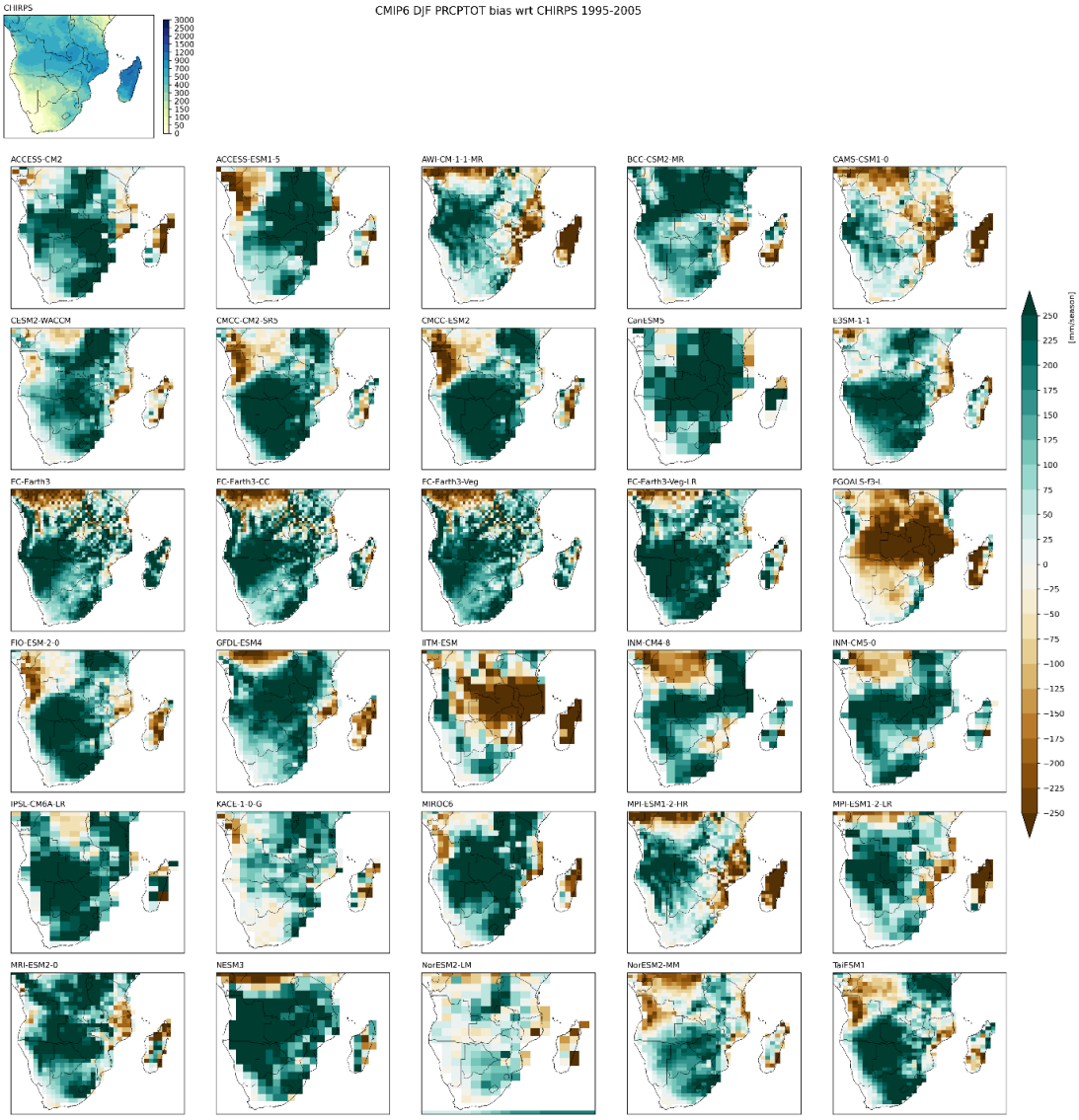

Figure 15 - CMIP6 total DJF seasonal rainfall bias (mm) relative to CHIRPS proxy observed rainfall for the period 1995-2005. CHIRPS total seasonal rainfall (mm) in upper left for reference.

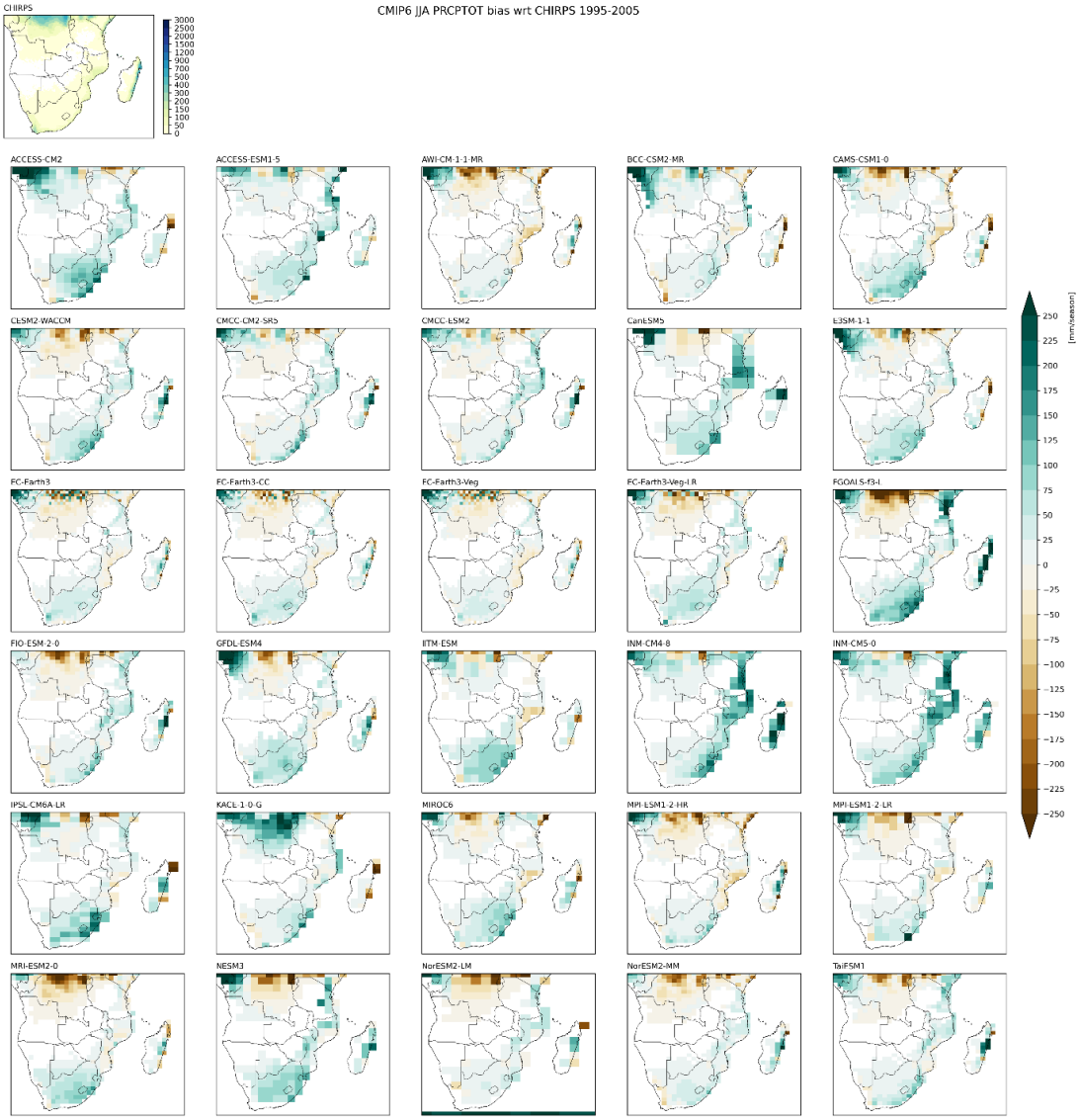

Figure 16 - CMIP6 total JJA seasonal rainfall bias (mm) relative to CHIRPS proxy observed rainfall for the period 1995-2005. CHIRPS total seasonal rainfall (mm) in upper left for reference.

Figure 17 (DJF) and Figure 18 (JJA) illustrate the absolute bias (model – observed) of the CMIP6 ensemble models relative to the CRU proxy 2m temperature values across the region for the reference period of 1995-2005. Longer reference periods were also tested and do not significantly affect the patterns.

For the warmer DJF season, almost all models exhibit a cold bias across the region except for the far western coastline where simulated ocean temperature biases related the cold boundary current may be responsible for warm biases observed across most models.

For the cooler JJA season, the cool bias is less prominent with some models exhibiting a warm bias across the region, though again strongest along the western coastal regions. The cool DJF bias and warmer JJA bias exhibited by many models suggests a suppressed seasonal cycle.

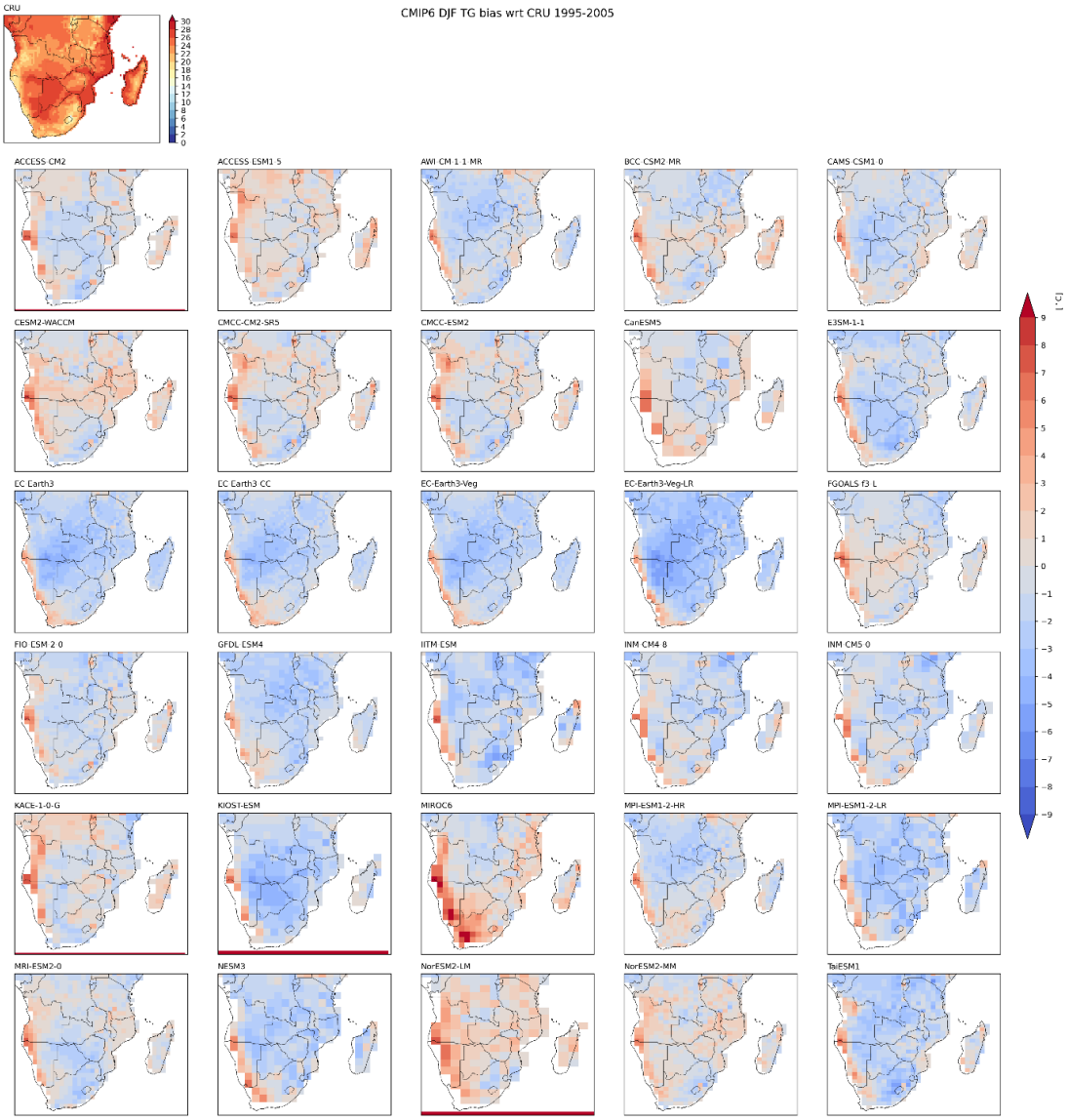

Figure 17 - Absolute mean temperature bias (C) for the DJF season for CMIP6 ensemble members relative to CRU proxy temperature values for the 1995-2005 reference period.

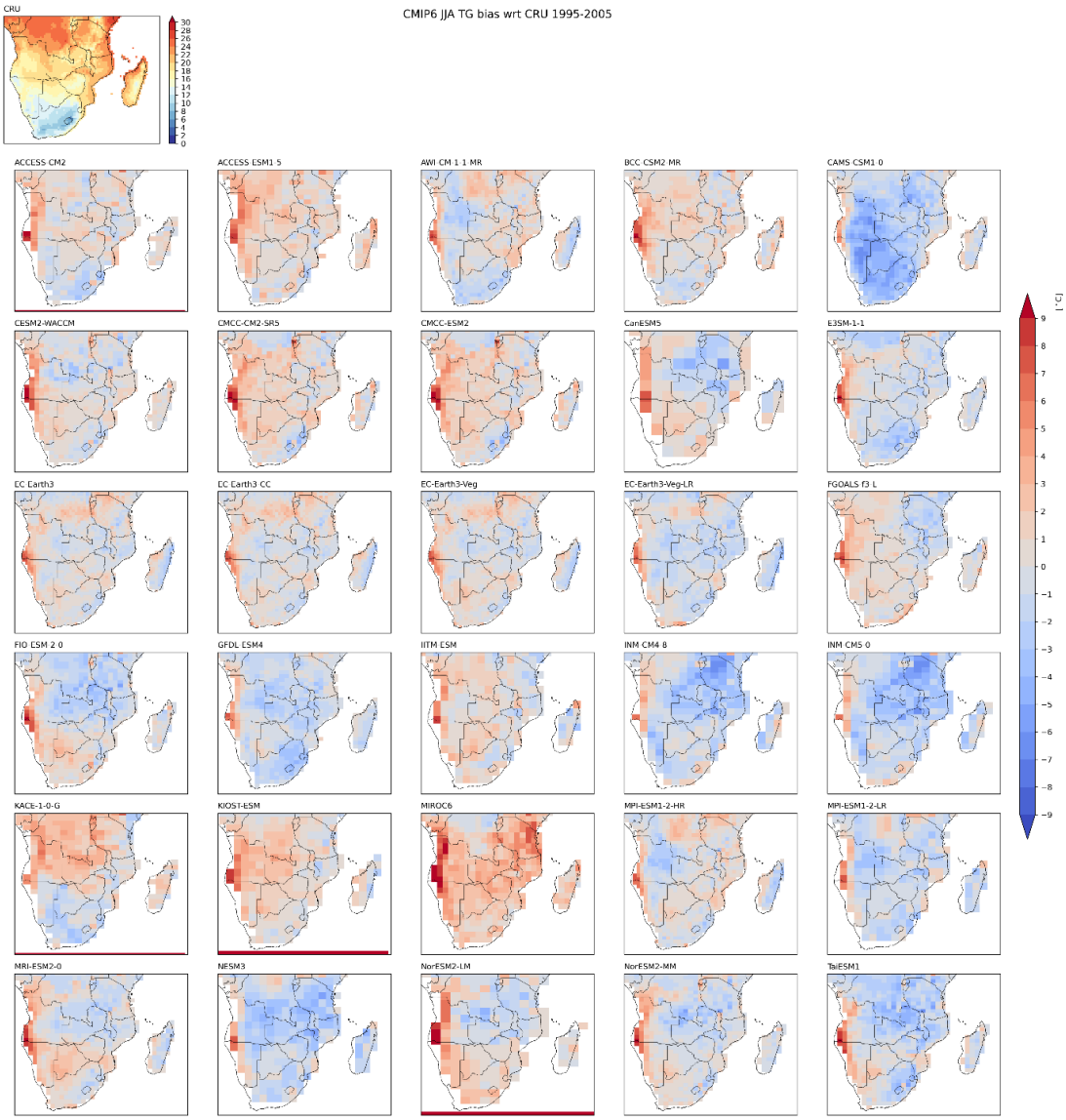

Figure 18 - Absolute mean temperature bias (C) for the JJA season for CMIP6 ensemble members relative to CRU proxy temperature values for the 1995-2005 reference period.

5.4 CCAM spatial representation of present-day climate over Southern Africa

At 8 km resolution, CCAM covers the Lower WSAF and ESAF regions. The topographically influenced spatial features of rainfall and temperature (Figure 19, top) are resolved in substantially more detail than in the CORDEX RCMs and CMIP5 and CMIP6 GCMs. For example, the annual rainfall total maxima along the eastern escarpment that stretch northward into the Limpopo Province of South Africa are clearly discernible in the 8 km resolution CCAM simulations. Similarly, the model simulations represent well the rainfall maxima over the Cape Fold mountains in the Western Cape Province in South Africa. Average temperature maxima such as those in the Orange and Limpopo river valleys are also clearly discernible in the simulations, and so are the effects of lapse rates along the steep eastern escarpment. The model has a general wet bias, which peaks over the eastern escarpment (Figure 19, bottom). An exception is the underestimation of rainfall totals over the Cape Fold mountains in the winter rainfall region. The model has a general cold bias, the exception being the Namibian coast, where temperatures are overestimated (Figure 19, bottom).

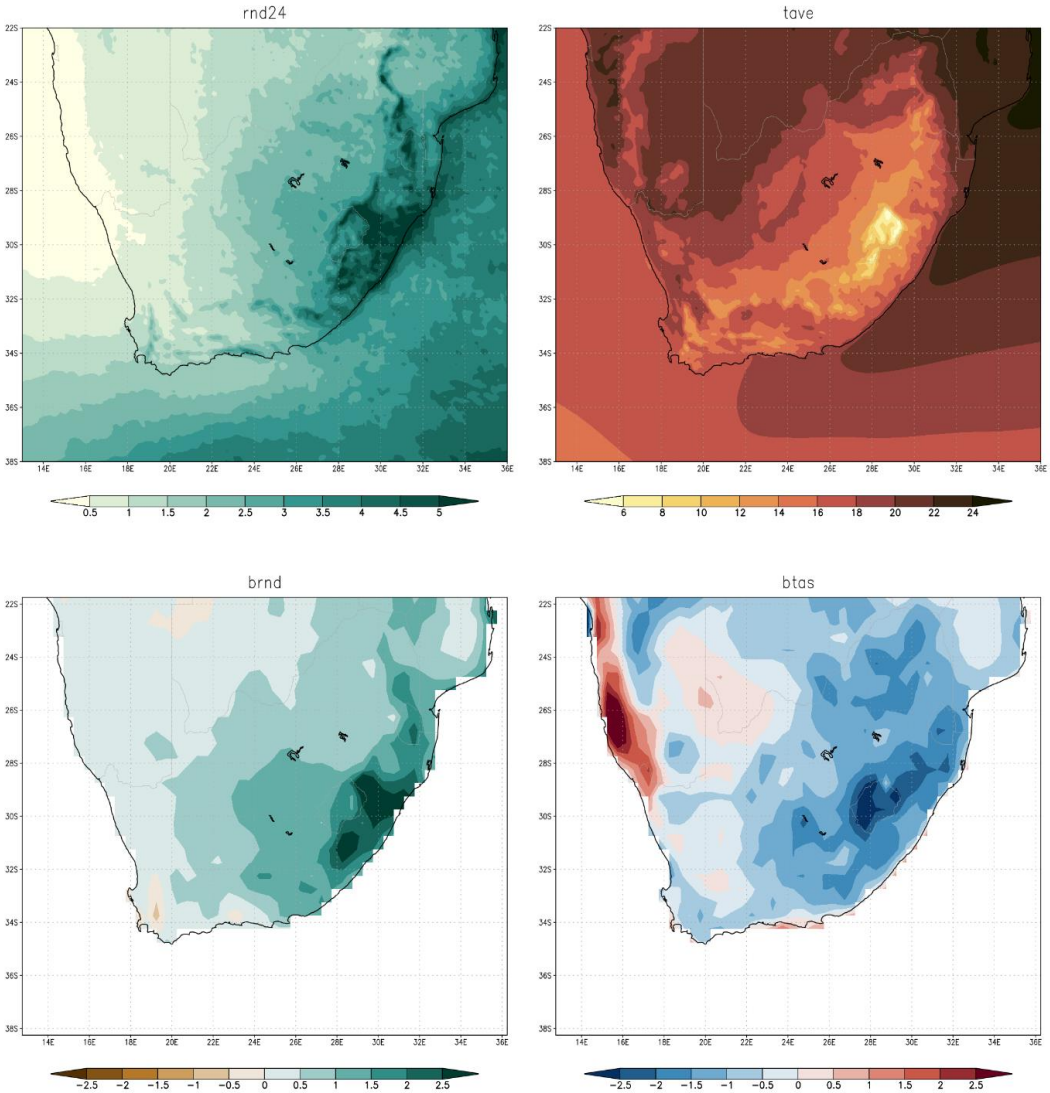

Figure 19 - CCAM downscaling (8 km resolution in the horizontal) of ERA reanalysis simulations, of annual rainfall totals (mm/day; top-left) and annual average temperature (°C; top right) over southern Africa for the time-slab 1995-2005 and corresponding biases (bottom)

The model realistically portrays the march of seasonal rainfall across southern Africa (Figure 20, top), but displays a wet bias across all seasons (Figure 20, bottom). The bias is largest over the eastern escarpment areas in summer (December to February). Winter rainfall totals are underestimated over the Cape Fold mountains in the Western Cape Province. The model realistically portrays the differential temperatures between winter and summer across southern Africa (Figure 21, top). The model's general cold bias is present across all seasons (Figure 21, bottom). An exception is the Namibian coast, where temperatures are persistently overestimated, as well as the Kalahari in Botswana, where temperatures are overestimated in autumn, winter, and spring.

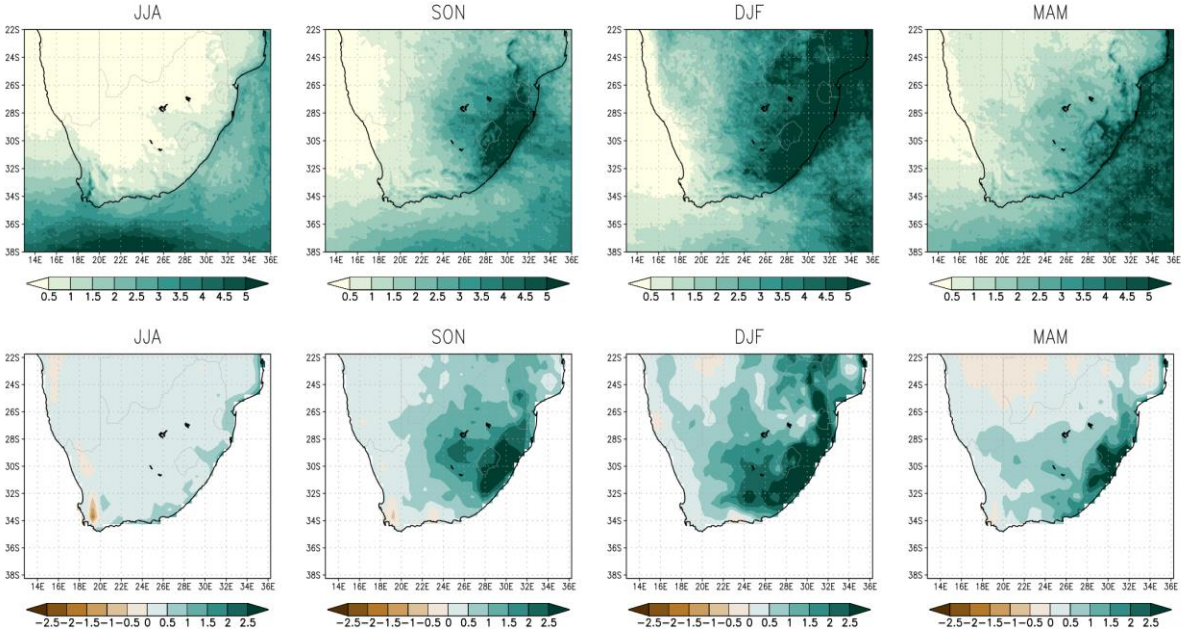

Figure 20 - CCAM downscalings (8 km resolution in the horizontal) of ERA reanalysis simulations, of seasonal rainfall totals (mm/day; top) and corresponding biases (mm/day, bottom) as calculated with respect to CRU TS4.02 data.

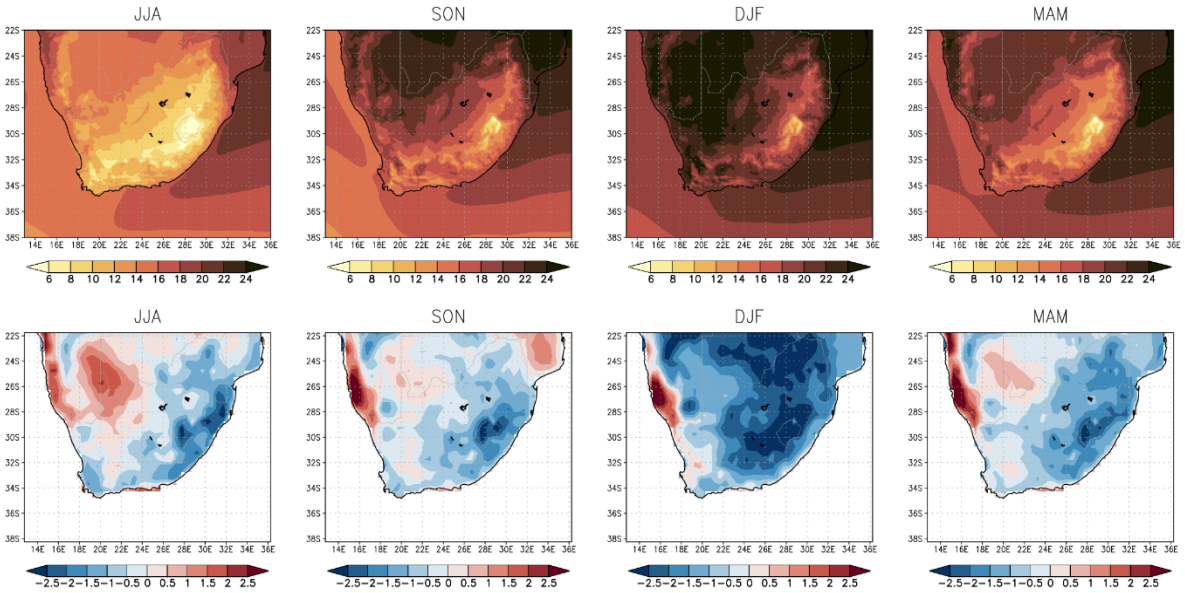

Figure 21 - CCAM downscalings (8 km resolution in the horizontal) of ERA reanalysis simulations, of seasonal average temperature (°C; top) and corresponding biases (°C, bottom) as calculated with respect to CRU TS4.02 data.

5.5 Summary

From the historical period performance assessment, there is no reason to exclude any of the models in our investigation of the future climate projections over SADC. The RCMs represent quite well precipitation and temperature spatially, improving in general the GCMs simulations especially in terms of rainfall, although there are variations in their simulated local features as described in Table 2 below.

Table 3 - Summary of all models' performance for the historical time period

Models' performance against observations	Temperature	Rainfall
CMIP5	Ensemble mean is close to observed temperatures across all regions. Only incm4 has a much colder bias than the other models	The ensemble mean follows observations well with a slight wet bias in most zones and a range of around 150mm in the first 3 zones. HadGEM2-ES is one of the best performing models here.
CMIP6	There is a cold bias across most of SADC during the warm season (DJF), with the west coast being the only acceptation to this. JJA has a reduced cold bias and more variable results. These results could suggest a muted seasonal cycle across CMIP6.	Wet seasons rainfall is variable across all models although there tends to be more of a wet bias across the models. The bias is smaller in the drier months (JJA), with South Africa being particularly wetter than the observations in most models
CORDEX (subset)	Both REMO2015 and RegCM4-7 have a warmer bias compared to observations while CCLM5-0-15 has a cold bias. The spatial representation of temperature is good across all models.	REMO2015 and RegCM4-7 both have a wetter bias compared to observations. CCLM5-0-15 on the other hand has a drier bias compared to its driving model, which leads to it falling within observer rainfall ranges between April and September. However, it does underestimate rainfall for the remaining months.
CP4A	CP4A's spatial representation of temperature is good although it does have a slightly colder bias when compared to observations.	The spatial patten of rain are well simulated except in areas with large amount of rainfall where it is strongly overestimated.
CCAM	This model has a cold bias over much of Southern Africa, with Botswana and the Namibian coast being among the only exceptions.	This model has a wet bias which peaks in the eastern escarpment. However, there is a dry bias across the Cape Fold Mountains.

6 Future climate projections

For analysing the future projections, we adopt the same structure as in Section 5. First, we analyse the spatial projections from CMIP5, the CORDEX sub-set, CP4A (Sections 6.1-6.4) and CMIP6 (Section 6.5) for 2090-2099 under RCP8.5. Secondly, we make use of plume plots to compare the projections from all CMIP5-6 and CORDEX models (Section 6.6). This gives a comprehensive overview of the projections from most of the models. Finally, the CCAM projections are analysed providing further insight of climate changes over the SADC region at high spatial resolution (Section 6.7).

6.1 DJF

December, January, and February were the wettest months in the present-day climate (Figure 7) and now exhibit some of the largest changes in rainfall under RCP8.5 (Figure 22). The projections vary between the GCMs, with some showing little change to rainfall (FGOALS-g2, inmcm4 and EC-EARTH) and others showing more dramatic changes (ACCESS1-3, MIROC-ESM and GFDL-CM3). It also illustrates the expected first-order pattern of climate change, with the wetter regions getting wetter (particularly in the west) and reduced rainfall in the drier regions such as Namibia and western South Africa. The three CORDEX models all show similar trends, with a key feature being the reduction in rainfall by around 80 mm on the east coast, as seen in the driving model (HadGEM2-ES). CP4A does also show a similar although less spread and less significant reduction in the same region. Projections for temperature all show a relatively uniform increase of around 4-7^{o}C in the regional models across the continent, as seen in the driving model (Figure 23). CCLM5-0-15 projects the smallest increase (4-6^{o}C) and CP4A the largest, with the greatest increase seen on the South Africa – Botswana border (7^{o}C).

6.2 MAM

In March, April, and May, most GCMs agree that the Western Cape will get drier and regions in the northern SADC will get wetter (Figure 24). However, the rest of the continent is more varied. Roughly half of the GCM in the ensemble show a reduction in rain through the southern SADC (from Zambia down) with the rest showing increases. The severity of the change is also diverse, for example, GFDL-ESM2G has both increases and decreases in rainfall up to and exceeding 100 mm/month, whereas models such as EC-EARTH and HadGEM2-ES show much smaller changes (-30 - ~+20 mm/month). The regional models all agree that a majority of southern SADC will become drier in these months as in HadGEM2-ES. There is some disagreement in northern SADC where CP4A shows a strong decrease in rainfall on the west coast with an increase in precipitation on the east. However, this is seen to some degree in HadGEM2-ES. RegCM4-7 shows the closest resemblance to HadGEM2-ES spatially, just with more extreme changes in precipitation. RegCM4-7 and CCLM5-0-15 differ the most from the driving model, with a large area of the Congo and the Demographic republic of Congo (DRC) seeing a decrease in rainfall, whereas HadGEM2-ES predicts an increase. However, in our region of focus, these models perform much better and replicate HadGEM2-ES's predicated changes well.

As expected, all models see some increase in temperature, with the highest most commonly in the south west of the continent where some models project increases in temperature of +10^{o}C (Figure 25). GCMs vary again in their projections with roughly half showing increases of between 1-3^{o}C and the rest ranging from 4-10^{o}C. The regional models all project similar changes in temperature although CP4A shows a consistently higher increase across the continent. All show the highest increase to be around Namibia and Angola, like their driving model.

6.3 JJA

In June, July and August, rainfall decreases across most of the continent in most models (MPI-ESM-MR, inmcm4 and CESM1-BGC being some of the exceptions) (Figure 26). Most of the disparity between projections occurs in the northern SADC region. Here, some models indicate an increase in rainfall by

up to 70 mm/month (MPI-ESM-MR) while others project a strong decrease (bcc-csm1-1-m). The regional models also differ from each other. HadGEM2-ES predicts a decrease in precipitation across SADC, particularly along the east coast, with small increases scattered though the northern reaches of SADC. This pattern is reproduced by RegCM4-7 and CCLM5-0-15 with differing intensities. REMO2015 also predicts a decrease across a majority of SADC but differs from its driving model with increased rainfall on the north east coast (Figure 26), but this does not affect our focus regions. CP4A differs from all the other RCMs, being the only model to suggest an increase in rainfall through much of the north / north-east SADC. However, like REMO2015, it still generally complies with HadGEM2-ES. Temperature in HadGEM2-ES is predicted to increase most in western SADC, which is also seen in the RCMs and CP4A. REMO2015, RegCM4-7 and CP4A all predict a more extreme increase in temperature in South Africa when compared to HadGEM2-ES, particularly in lower ESAF (Zone 3) (Figure 27).

6.4 SON

For the remaining months, most models agree that precipitation in central and southern SADC will decrease to some degree, with higher elevations potentially being an exception (Figure 28). A substantial proportion the models also agree that north SADC will see an increase in rainfall through these months by up to 100 mm/month. HadGEM2-ES is an exception to this, with most of SADC predicted to see a decrease in rainfall, and minor increases in northern countries and South Africa. This is replicated in the CORDEX subset, with these models having a similar output to their driving model. CP4A does not manage to replicate that of HadGEM2-ES in this season, with northern SADC predicted to see an increase in rainfall, affecting Zones 1 and 2. On the other hand, it does replicate the decreased rainfall over parts of Mozambique and the general patterns for South Africa. Temperatures are again consistent and similar changes are observed to those seen in previous months (Figure 29), with all RCMs and CP4A showing comparable results to HadGEM2-ES.

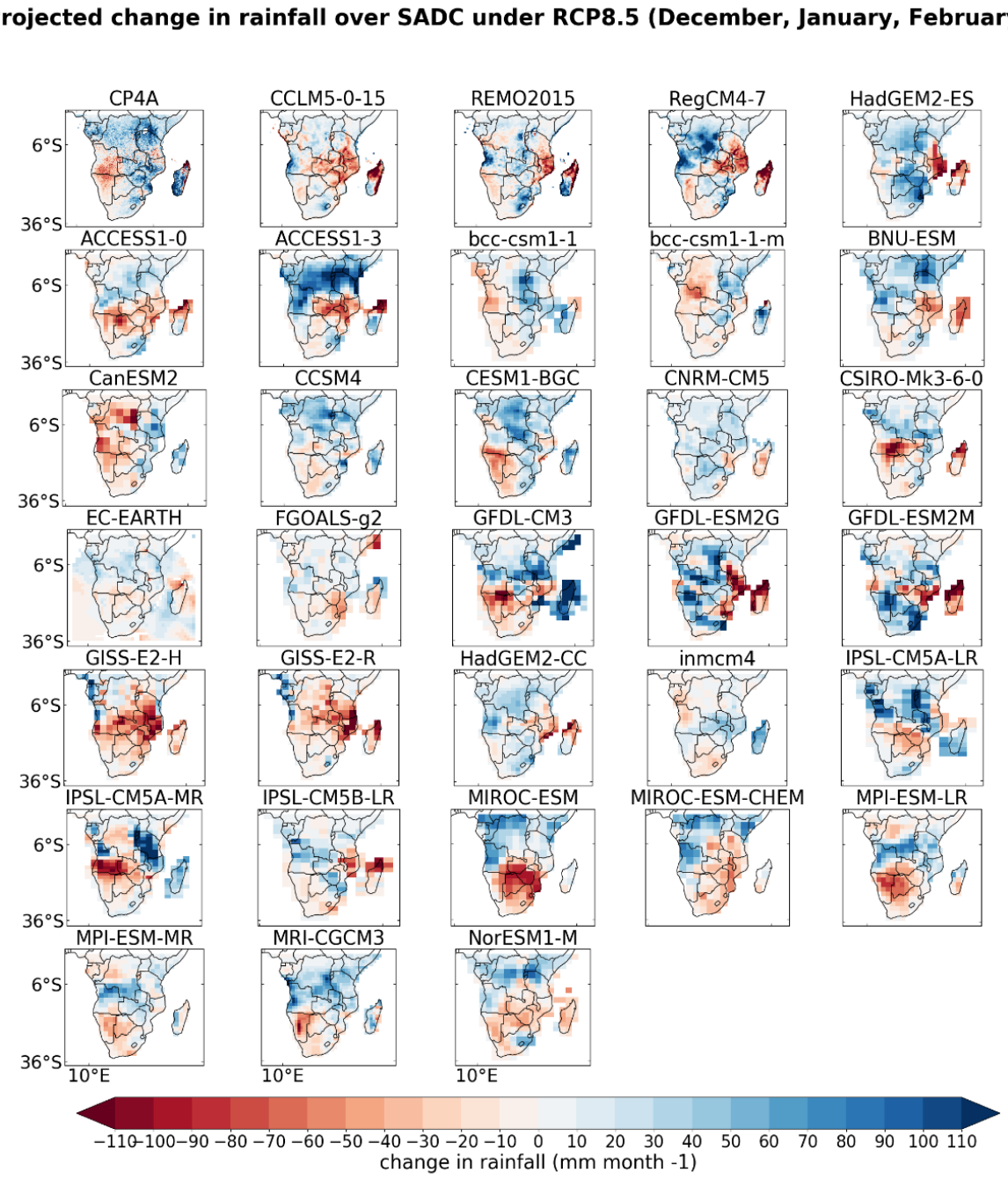

Figure 22 - Projected change in average rainfall under an RCP8.5 scenario in December, January, and February

Projected change in temperature over SADC under RCP8.5 (December, January, February)

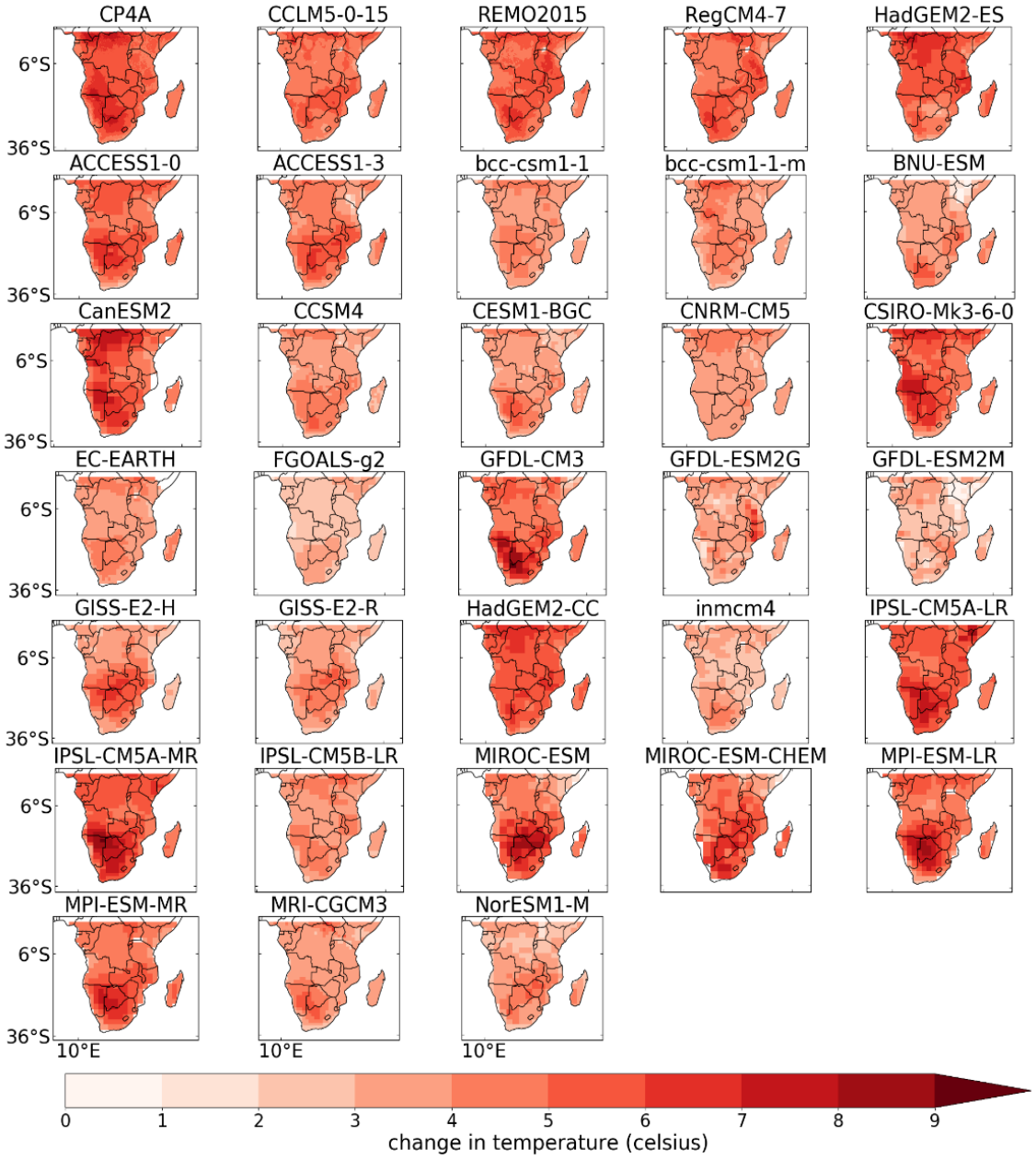

Figure 23 - Projected change in average temperature under an RCP8.5 scenario in December, January, and February

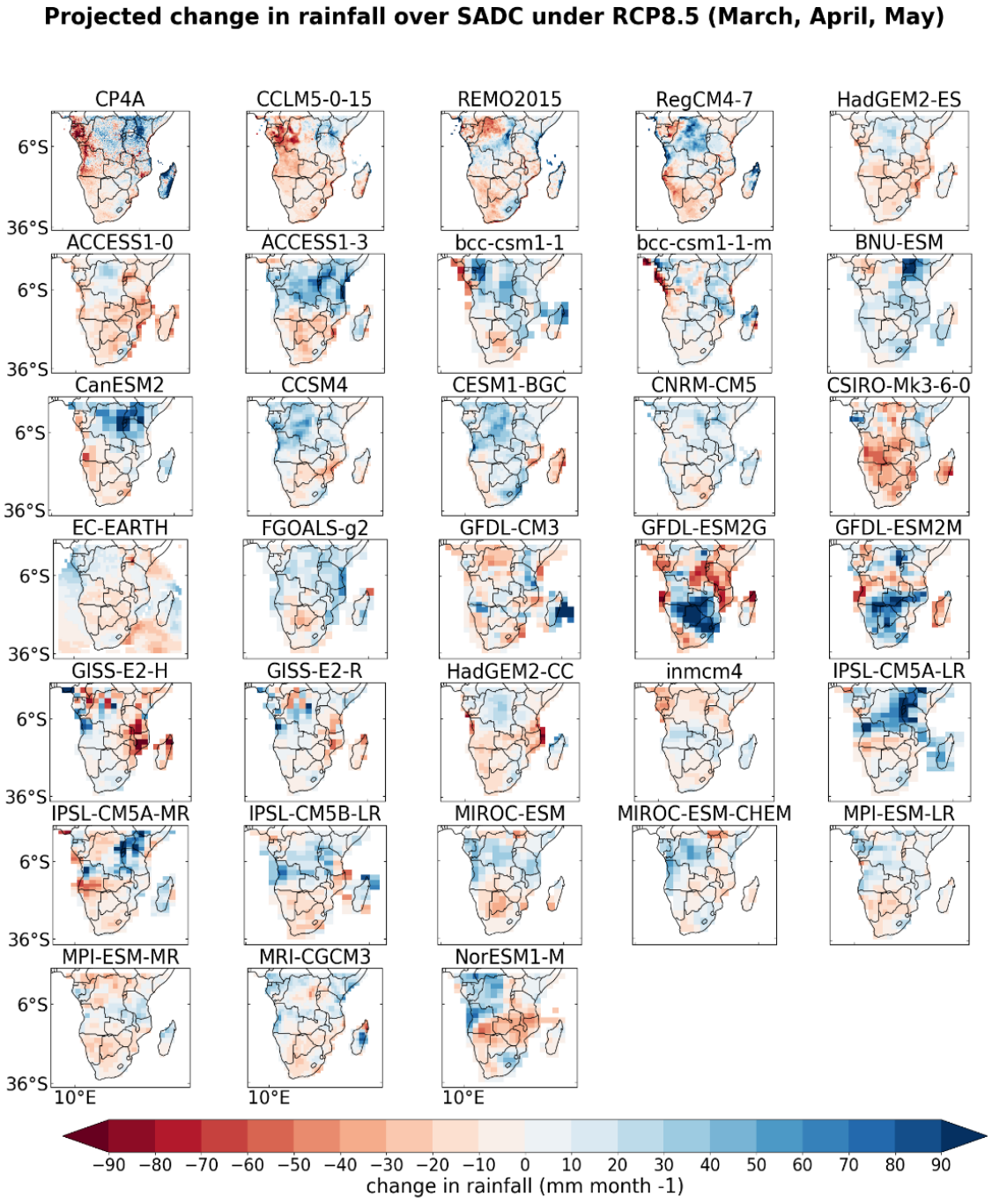

Figure 24 - Projected change in average rainfall under an RCP8.5 scenario in March, April, and May

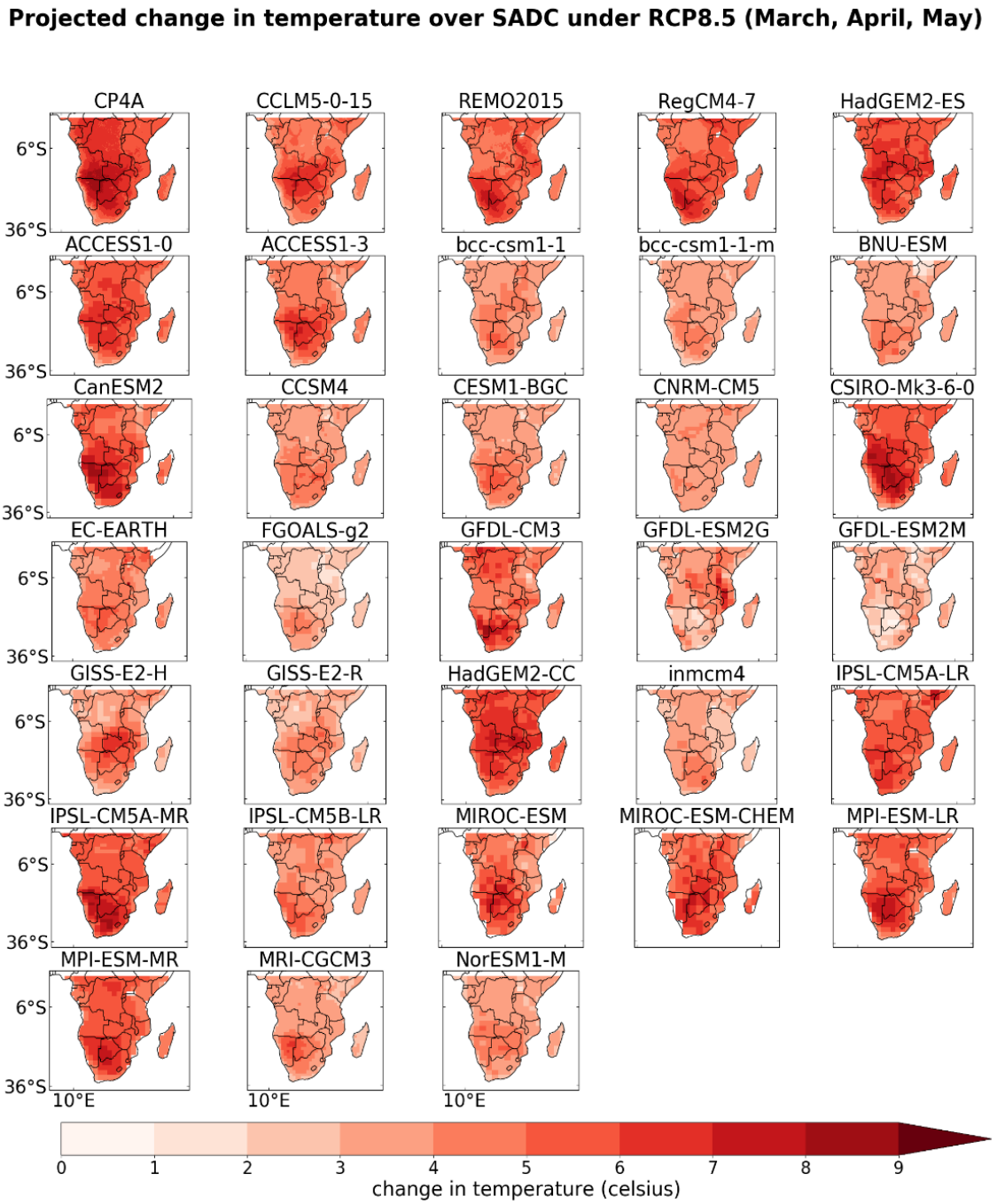

Figure 25 - Projected change in average temperature under an RCP8.5 scenario in March, April, and May

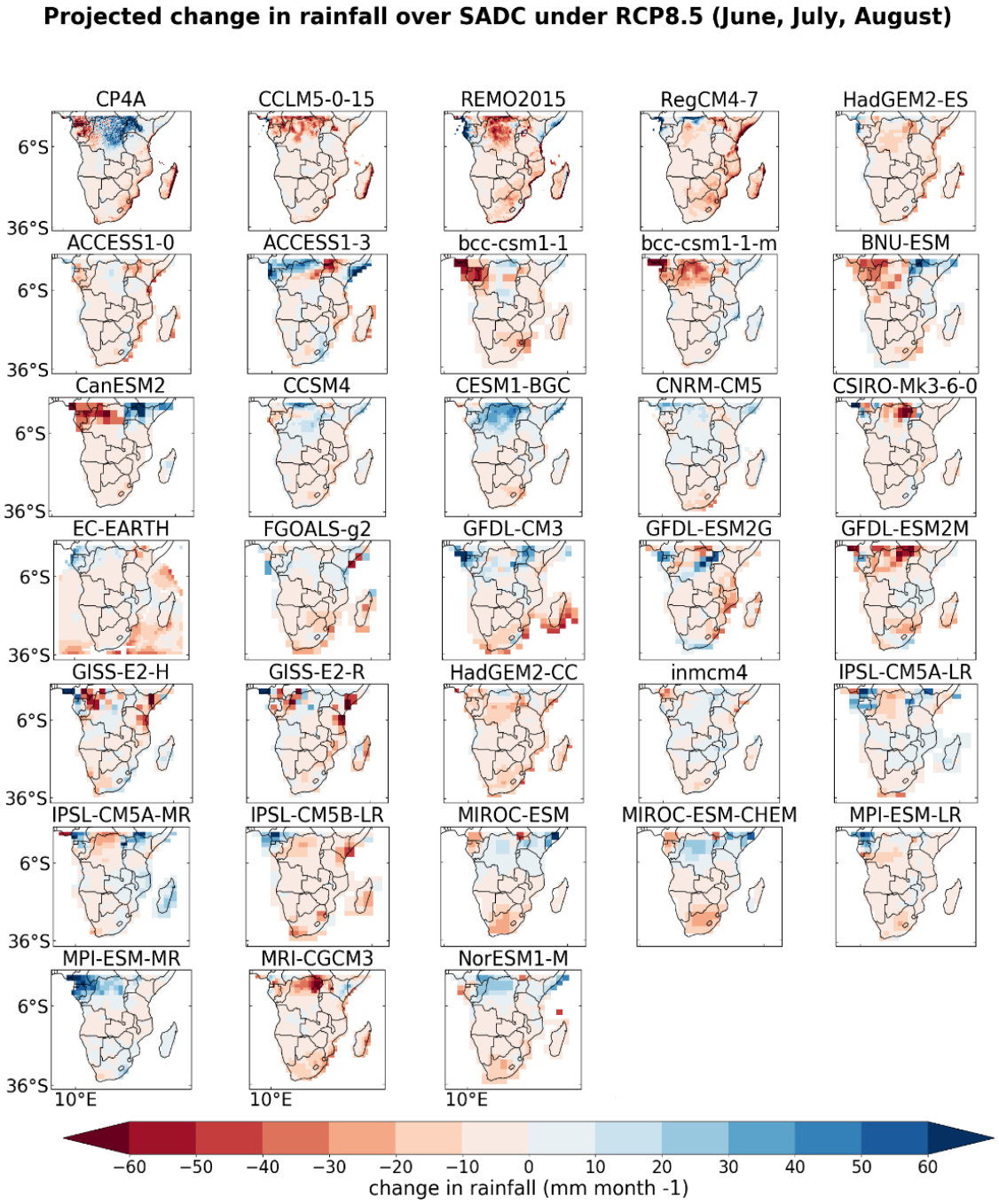

Figure 26 - Projected change in average rainfall under an RCP8.5 scenario in June, July, and August

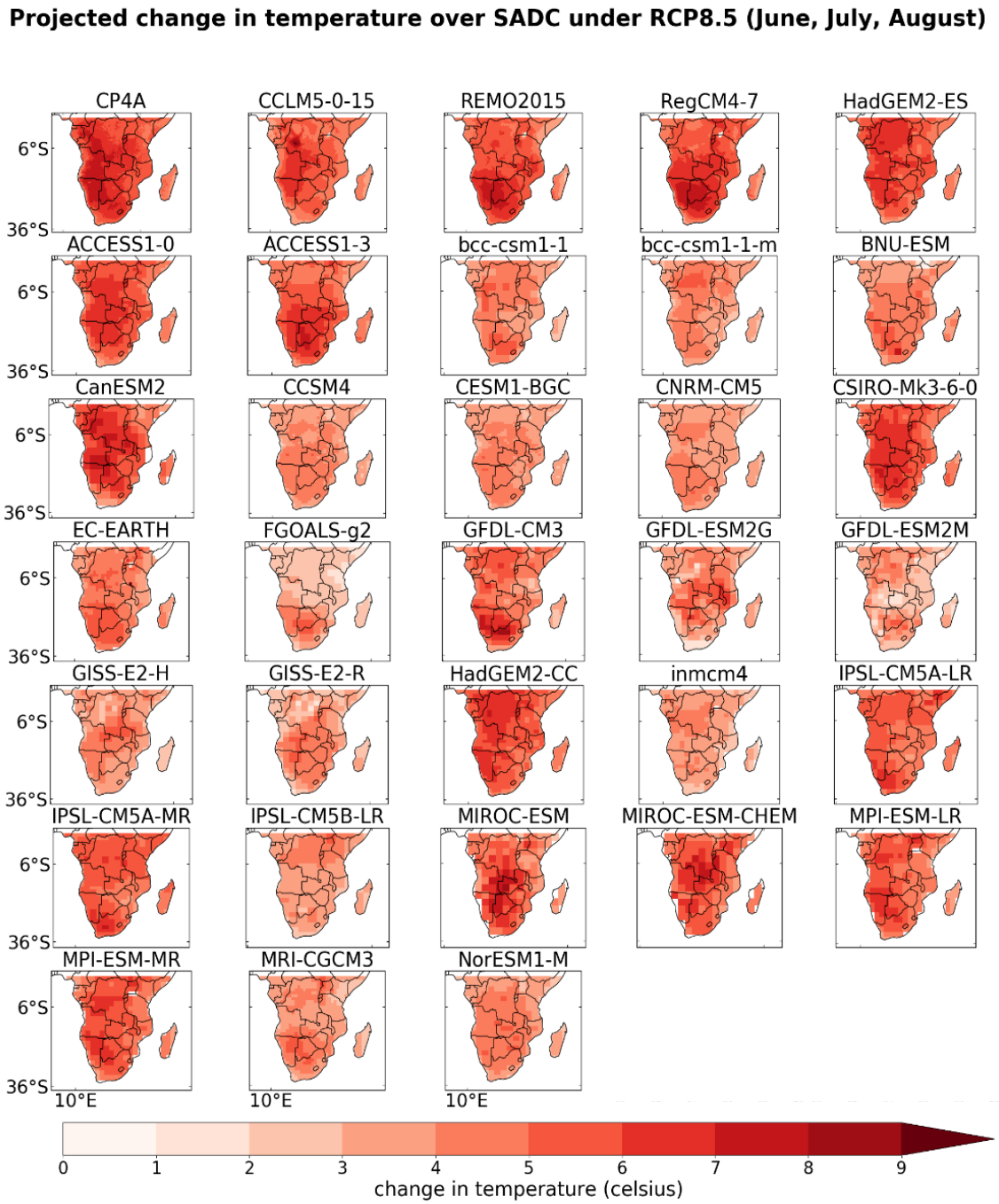

Figure 27 - Projected change in average temperature under an RCP8.5 scenario in June, July, and August

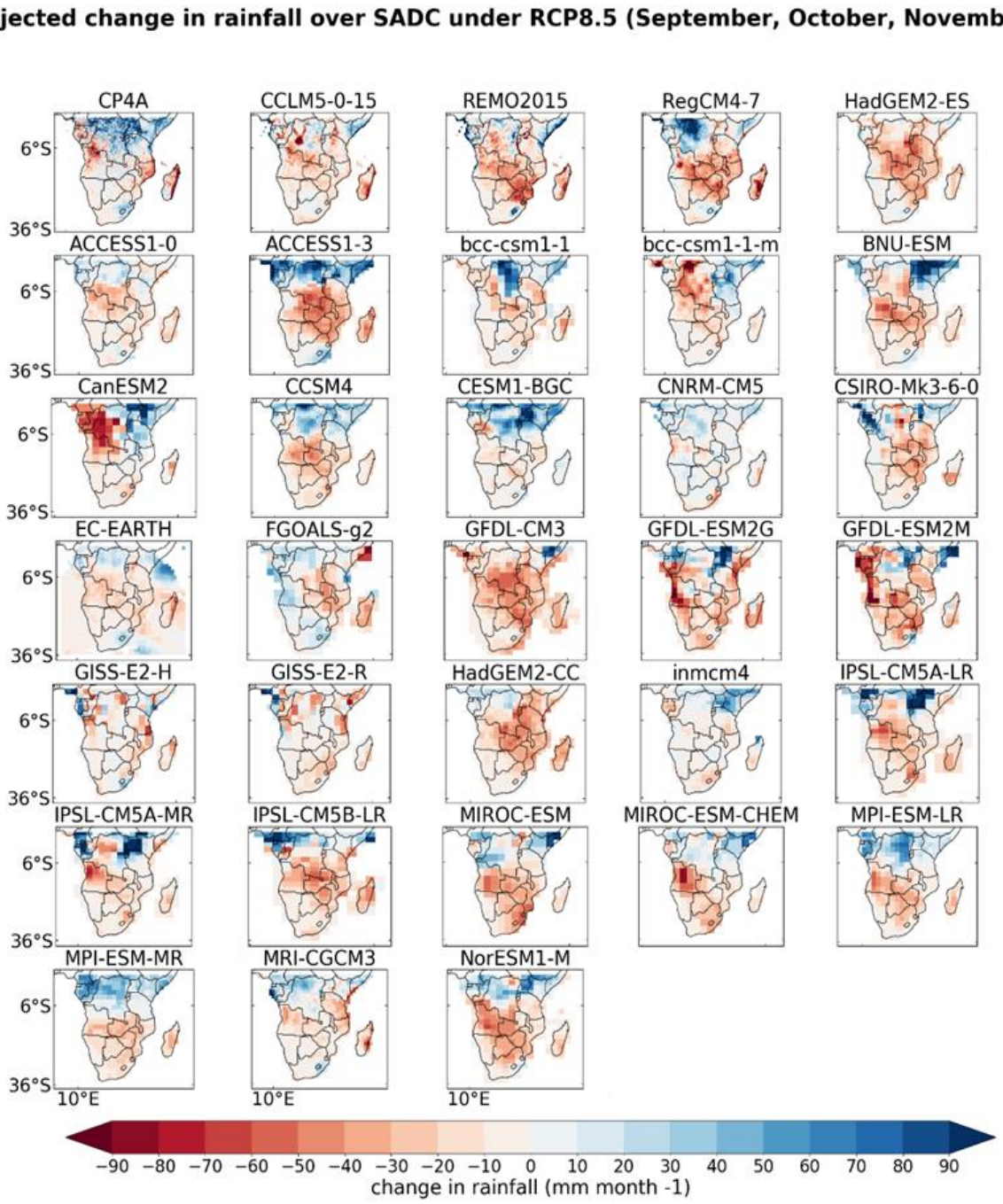

Figure 28 - Projected change in average rainfall under an RCP8.5 scenario in September, October, and November

Projected change in temperature over SADC under RCP8.5 (September, October, November)

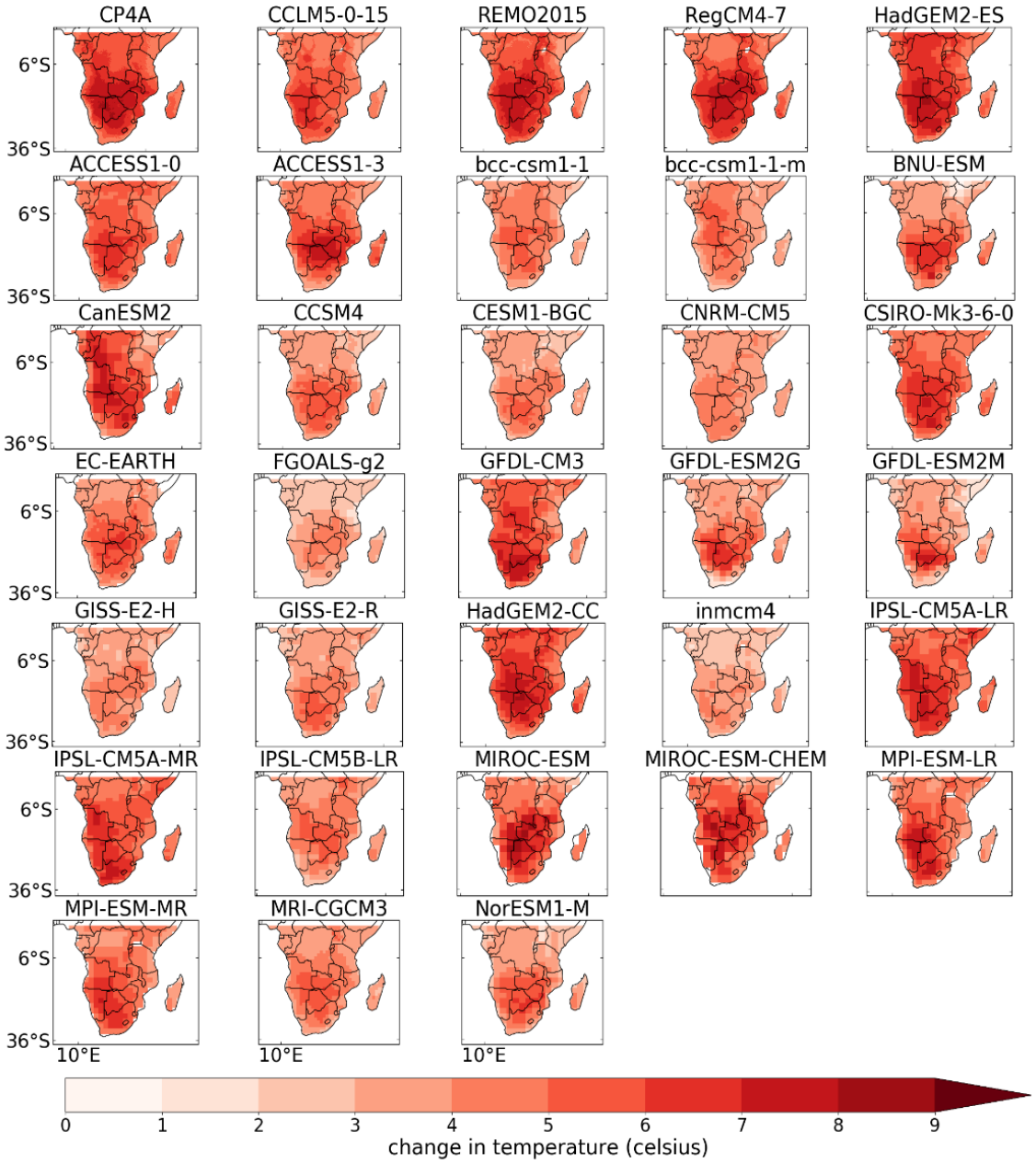

Figure 29 - Projected change in average temperature under an RCP8.5 scenario in September, October, and November

6.5 CMIP6 Future Projections

Figure 30 and Figure 31 below illustrate CMIP6 ensemble projected changes in seasonal total rainfall for the period 2090-2099 relative to the 1995-2005 reference period for DFJ and JJA seasons under SSP5-8.55. Hatching indicates areas where the projected change is not statistically significant given natural variability and the 10-year sample size, and a threshold of $p < 0.5$ for a two-sided t-test.

There is little consistency in projected rainfall changes across the ensemble members across the entire region. Tropical increases in rainfall appear to be the most consistent pattern across members with only a few exceptions. Models of the same family (e.g., EC-EARTH) show some consistency suggesting that underlying physics may be driving consistent changes. Several models show significant drying over the sub-tropics (e.g., CESM2-WACCM, E3SM-1-1). For the dry JJA season, there are almost no significant changes projected though there is much more consistency of drying (not significant in magnitude) across the region especially across the south Eastern ocean areas. Considering the consistent wet bias across the ensemble for the reference period, this drying suggests that most models are projected changes that reduce the wet bias (i.e., closer to observations).

Subsequently, we only included the projected changes for the DJF season (Figure 32) as temperature projections are consistent across seasons (other seasonal plots available in the appendix). All ensemble members show significant warming into the future ranging from 3°C up to as much as 9°C in the western and southern interior. Most models are consistent in showing the strongest warming in this western central interior region which aligns with historical trend analysis. The large range and the associated high upper warming rate are concerning as this leads to significant uncertainties in the future projections.

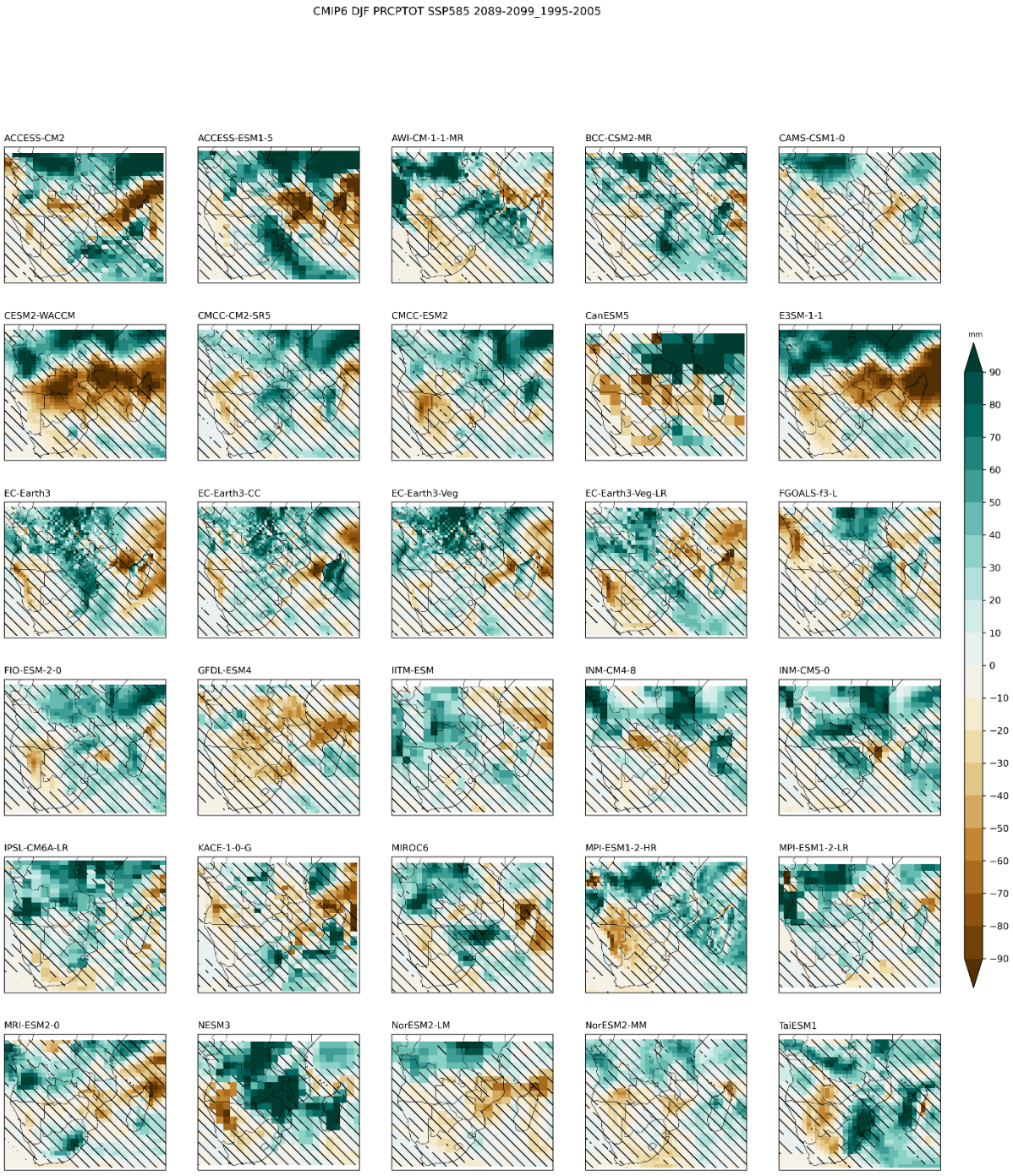

Figure 30 - Projected changes in seasonal total rainfall (mm) for DJF season across the CMIP6 ensemble members. Anomalies are for 2090-2099 relative to 1995-2005 and hatching indicates changes that are not statistically significant for p > 0.05 threshold.

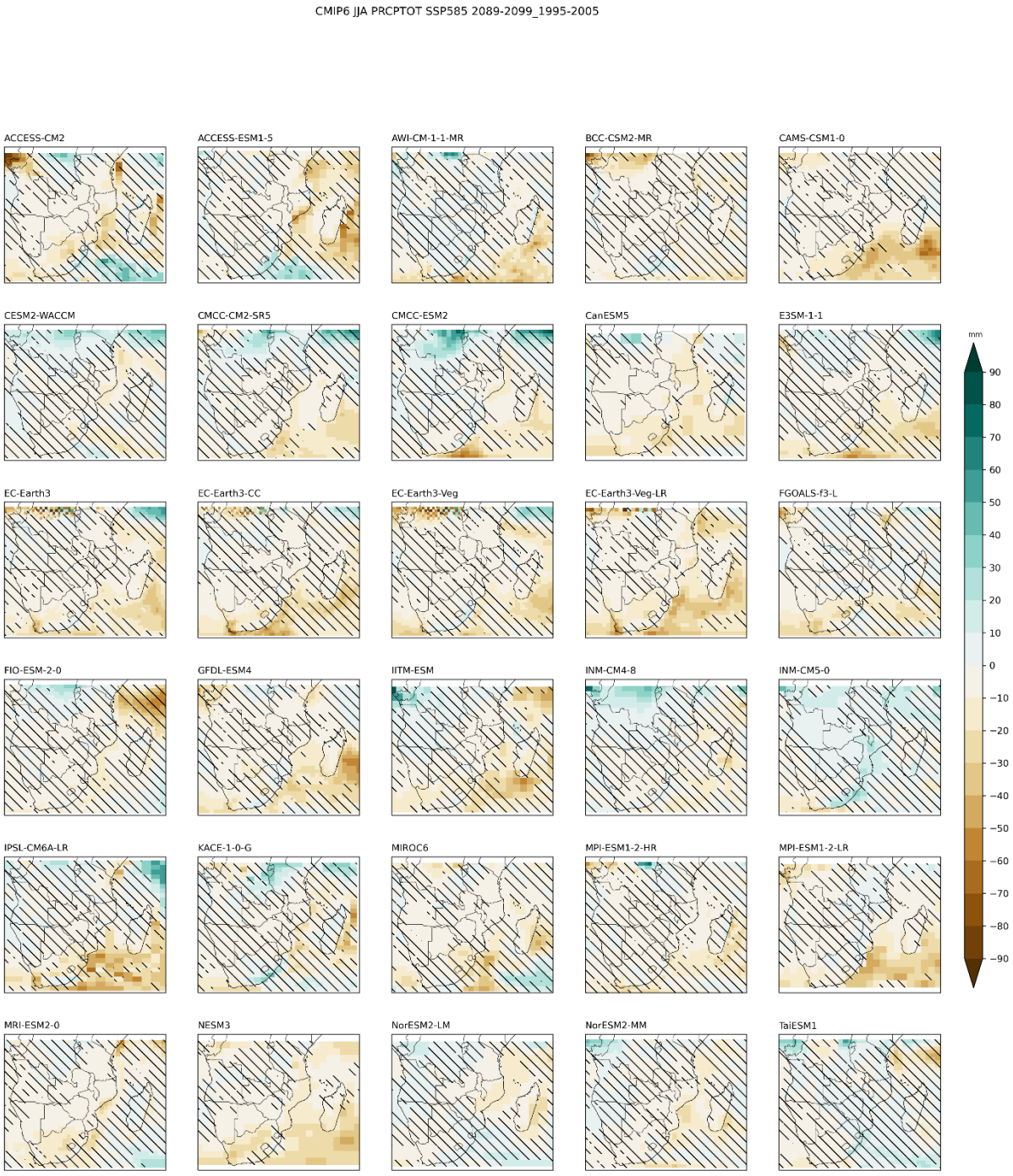

Figure 31 - Projected changes in seasonal total rainfall (mm) for JJA season across the CMIP6 ensemble members. Anomalies are for 2090-2099 relative to 1995-2005 and hatching indicates changes that are not statistically significant for p > 0.05 threshold.

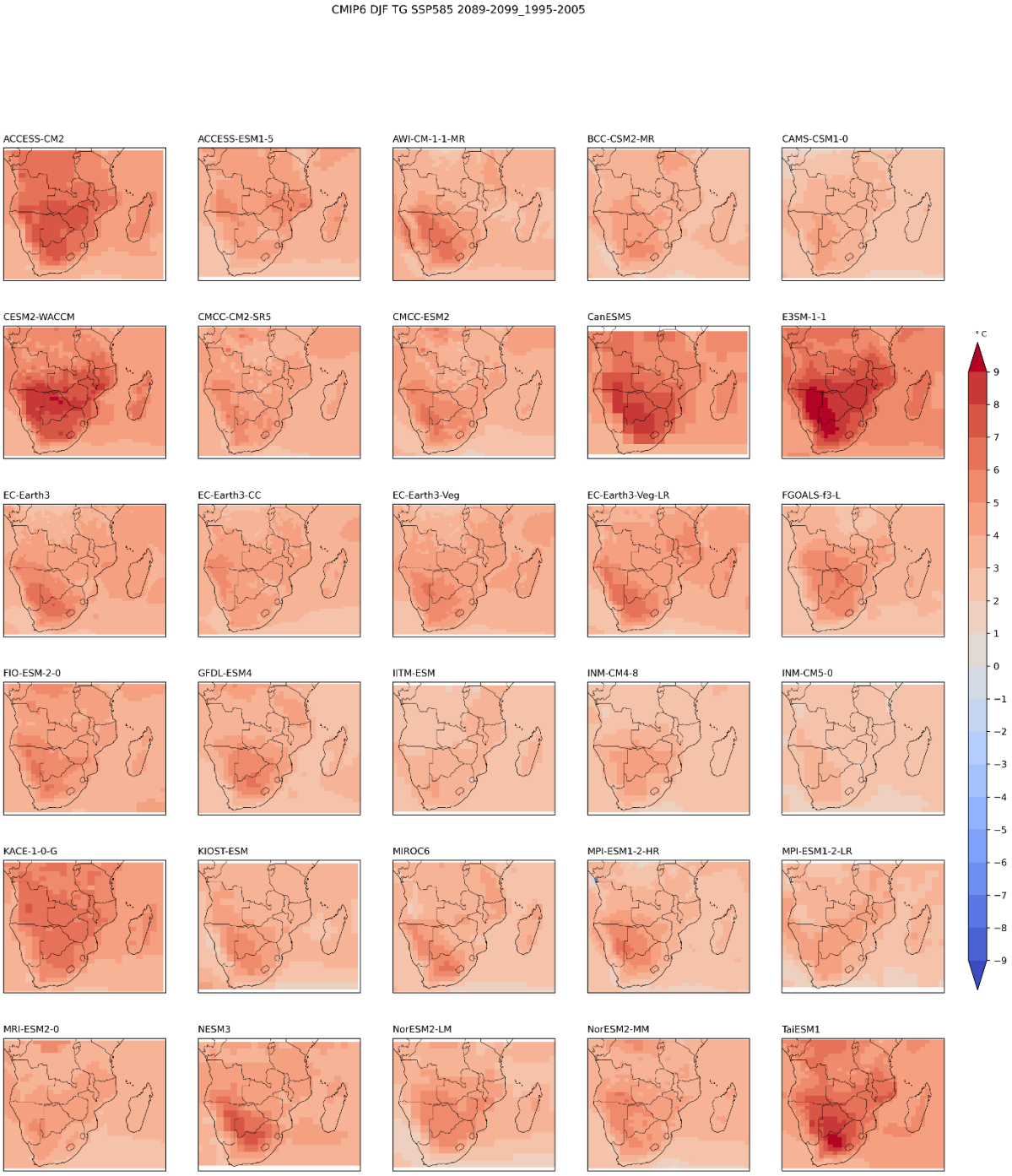

Figure 32 - Projected changes in seasonal mean temperature (C) for DJF season across the CMIP6 ensemble members. Anomalies are for 2090-2099 relative to 1995-2005 and hatching indicates changes that are not statistically significant for p > 0.05 threshold.

This is corroborated when examining the interannual mean annual signal for a specific location of interest for the project, for example, Malawi from 1995 to 2100 (Figure 33). The winter precipitations show no trend and Figure 33 also illustrates that there is no clear separation between the emission scenarios SSP2-4.5 and SSP5-8.5 (black line for historical; blue for SSP2-4.5 and purple for SSP5-8.5) time periods. All the selected GCMs are plotted with lines while bold lines stand for the ensemble means. Furthermore, by the end of the century in Malawi, raw projections would induce mean temperature of 24°C against 22°C in the late 1990s for SSP2-4.5, and above 26°C for SSP5-8.5.

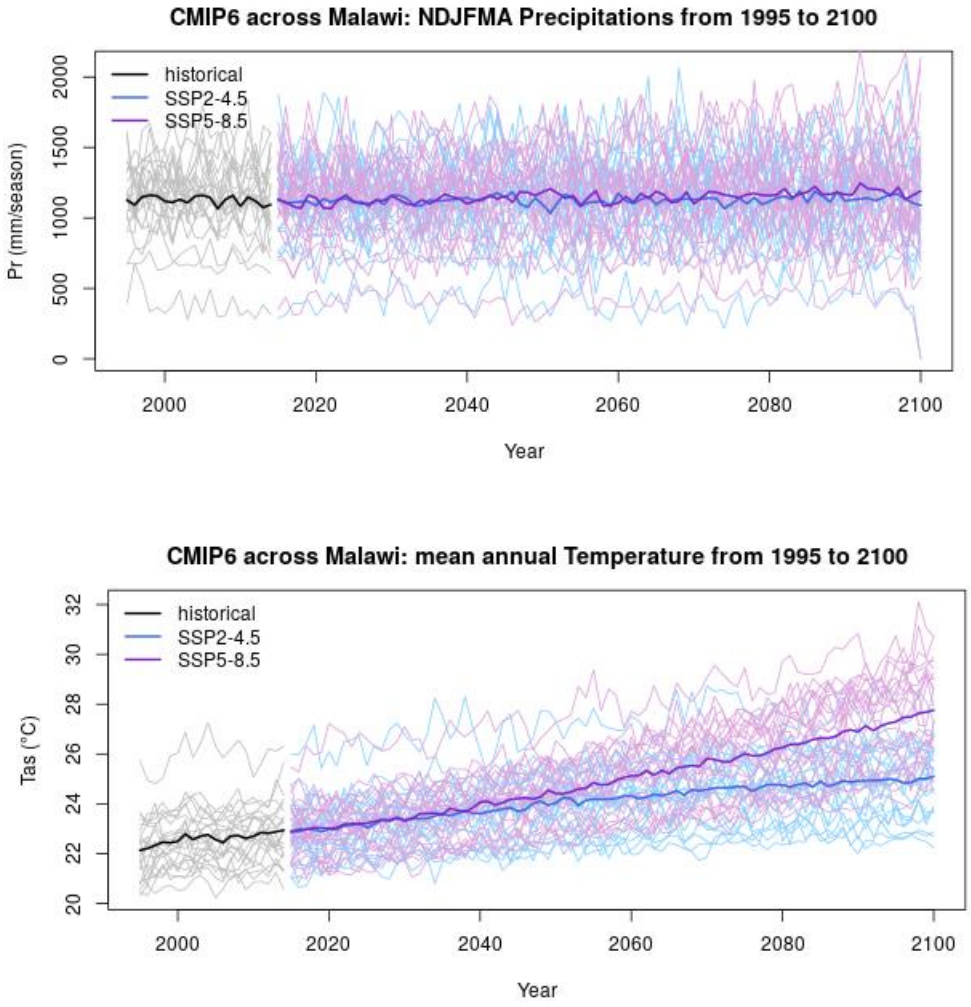

Figure 33 - Winter precipitations (top) and mean temperature (bottom) across Malawi for the historical time (black), SSP2-4.5 (blue), and SSP5-8.5 (purple). Thin lines: each GCM, bold lines: ensemble mean for each scenario.

6.6 CMIP5-6 and CORDEX models' intercomparison

Plume plots have been constructed to compare the relative behaviour of the different models' ensembles and include the observations. These plume plots illustrate the 90% range of each ensemble along with the median. Different ensembles are plotted in assorted colours. All ensemble medians and observation means are adjusted to have the same mean during the reference period to allow the comparison of relative changes rather than the absolute bias. It is only presented the results for the DJF months as these are the wettest months and those with most differences in the models' projections.

It is important to note that the ensembles are of varied sizes, and in the case of CORDEX downscaling, represent different sub-samplings of the driving GCM ensemble (CMIP5 in this case). The spread of the ensembles cannot therefore be interpreted as a different total uncertainty. In many cases CORDEX ensembles exhibit a smaller ensemble range but this is due to the smaller sampling of the forcing GCMs.

6.6.1 Temperature plume plots

Figure 35- Figure 36 illustrate that all ensembles are consistent with DJF warming through the 20th century and accelerated warming into the 21st century for the four Zones. Observations (CRU) generally lie within the ensemble ranges for the 20th century. However, in the Upper ESAF region, the CRU temperature observations show a cooling trend during the mid-20th Century with warming only occurring post 1970. This would require further investigation to determine the role of station observation density in the region during this period.

RCP8.5 and SSP 5.85 emission scenarios have been analysed which represent low mitigation futures. Consistent with many analyses, CMIP6 (yellow) exhibits stronger warming at the 95th percentile of the ensemble range than CMIP5 (green), or the CMIP5 forced CORDEX simulations.

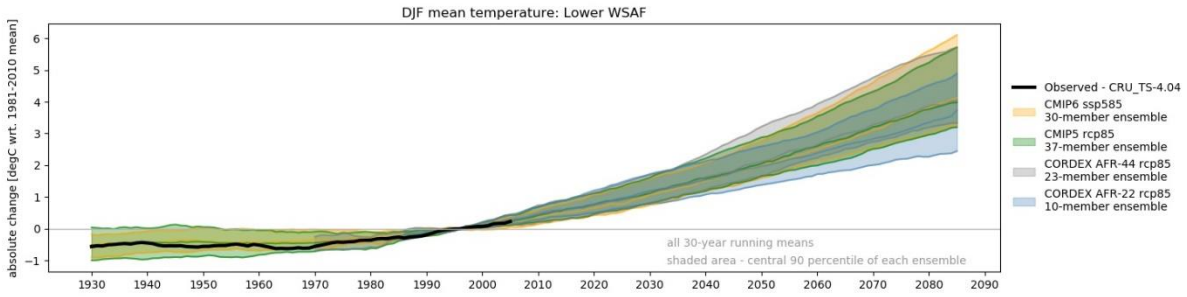

Figure 34 - Plume plot of DJF absolute 2m temperature change for CRU, CMIP5, CMIP6, CORDEX AFR-44, and CORDEX AFR-22 for Lower WSAF region

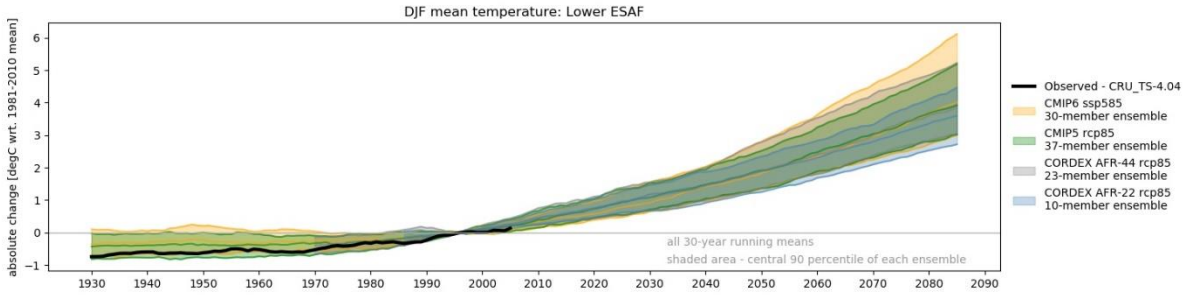

Figure 35 - Plume plot of DJF absolute 2m temperature change for CRU, CMIP5, CMIP6, CORDEX AFR-44, and CORDEX AFR-22 for Lower ESAF region

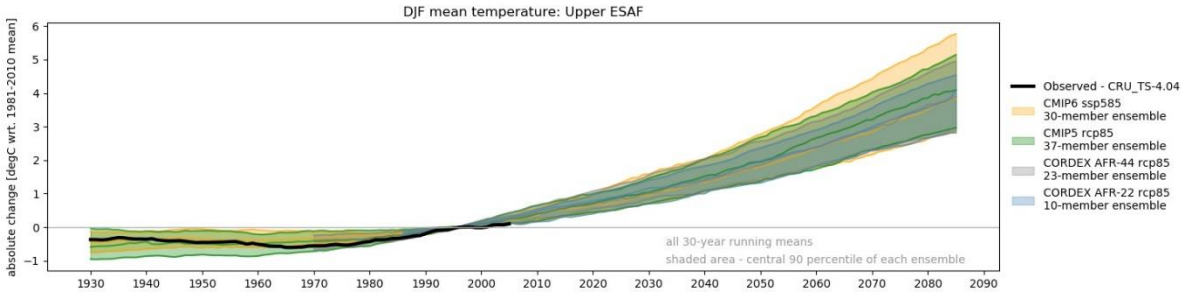

Figure 37 - Plume plot of DJF absolute 2m temperature change for CRU, CMIP5, CMIP6, CORDEX AFR-44, and CORDEX AFR-22 for Upper ESAF region

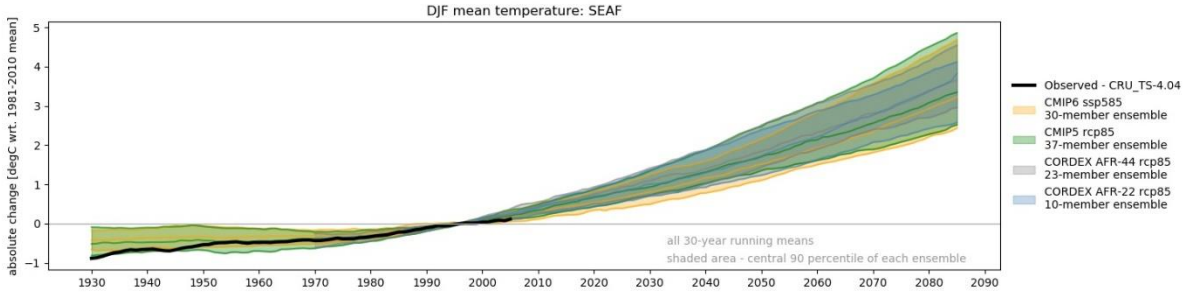

Figure 36 - Plume plot of DJF absolute 2m temperature change for CRU, CMIP5, CMIP6, CORDEX AFR-44, and CORDEX AFR-22 for SEAF region

6.6.2 Precipitation plume plots

Figure 38 -Figure 41 below indicate that, as expected, changes in DJF rainfall are far less consistent both in terms of direction of change, and magnitude, than for temperature changes.

For the Lower ESAF region the observations are largely within the range of historical simulations for the 20th century, however natural variability, even with 30 year rolling averages is large, with many wet and dry decades, and no clear systematic trend. Projected changes in rainfall range from increases of more than 15% through to decreases of more than 15%. While the CMIP5 based projections tend towards a reduction in rainfall, the more recent CMIP6 projections seem to indicate a stronger tendency towards increasing rainfall across the region.

For the Lower WSAF region, once again the observations are generally within the ensemble range for the 20th century, however natural variability in this generally drier region is much larger. There does appear to be a positive rainfall trend in the observations, however trends in these regions are strongly influenced by changes in station density so would require further analysis. Projected changes show more consistency in a reduction in a rainfall across the region with more consistency across the different ensembles. The CORDEX simulations do have a narrower range, however, as noted above this likely due to the smaller ensemble size and the small sub-sample of driving CMIP5 models. It should not be interpreted as a reduction in uncertainty.

For the SEAF region the observations show low natural variability percentage wise because of the high absolute rainfall in this region. The observations lie well within the range of the ensemble simulations for the 20th century. There is not clear trend in observations but may be a slight increasing trend over-all, this would require further analysis. Ensemble projections for the 21st Century demonstrate some

inconsistency across the ensembles with CMIP6 once again showing larger rainfall increases, as high as +50%, at the upper bounds of the ensemble range compared with CMIP5 and the CMIP5 forced CORDEX simulations. The CORDEX simulations project the least increase in rainfall into the future with some members projected decreasing rainfall.

The Lower ESAF plume plot shows that the historical observations, while largely within the ensemble ranges for the 20th century, does have large multi-decadal variability with what appears to be consistent drying from the 1960s onwards. Again, this would need to be explored further. The ensemble projections of future rainfall changes are more consistent than for the other regions but also show an even spread between increasing and decreasing rainfall.

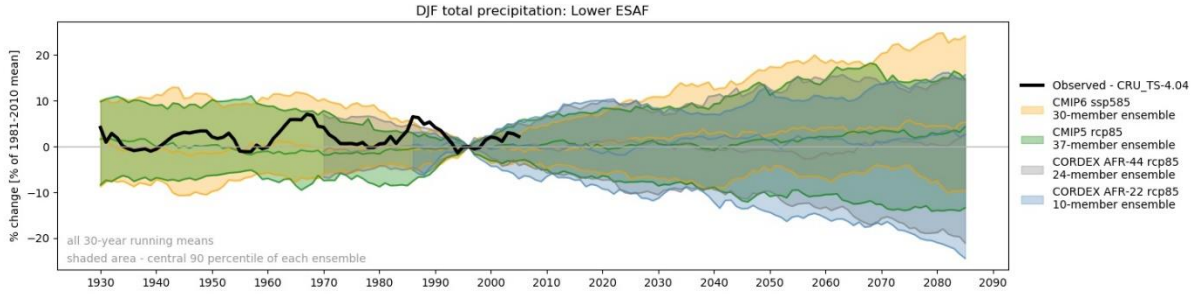

Figure 38 - Plume plot of DJF relative total precipitation changes for CRU, CMIP5, CMIP6, CORDEX AFR-44, and CORDEX AFR-22 for Lower ESAF region.

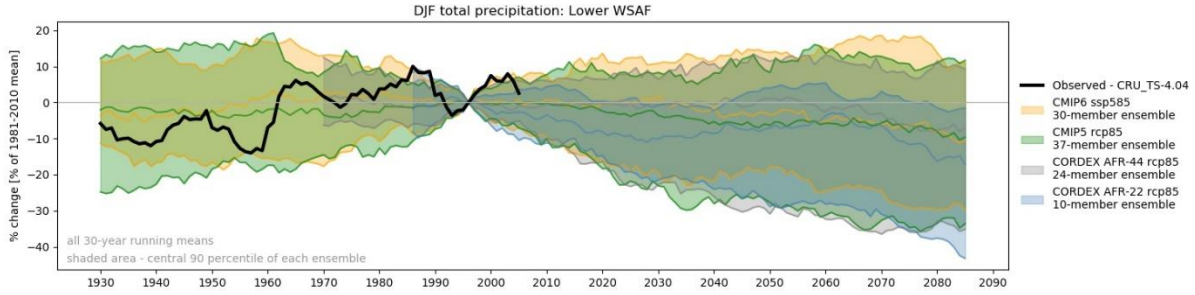

Figure 39 - Plume plot of DJF relative total precipitation changes for CRU, CMIP5, CMIP6, CORDEX AFR-44, and CORDEX AFR-22 for Lower WSAF region.

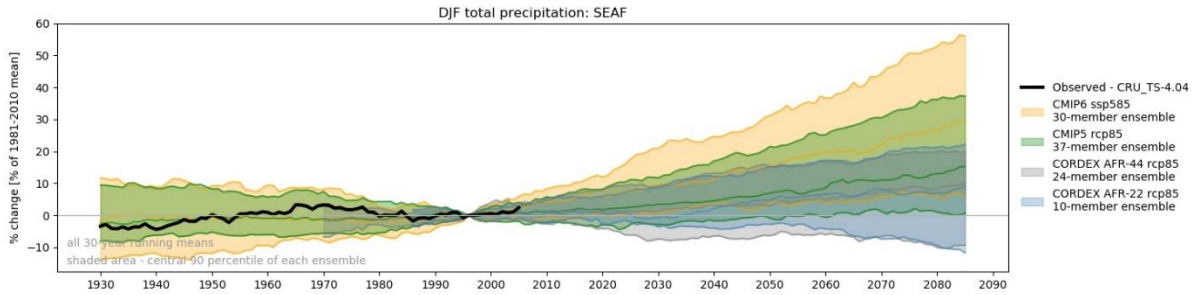

Figure 40 - Plume plot of DJF relative total precipitation changes for CRU, CMIP5, CMIP6, CORDEX AFR-44, and CORDEX AFR-22 for SEAF region.

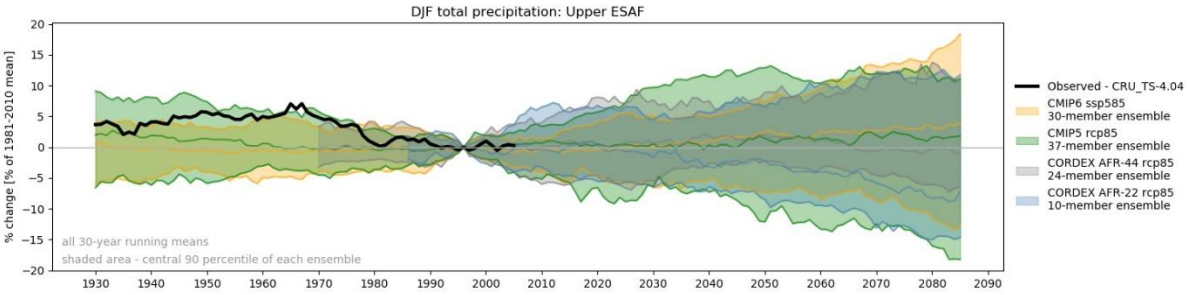

Figure 41 - Plume plot of DJF relative total precipitation changes for CRU, CMIP5, CMIP6, CORDEX AFR-44, and CORDEX AFR-22 for Upper ESAF region.

6.7 CCAM Future Climate Projections

The simulations are indicative of general rainfall decreases over southern Africa for the period 2089-2099 for RCP8.5 with respect to 1995-2005 (Figure 42- Figure 45). An important exception is summer (Figure 42), for which most models project rainfall increases over the eastern escarpment regions. In several of these simulations, rainfall increases stretch into southern Mozambique, and in one of them the increases stretch westwards into the southern African interior. Substantial rainfall reductions in winter rainfall are projected, consistently across the simulations (Figure 44). Drastic warming is projected for all seasons, exceeding 5°C over substantial portions of the interior in all the projections (Figure 46- Figure 49**Error! Reference source not found.**).

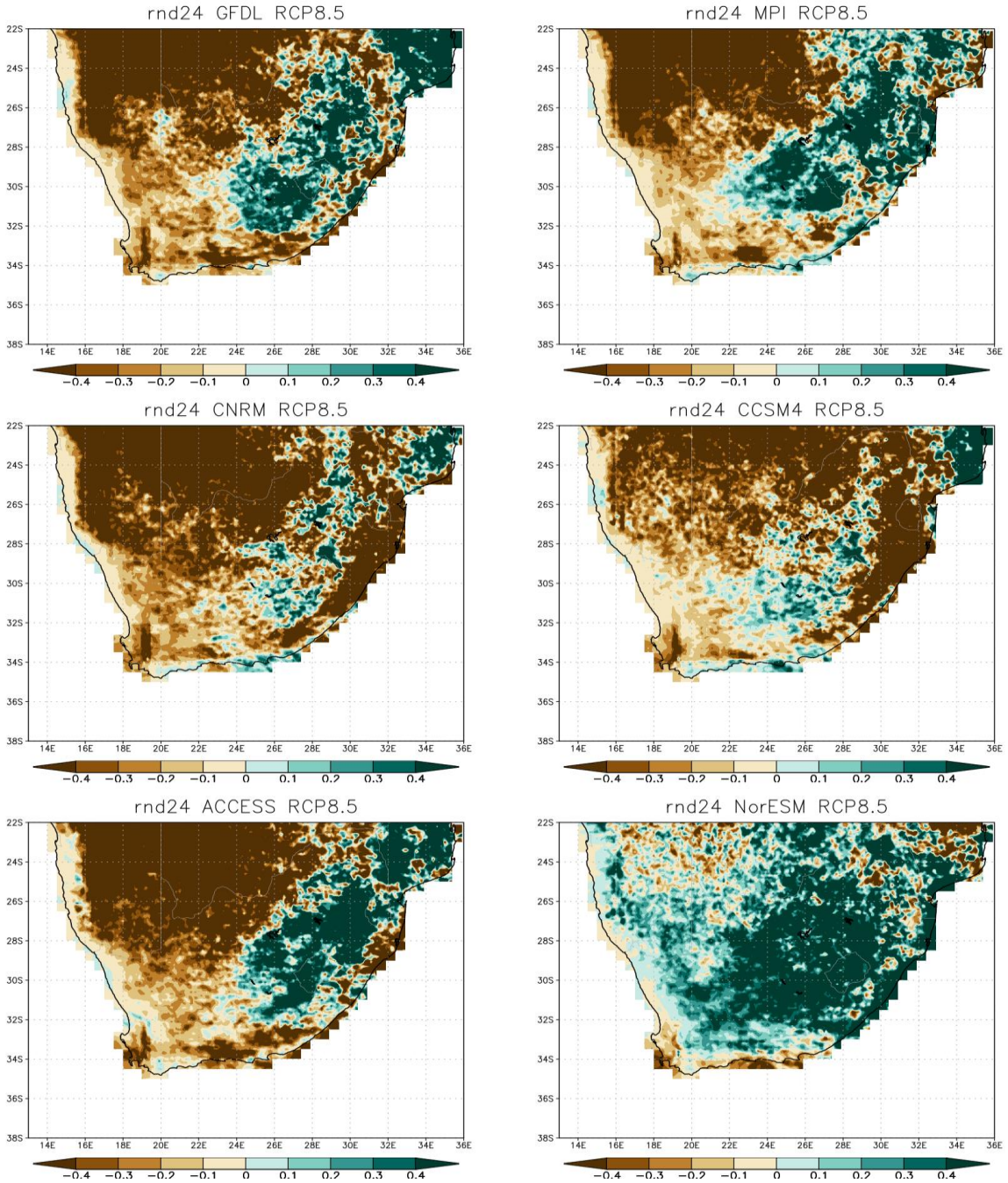

Figure 42 - CCAM downscalings (8 km resolution in the horizontal) of the change in summer (December to February) rainfall totals (mm/day) over southern Africa for the time-slab 2089-2099 relative to 1995-2005, for six different GCMs under RCP8.5.

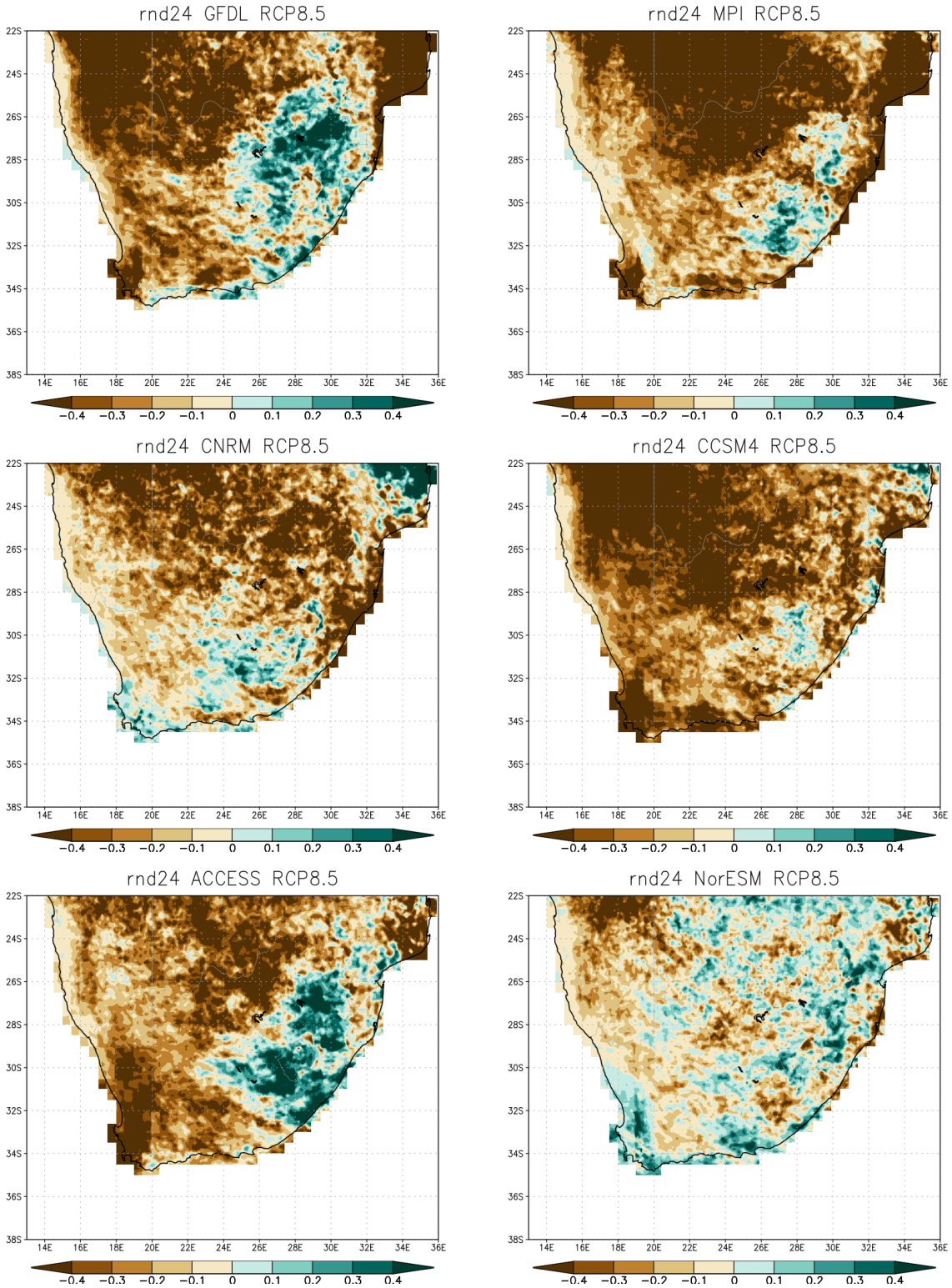

Figure 43 - CCAM downscalings (8 km resolution in the horizontal) of the change in autumn (March to May) rainfall totals (mm/day) over southern Africa for the time-slab 2089-2099 relative to 1995-2005, for six different GCMs under RCP8.5.

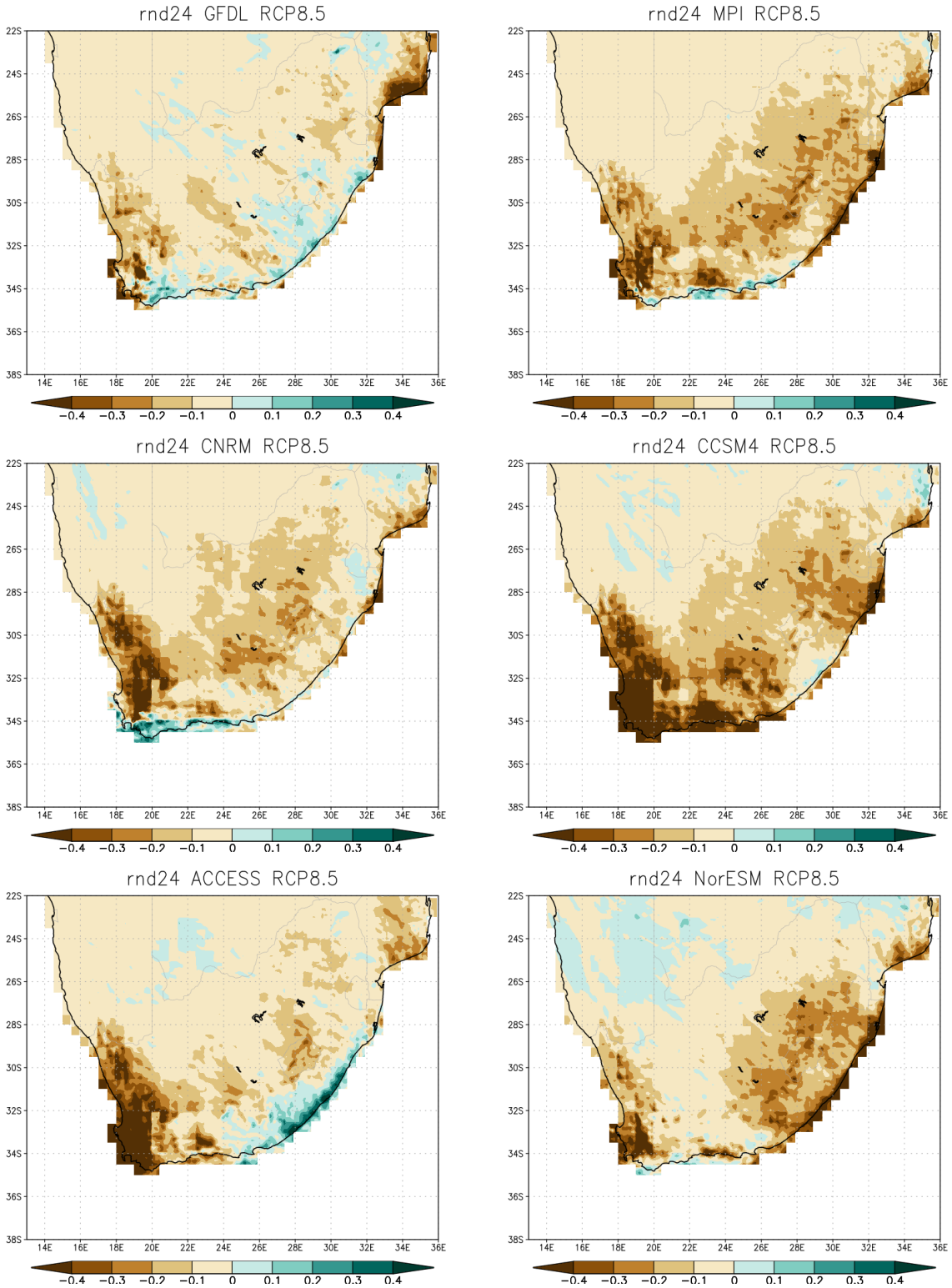

Figure 44 - CCAM downscalings (8 km resolution in the horizontal) of the change in winter (July to August) rainfall totals (mm/day) over southern Africa for the time-slab 2089-2099 relative to 1995-2005, for six different GCMs under RCP8.5.

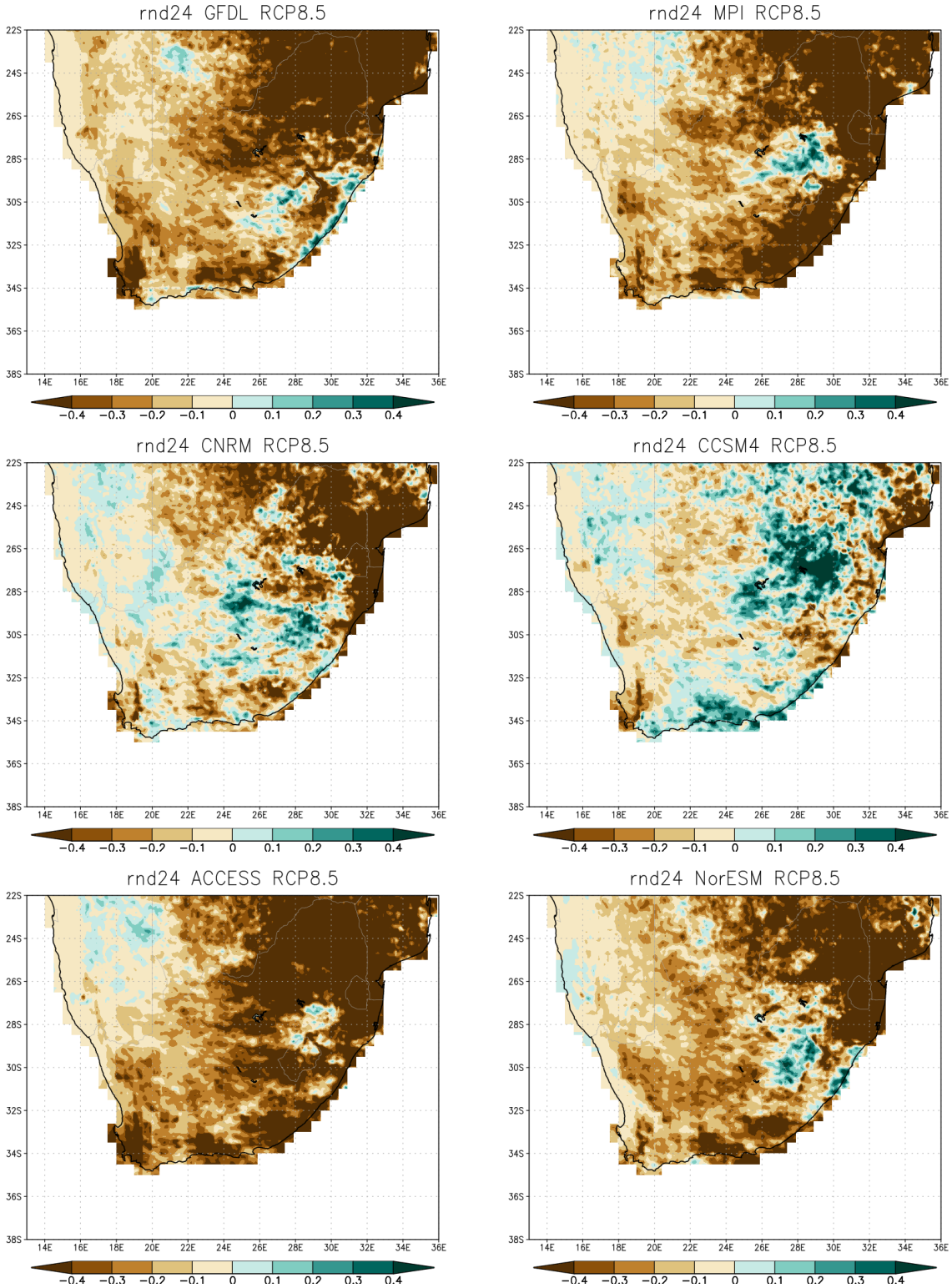

Figure 45 - CCAM downscalings (8 km resolution in the horizontal) of the change in spring (September to November) rainfall totals (mm/day) over southern Africa for the time-slab 2089-2099 relative to 1995-2005, for six different GCMs under RCP8.5

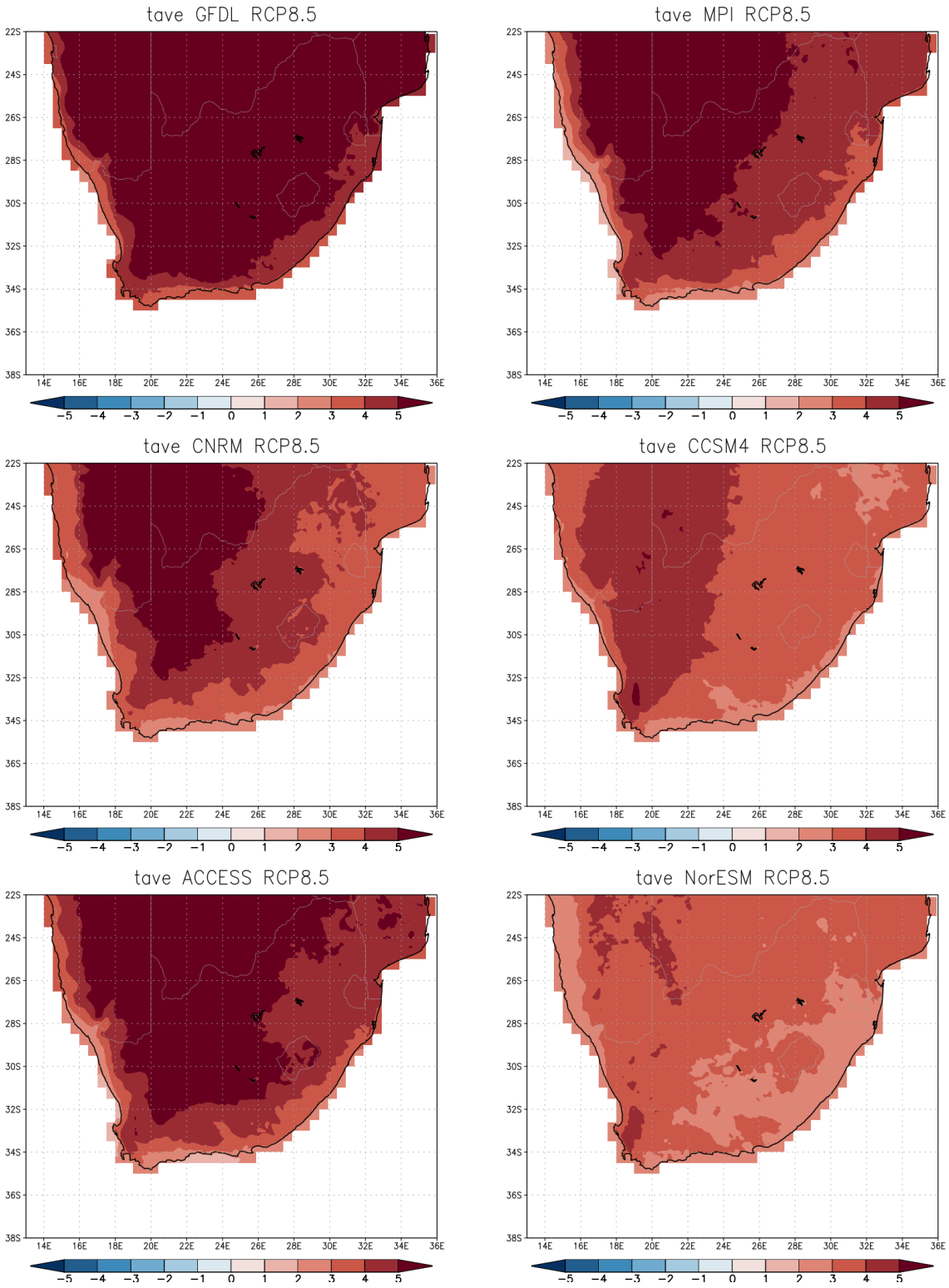

Figure 46 - CCAM downscalings (8 km resolution in the horizontal) of the change in summer (December to February) average temperature (°C) over southern Africa for the time-slab 2089-2099 relative to 1995-2005, for six different GCMs under RCP8.5.CCAM downscalings

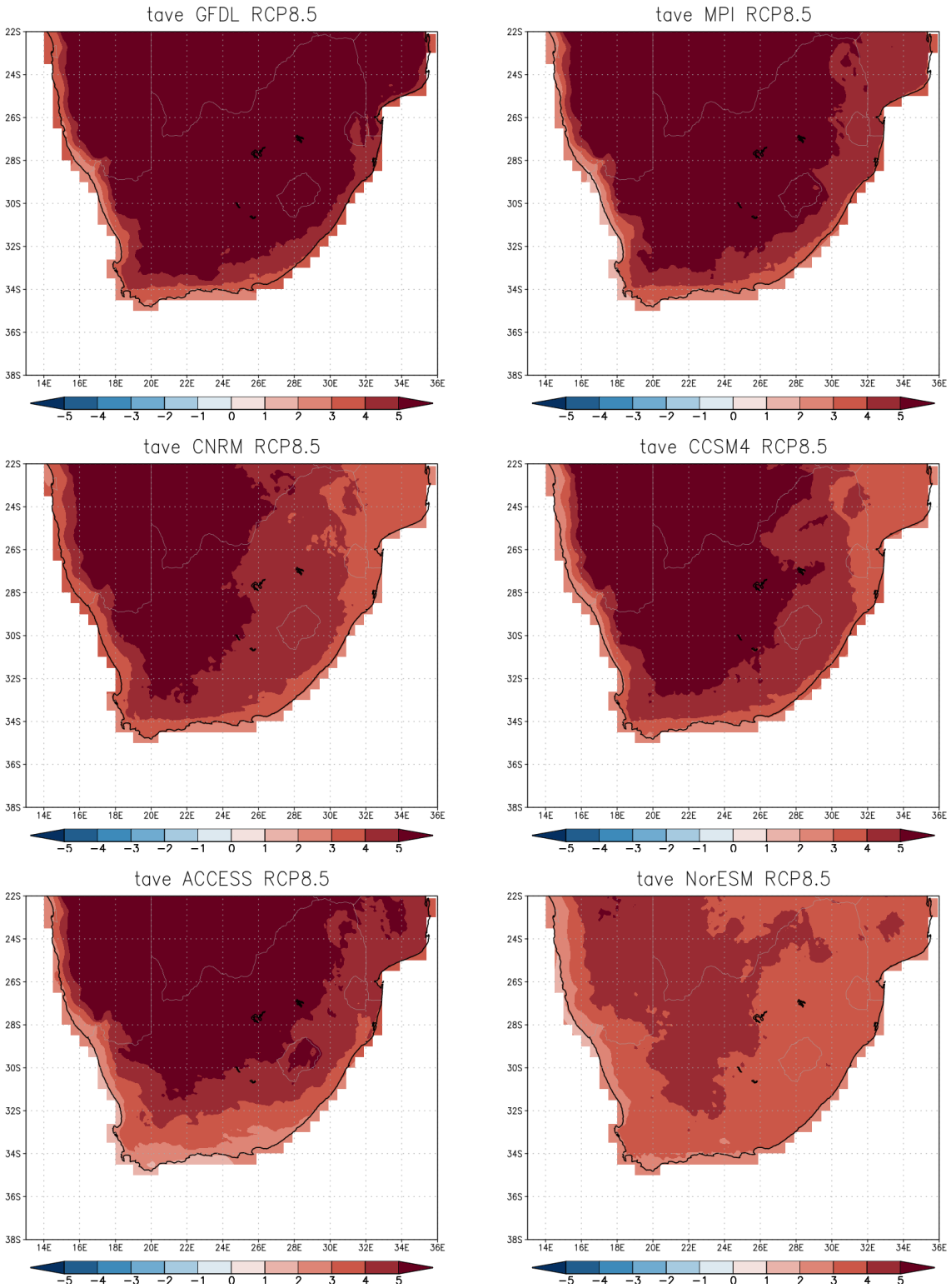

Figure 47 - CCAM downscalings (8 km resolution in the horizontal) of the change in autumn (March to May) average temperature (°C) over southern Africa for the time-slab 2089-2099 relative to 1995-2005, for six different GCMs under RCP8.5.

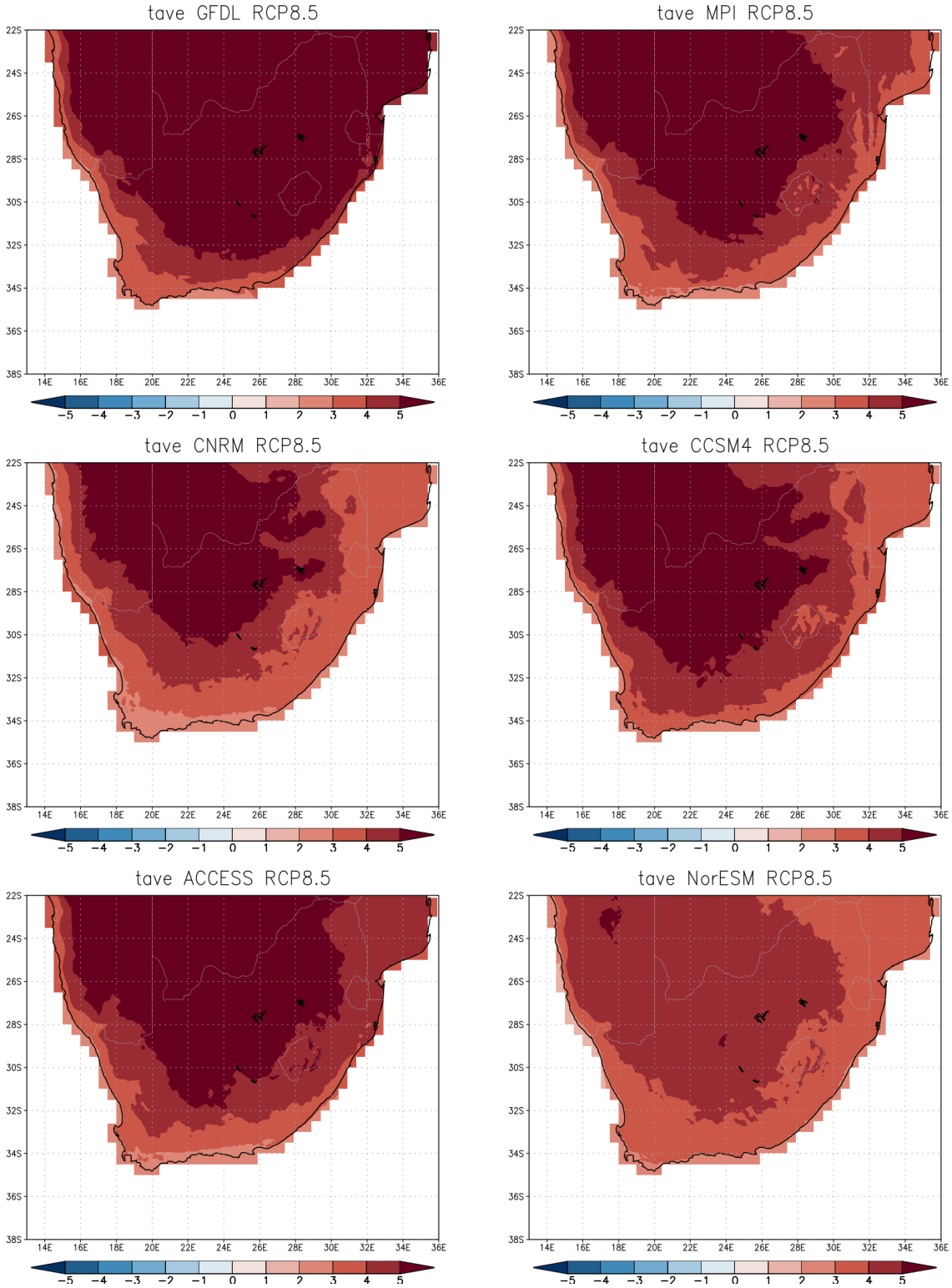

Figure 48 - CCAM downscalings (8 km resolution in the horizontal) of the change in winter (July to August) average temperature (°C) over southern Africa for the time-slab 2089-2099 relative to 1995-2005, for six different GCMs under RCP8.5.

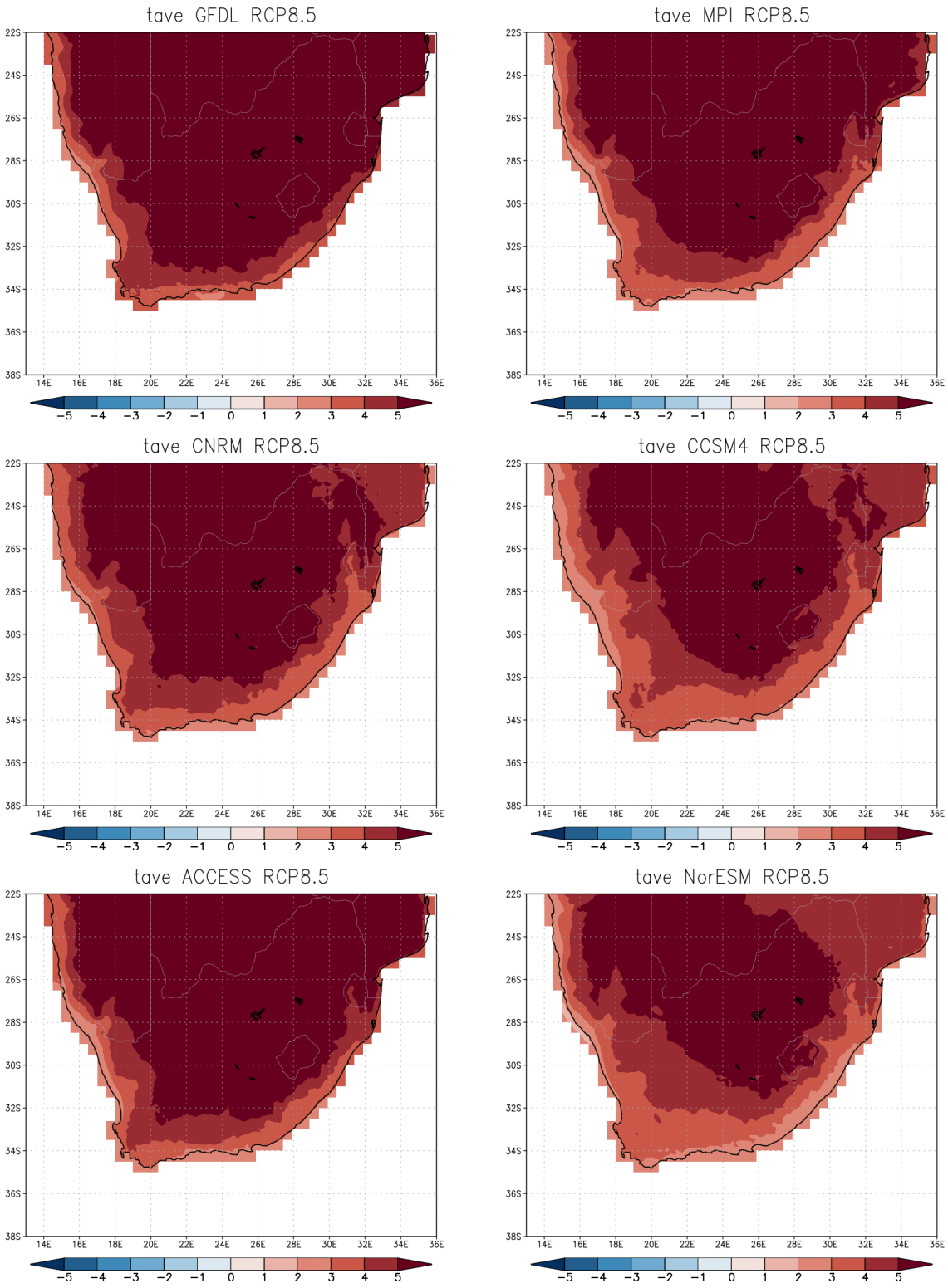

Figure 49 - CCAM downscalings (8 km resolution in the horizontal) of the change in spring (September to October) average temperature (°C) over southern Africa for the time-slab 2089-2099 relative to 1995-2005, for six different GCMs under RCP8.5.

6.8 Summary

6.8.1 Air Temperature

CMIP5 models show an increase across all models with the largest values around Botswana. The degree of change varies across the ensemble with ranges of between 1-3°C in some models and 4-8°C in others. In the regions of interest, this is ranging between 3-5°C. For CMIP6, there is also an Increase across all models ranging 3-9°C, with the greatest increases being found in the southern and western interior of SADC. CMIP6 generally shows a stronger warming in the 95 percentiles when compared to the other models in this study over the focused regions. In these regions the increases ranges within 2-6°C. The CORDEX models have the smallest range, likely due to the smaller ensemble size, but also the smallest increases in temperature, with ranges between 1-7°C over the whole of SADC and 1-3°C over the focused regions.

However, CP4A projects a more extreme increase in temperature across SADC with a range of around 6-8°C. This is in part, due to the lack of anomalous aerosols in the forcing scheme used, which leads to a higher warming than CMIP models. The highest increases are seen in Namibia, Botswana, and Angola while CCAM warming across South Africa exceeds 5°C for large portions of the interior regions.

6.8.2 Precipitation

In the wetter seasons (DJF), most models agree that rainfall will increase across most of northern SADC, with southern SADC becoming drier. JJA sees a reduction in rainfall across a majority of SADC except for a few northern countries. CMIP6 ensemble mean is overall aligned with CMIP5 results, however, in both cases there is generally little consistency across the models. Several CMIP6 models project severe drying across the sub-tropics, but this is not a consistent pattern. There is some consistency in JJA with a general drying across most models. Compared to the other models, again, CMIP6 tends to project greater increases in the upper percentiles.

As for air temperature, the CORDEX models also project the smallest changes in rainfall compared to the other models. However, the results are still generally well aligned with CMIP5 and 6 projections.

CP4A predicts that wet seasons (DJF) will get wetter across most of SADC except for Namibia and Angola. Drier seasons (JJA) shows a slight decrease in rainfall across a majority of SADC with the only exception being Demographic Republic of Congo. CCAM simulates a similar decrease in rainfall with a substantial reduction in the winter months. The only exception to this rainfall reduction is in the summer where there is an increase over the eastern escarpment region.

7 Conclusion

It is demonstrated that the selected models perform reasonably well at simulating the present-day conditions for near-surface air temperature and rainfall over the SADC region. The simulations from CP4A (4.5 km) and CCAM (8 km) exhibit some improvements compared to the lower resolution models especially for the DJF rainfall. There was thus no reason to exclude any of these models in our evaluation of the future SADC climate projections and this is conformed to the selection undertaken by Rowell et al. (2016) and Kolusu et al. (2021).

For the end of century climate projections, there is a common agreement from all the models on an air temperature increase across the SADC region. However, the high-resolution models exhibit larger values with increase average around 5°C. For the precipitation, as shown in Table 3, there is a general reduction projected across the region except for (1) DJF months in the Upper ESAF and SEAF regions, (2) MAM months in SEAF. However, there are significant discrepancies between the models in (1) Lower ESAF in DJF and MAM, (2) Upper ESAF in MAM and (3) SEAF in SON. However, it should be kept

in mind that there are large differences between the models and thus some uncertainties which need to be characterize better in the follow-up activities targeting the individual case studies.

Table 4: Summary of the projected change in precipitation for the end of the century under RCP8.5. The symbol "+" indicates an increase, "-" a decrease and "=" no significant change. The Green columns show areas with significant discrepancies between the models.

Precipitation	LOWER ESAF				LOWER WSAF				UPPER ESAF				SEAF			
MODEL	DJF	MAM	JJA	SON	DJF	MAM	JJA	SON	DJF	MAM	JJA	SON	DJF	MAM	JJA	SON
CMIP5	-	-	-	-	-	-	-	-	+	=	-	-	+	+	=	+
CMIP6	+	-	-	-	-	-	-	-	+	+	-	-	+	+	=	+
CORDEX	-	-	-	-	-	-	-	-	=	-	-	-	+	+	-	+
CCAM	+	+	-	-	-	-	-	-								
CP4A	+	+	-	+	-	-	-	-	+	+	-	-	+	+	-	-

Bibliography

Archer E, Engelbrecht F, Hänsler A, Landman W, Tadross M and Helmschrot J. (2018) Seasonal prediction and regional climate projections for southern Africa. In: Climate change and adaptive land management in southern Africa – assessments, changes, challenges, and solutions, pp. 14-21, Biodiversity & Ecology, 6, Klaus Hess Publishers, Göttingen & Windhoek. doi:10.7809/b-e.00296.

Berrisford, P., Dee, D., Fielding, K., Fuentes, M., Kallberg, P., Kobayashi, S., & Uppala, S. (2009). The ERA-Interim Archive. Retrieved from http://www.ecmwf.int/publications/library/do/references/list/782009%5Cnhttp://centaur.reading.ac.uk/1997/

Conway, D., Dalin, C., Landman, W.A. et al. Hydropower plans in eastern and southern Africa increase risk of concurrent climate-related electricity supply disruption. Nat Energy 2, 946–953 (2017). https://doi.org/10.1038/s41560-017-0037-4)

Ekine-Dzivenu, C.C., Mrode, R., Oyieng, E., Komwihangilo, D., Lyatuu, E., Msuta, G., Ojango, J.M.K., Okeyo, A.M., 2020. Evaluating the impact of heat stress as measured by temperature-humidity index (THI) on test-day milk yield of small holder dairy cattle in a sub-Sahara African climate. Livest. Sci. 242, 104314. doi:10.1016/j.livsci.2020.104314

Engelbrecht F, Adegoke J, Bopape MM, Naidoo M, Garland R, Thatcher M, McGregor J, Katzfey J, Werner M, Ichoku C and Gatebe C (2015). Projections of rapidly rising surface temperatures over Africa under low mitigation. Environmental Research Letters **10** doi: 10.1088/1748-9326/10/8/085004.

Engelbrecht FA, Marean CW, Cowling R, Engelbrecht C, Nkoana R, O'Neal D, Fisher E, Shook E, Franklin J, Neumann FH, Scott L, Thatcher M, McGregor JL, Van der Merwe J, Dedekind Z and Difford M (2019). Downscaling Last Glacial Maximum climate over southern Africa. Quaternary Science Reviews **226** 105879 https://doi.org/10.1016/j.quascirev.2019.105879.

Eyring, V., Bony, S., Meehl, G. A., Senior, C. A., Stevens, B., Stouffer, R. J., & Taylor, K. E. (2016). Overview of the Coupled Model Intercomparison Project Phase 6 (CMIP6) experimental design and organization. *Geoscientific Model Development*, *9*(5), 1937–1958. https://doi.org/10.5194/gmd-9-1937-2016

Funk, C., Peterson, P., Landsfeld, M., Pedreros, D., Verdin, J., Shukla, S., … Michaelsen, J. (2015). The climate hazards infrared precipitation with stations—a new environmental record for monitoring extremes. *Scientific Data*, *2*(1), 150066. https://doi.org/10.1038/sdata.2015.66

Harris, I., Jones, P. D., Osborn, T. J., & Lister, D. H. (2014). Updated high-resolution grids of monthly climatic observations - the CRU TS3.10 Dataset. *International Journal of Climatology*, *34*(3), 623–642. https://doi.org/10.1002/joc.3711

Horowitz HM, Garland RM, Thatcher M, Landman WA, Dedekind Z, Van der Merwe J, and Engelbrecht F.A. (2017). Evaluation of climate model aerosol variability over Africa using AERONET. Atmospheric Chemistry and Physics **17** 13999-14023. DOI 10.5194/acp-17-13999-2017..

Huffman, G. J., Adler, R. F., Bolvin, D. T., & Gu, G. (2009). Improving the global precipitation record: GPCP Version 2.1. *Geophysical Research Letters*, *36*(17), L17808. https://doi.org/10.1029/2009GL040000

IPCC, 2021: Climate Change (2021). The Physical Science Basis. Contribution of Working Group I to the Sixth Assessment Report of the Intergovernmental Panel on Climate Change [Masson-Delmotte, V., P. Zhai, A. Pirani, S. L. Connors, C. Péan, S. Berger, N. Caud, Y. Chen, L. Goldfarb, M. I. Gomis, M. Huang, K. Leitzell, E. Lonnoy, J. B. R. Matthews, T. K. Maycock, T. Waterfield, O. Yelekçi, R. Yu and B. Zhou (eds.)]. Cambridge University Press. In Press.

Iturbide, M., Gutiérrez, J. M., Alves, L. M., Bedia, J., Cerezo-Mota, R., Cimadevilla, E., … Vera, C. S. (2020). An update of IPCC climate reference regions for subcontinental analysis of climate model data: definition and aggregated datasets. *Earth System Science Data*, *12*(4), 2959–2970. https://doi.org/10.5194/essd-12-2959-2020

Kolusu, S. R., Shamsudduha, M., Todd, M. C., Taylor, R. G., Seddon, D., Kashaigili, J. J., Ebrahim, G. Y., Cuthbert, M. O., Sorensen, J. P. R., Villholth, K. G., MacDonald, A. M., and MacLeod, D. A. (2019) The El Niño event of 2015–2016: climate anomalies and their impact on groundwater resources in East and Southern Africa, Hydrol. Earth Syst. Sci., 23, 1751–1762

Kolusu, S.R., Siderius, C., Todd, M.C. et al. Sensitivity of projected climate impacts to climate model weighting: multi-sector analysis in eastern Africa. Climatic Change 164, 36 (2021). https://doi.org/10.1007/s10584-021-02991-8

Mabhaudhi, T., Simpson, G., Badenhorst, J., Senzanje, A., Jewitt, G.P.W., Chimonyo, V.G.P., Mpandeli, S., Nhamo, L., (2021). Developing a Framework for the Water-Energy-Food Nexus in South Africa, in: Climate Change and Water Resources in Africa. Springer International Publishing, Cham, pp. 407–431. doi:10.1007/978-3-030-61225-2_18

McGregor JL (2005) C-CAM geometric aspects and dynamical formulation. *CSIRO Atmospheric Research Technical paper*, 70.

Nhemachena, C., Nhamo, L., Matchaya, G., Nhemachena, C.R., Muchara, B., Karuaihe, S.T., Mpandeli, S., (2020). Climate Change Impacts on Water and Agriculture Sectors in Southern Africa: Threats and Opportunities for Sustainable Development. Water 12, 2673. doi:10.3390/w12102673

Nikulin, G., Jones, C., Giorgi, F., Asrar, G., Büchner, M., Cerezo-Mota, R., … Sushama, L. (2012). Precipitation Climatology in an Ensemble of CORDEX-Africa Regional Climate Simulations. *Journal of Climate*, *25*(18), 6057–6078. https://doi.org/10.1175/JCLI-D-11-00375.1

O'Neill, B. C., Tebaldi, C., van Vuuren, D. P., Eyring, V., Friedlingstein, P., Hurtt, G., … Sanderson, B. M. (2016). The Scenario Model Intercomparison Project (ScenarioMIP) for CMIP6. *Geoscientific Model Development*, *9*(9), 3461–3482. https://doi.org/10.5194/gmd-9-3461-2016

Pequeno, N. L. D., Hernandez-Ochoa, I.M., Reynolds, M., Sonder, K., Molero-Milan, A., Robertson, R., da Silva Sabino Lopes, M., Xiong, W., Kropff, M., Asseng, S., (2021). Climate impact and adaptation to heat and drought stress of regional and global wheat production. Environ. Res. Lett. doi:10.1088/1748-9326/abd970

Prein, A. F., Langhans, W., Fosser, G., Ferrone, A., Ban, N., Goergen, K., … Leung, R. (2015). A review on regional convection-permitting climate modeling: Demonstrations, prospects, and challenges. *Reviews of Geophysics*, *53*(2), 323–361. https://doi.org/10.1002/2014RG000475

Ramirez-Villegas J, Ghosh A, Craparo A, Thornton P, Manvatkar R, Bogart B, Läderach P . (2021). Climate change and its impacts in Southern Africa: A synthesis of existing evidence in support of the World Food Programme's 2021 Climate Change Position Paper CCAFS Working paper No. 358. CGIAR Research Program on Climate Change, Agriculture and Food Security (CCAFS).

Remedio, A. R., Teichmann, C., Buntemeyer, L., Sieck, K., Weber, T., Rechid, D., … Jacob, D. (2019). Evaluation of New CORDEX Simulations Using an Updated Köppen–Trewartha Climate Classification. *Atmosphere*, *10*(11), 726. https://doi.org/10.3390/atmos10110726

Riahi, K., van Vuuren, D. P., Kriegler, E., Edmonds, J., O'Neill, B. C., Fujimori, S., … Tavoni, M. (2017). The Shared Socioeconomic Pathways and their energy, land use, and greenhouse gas emissions implications: An overview. *Global Environmental Change*, *42*, 153–168. https://doi.org/10.1016/j.gloenvcha.2016.05.009

Rowell DP, Senior CA, Vellinga M, Graham RJ (2016) Can climate projection uncertainty be constrained over Africa using metrics of contemporary performance? *Climatic Change,* 134:621–633. https://doi.org/10.1007/s10584-015-1554-4

Schneider, U., Becker, A., Finger, P., Meyer-Christoffer, A., Rudolf, B., & Ziese, M. (2011). GPCC full data reanalysis version 6.0 at 0.5: Monthly land-surface precipitation from rain-gauges built on GTS-based and historic data.

Senior, CA, Marsham, JH, Berthou, S et al. (2021) *Convection-Permitting Regional Climate Change Simulations for Understanding Future Climate and Informing Decision-Making in Africa*. Bulletin of the American Meteorological Society, 102 (6). E1206-E1223. ISSN 1520-0477

Siderius, Christian, Seshagiri R. Kolusu, Martin C. Todd, Ajay Bhave, Andy J. Dougill, Chris JC Reason, David D. Mkwambisi et al. (2021). "Climate variability affects water-energy-food infrastructure performance in East Africa." One Earth 4, no. 3, 397-410

Steppeler, J., Doms, G., Schuttler, U., Bitzer, H. W., Gassmann, A., Damrath, U., & Gregoric, G. (2003). Meso-gamma scale forecasts using the nonhydrostatic model LM. *Meteorology and Atmospheric Physics*, *82*(1–4), 75–96. https://doi.org/10.1007/s00703-001-0592-9

Stouffer, R. J., Eyring, V., Meehl, G. A., Bony, S., Senior, C., Stevens, B., & Taylor, K. E. (2017). CMIP5 Scientific Gaps and Recommendations for CMIP6. *Bulletin of the American Meteorological Society*, *98*(1), 95–105. https://doi.org/10.1175/BAMS-D-15-00013.1

Stratton, R. A., Senior, C. A., Vosper, S. B., Folwell, S. S., Boutle, I. A., Earnshaw, P. D., … Wilkinson, J. M. (2018). A Pan-African Convection-Permitting Regional Climate Simulation with the Met Office Unified Model: CP4-Africa. *Journal of Climate*, *31*(9), 3485–3508. https://doi.org/10.1175/JCLI-D-17-0503.1

Taylor, K. E., Stouffer, R. J., & Meehl, G. A. (2012). An Overview of CMIP5 and the Experiment Design. *Bulletin of the American Meteorological Society*, *93*(4), 485–498. https://doi.org/10.1175/BAMS-D-11-00094.1

8 Appendix

8.1 List of CMIP5 models

Model	Resolution	Country
ACCESS1-0	1.875° ×1.875°	Australia
ACCESS1-3	1.875° ×1.875°	Australia
bcc-csm1-1	2.8° × 2.8°	China
bcc-csm1-1-m	2.8° × 2.8°	China
BNU-ESM	2.8° × 2.8°	China
CanESM2	2.8° × 2.8°	Canada
CCSM4	0.9° × 1.25°	USA

CESM1-BGC	0.9° × 1.25°	USA
CMCC-CM	0.75° × 0.75°	Italy
CNRM-CM5	1.4° × 1.4°	France
CSIRO-Mk3-6-0	1.875° ×1.875°	Australia
EC-EARTH	2.8° × 2.8°	Europe
FGOALS-g2	2.8° × 2.8°	China
GFDL-CM3	2° × 2.5°	USA
GFDL-ESM2G	2° × 2.5°	USA
GFDL-ESM2M	2° × 2.5°	USA
GISS-E2-H	2° × 2.5°	USA
GISS-E2-R	2° × 2.5°	USA
HadGEM2-CC	1.25° × 1.875°	UK
HadGEM2-ES	1.25° × 1.875°	UK
inmcm4	1.5° × 2°	Russia
IPSL-CM5A-LR	1.89° ×3.75°	France
IPSL-CM5A-MR	1.27° × 2.5°	France
IPSL-CM5B-LR	1.89° × 3.75°	France
MIROC5	1.4° × 1.4°	Japan
MIROC-ESM	2.79° × 2.81°	Japan
MIROC-ESM-CHEM	2.79° × 2.81°	Japan
MPI-ESM-LR	1.865° × 1.875°	Germany
MPI-ESM-MR	1.865° × 1.875°	Germany
MRI-CGCM3	1.121° × 1.125°	Japan
NorESM1-M	2.9° × 1.895°	Norway

8.2 List of CMIP6 Models

CMIP6 model	Latitude Spatial resolution	Longitude Spatial resolution
ACCESS-ESM1-5	1.25	1.875
ACCESS-CM2	1.25	1.875
AWI-CM-1-1-MR	0.93	0.93
AWI-ESM-1-1-LR	1.865	1.875
BCC-CSM2-MR	1.121	1.125
BCC-ESM1	2.8	2.8
CanESM5	2.8	2.8
CESM2-FV2	1.9	2.5
CESM2	0.94	1.25
CESM2-WACCM-FV2	1.9	2.5
CESM2-WACCM	0.94	1.25
CMCC-CM2-HR4	0.94	1.25
CMCC-CM2-SR5	0.94	1.25
CMCC-ESM2	0.94	1.25
CNRM-CM6-1	1.4	1.4
CNRM-CM6-1-HR	0.5	0.5
CNRM-ESM2-1	1.4	1.4
EC-Earth3-AerChem	0.70	0.70
EC-Earth3-CC	0.70	0.70
EC-Earth3	0.70	0.70
EC-Earth3-Veg	0.70	0.70
EC-Earth3-Veg-LR	1.121	1.125
FGOALS-f3-L	1.0	1.25
FGOALS-g3	2.0	2.0
GFDL-CM4	2.0	2.5
GFDL-ESM4	1.0	1.25
HadGEM3-GC31-LL	1.25	1.87
HadGEM3-GC31-MM	0.55	0.83
IITM-ESM	1.90	1.87
INM-CM4-8	1.5	2

INM-CM5-0	1.5	2
KACE-1-0-G	1.25	1.87
MIROC6	1.4	1.40
MIROC-ES2L	2.79	2.81
MPI-ESM-1-2-HAM	1.86	1.87
MPI-ESM1-2-HR	0.93	0.93
MPI-ESM1-2-LR	1.86	1.87
MRI-ESM2-0	1.121	1.125
NESM3	1.86	1.87
NorCPM1	1.89	2.5
NorESM2-LM	1.89	2.5
NorESM2-MM	0.942	1.25
SAM0-UNICON	0.942	1.25
TaiESM1	0.942	1.25
UKESM1-0-LL	1.25	1.87